CONTROL OF CARDIOMYOCYTE LIPOPROTEIN LIPASE SECRETION FOLLOWING DIABETES

by

Min Suk Kim

B.Sc., University of Kyung Hee, Korea 2001

M.D., University of Kyung Hee, Korea 2003

A THESIS SUBMITTED IN PARTIAL FULFILMENT OF THE REQUIREMENTS FOR THE DEGREE OF

DOCTOR OF PHILOSOPHY

in

THE FACULTY OF GRADUATE STUDIES

(Pharmaceutical Sciences)

THE UNIVERSITY OF BRITISH COLUMBIA
(Vancouver)

March 2010

ABSTRACT

During diabetes, when cardiac glucose utilization is impaired, the heart switches to exclusively using fatty acid (FA) for energy supply. This metabolic switching could lead to cardiomyocyte cell death, and eventually to heart disease. One mechanism for providing the heart with FA is lipoprotein lipase (LPL). LPL, synthesized in cardiomyocytes, is transferred to the vascular lumen where it catalyzes the breakdown of lipoprotein-triglyceride (TG) to provide FA to the heart. Following diabetes, heparin-releasable LPL activity at the coronary lumen increases by mechanisms that have yet to completely elucidated. Using diazoxide (DZ), an agent that decreases insulin secretion and causes hyperglycemia, we induced a substantial increase in LPL activity at the vascular lumen. In these hyperglycemic animals, we demonstrate that phosphorylation of AMPK, p38 MAPK, and heat shock protein (Hsp)25 produced actin cytoskeleton rearrangement. This structural rearrangement facilitated LPL translocation to the myocyte cell surface and eventually, the vascular lumen. Parallel to this mechanism, the robust phosphorylation of Hsp25 allowed PKCδ to activate protein kinase D (PKD), an important kinase that regulates fission of vesicles from Golgi membranes. Rottlerin, a PKCδ inhibitor, prevented PKD phosphorylation and the subsequent increase in coronary LPL. In myocytes in which PKD was silenced or a mutant form of PKCδ was expressed, these cells were incapable of increasing LPL. Results from these studies could help in restricting cardiac LPL translocation, lowering FA delivery to the heart, and strategies to overcome contractile dysfunction following diabetes. We also evaluated the process which restricts LPL at the vascular lumen, especially during severe diabetes with its associated increase in hepatic lipoprotein TG secretion and adipose tissue lipolysis. Following severe hypoinsulinemia and hyperlipidemia induced by streptozotocin, we reported that activation of caspase-3, together with loss of 14-3-3ζ, restricted

LPL translocation to the vascular lumen. When caspase-3 was inhibited, this compensatory response was lost, leading to profound lipid accumulation in the heart through promotion of LPL activity. Thus, although caspase-3 inhibition has been suggested to attenuate cardiac dysfunction, its inhibition following severe diabetes may induce cardiac damage through striking TG accumulation in the heart.

TABLE OF CONTENTS

LIST OF TABLES

LIST OF FIGURES

LIST OF ABBREVIATIONS

FA	Fatty acids
GLUT	Glucose transporters
ATP	Adenosine triphosphate
$FABP_{PM}$	Fatty acid-binding protein
FAT/CD36	Fatty acid translocase
FATP	Fatty acid-transport protein
LPL	Lipoprotein lipase
TG	Triglyceride
HSPG	Heparan sulfate proteoglycans
ER	Endoplasmic reticulum
ROCK	Rho kinase
Hsp25	Heat shock protein 25
AMPK	AMP-activated protein kinase
Ara-A	9-β-D-arabinofuranoside
MAPK	mitogen activated protein kinase
TAB1	Transforming growth factor β-activated protein kinase 1-binding protein 1
Thr	Threonine
Tyr	Tyrosine
Ser	Serine
MKK	MAPK Kinases
PKC	Protein kinase C
PKD	Protein kinase D
CAMK	Calcium/calmodulin-dependent protein kinase
Cys	Cysteine-rich domain
PDZ	**P**ost synaptic density protein, **d**rosophila disc large tumor suppressor, **z**onula occludens-1 protein
AKAP	A-kinase anchoring protein
JNK	C-Jun N-terminal kinase
ERK	Extracellular signal regulated kinase
CERT	Ceramide transport
HDAC	Class IIa histone deacetylase
MEF2	Myocyte enhancer factor 2
AP	Activator protein
ABCA	ATP-binding cassette transporter A
HDL	High-density lipoprotein
$PI_4KIII\text{-}\beta$	Phosphatidylinositol 4-kinase IIIβ
PKA	Protein kinase A
DAG	Diacylglycerol
GPCR	G-protein coupled receptor
LPA	Lysophosphatidic acid
COP	Coat protein
SNARE	Soluble NSF (N-ethylmaleimide sensitive fusion protein) attachment protein receptor
VAMP	Vesicle associated membrane protein

VLDL	Very low-density lipoprotein
Angptl	Angiopoietin-like protein
Apo	Apolipoprotein
DZ	Diazoxide
STZ	Streptozotocin
ROS	Reactive oxygen species
MHC-β	Myosin heavy chain β
PPARα	Peroxisome proliferator activated receptor α
LPC	Lysophosphatidylcholine
mRNA	Messenger ribonucleic acid
HEPES	4-(2-hydroxyethyl)-1-piperazineethanesulfonic acid
HR	Heparin releasable
HSPG	Heparin sulphate proteoglycan
Src	Sarcoma
i.p.	Intraperitoneal
i.v.	Intravenous
PH	Pleckstrin homology
PBS	Phosphate buffered saline
SDS	Sodium dodecyl sulfate
HRP	Horse radish peroxidase
EDTA	Ethylenediaminetetraacetic acid
EGFP	Enhanced green fluorescent protein
EGTA	Ethylene glycol tetraacetic acid
DTT	Dithiothreitol
PMSF	Phenylmethylsulphonyl fluoride
TGN	Trans golgi network
DMEM	Dulbecco's Modified Eagle Medium
GST	Glutathione S transferases
PAC-1	First procaspase activating compound
OXPAT	Lipid droplet proteins (**P**erilipin, **A**dipophilin, and **T**IP47) in oxidative tissues.
PCR	Polymerase chain reaction
IP	Immunoprecipitation
WB	Western blot
SiRNA	Small interfering RNA
PMA	Phorbol 12-myristate 13-acetate
HPLC	High performance liquid chromatography
PA	Palmitic acid
PPAR	Peroxisome proliferator activated receptor

ACKNOWLEDGEMENTS

Carrying out the sheer volume and depth of this research was no easy task without the help of so many people.

First, I am deeply grateful to my doctoral supervisor, Dr. Brian Rodrigues for his continual support, advice and guidance throughout this project. His trust, encouragement and instruction have allowed me to complete this challenging work. It is a great honor and pleasure to work with him.

I also appreciate the members of my supervisory committee: Dr. Bruce Verchere, Dr. John Hill, Dr. Judy Wong, and Dr. David Fielding for their valuable suggestions and encouragement during my doctoral training. And this study would not have been possible without the generous support of the Heart & Stroke Foundation and Canadian Diabetes Association who provided me funding in the form of a Ph.D. scholarship.

Many thanks also to my colleagues and friends: Ashraf, Prasanth and Fang for their friendship and support.

Finally, I would like to take this opportunity to thank my parents and brother for their love, support and understanding.

DEDICATION

To my family, whose love and nurturing made this all possible

CO-AUTHORSHIP STATEMENT

For the three manuscripts in which I was the lead author, I was responsible for reviewing the literature, conceiving the hypothesis, designing the experiments, and writing manuscripts with help from my supervisor. The co-authors listed in my three manuscripts, Fang Wang, Prasanth Puthanveetil, and Ujendra Kumar helped with the obtaining of the immunofluoresence data. The analysis of cardiac TG was done by Sheila Innis using high performance liquid chromatography. The PKCδ and PKD mutant viruses were provided by Christopher G. Proud and Susan F. Steinberg. Travis D. Webber and Timothy J. Kieffer helped with the virus transfection in cardiomyocytes. Vivian Lee, Ding An and Ashraf Abrahani helped with the preparation of the cardiomyocytes. Lucy Marzban was instrumental in helping with the caspase-3 studies. Finally, Girish Kewalramani, Elham Hosseini-Beheshti, Natalie Ng, and Yanni Wang, at various stages of the projects, assisted with some aspects of the Western blot.

1. INTRODUCTION

1.1. Cardiac energy metabolism

1.1.1. Glucose utilization

To supply blood to all organs in the body, the heart uses vast amounts of ATP per day. Associated with this high energy demand, ATP is obtained via the oxidation of various substrates including glucose, fatty acids (FA), amino acids, lactate and ketones(1-3). Among these substrates, glucose and FA produce the bulk of ATP(1,4). Under normal physiological conditions, cardiac glucose uptake is dependent on glucose transporters (GLUT1 and GLUT4)(5). GLUT1 is located at the plasma membrane, and is responsible for basal glucose uptake(6). Compared to GLUT1, GLUT4 is predominantly located in an intracellular pool, and can be recruited to the cell surface on stimulation by insulin or muscle contraction(7,8). Inside the cardiomyocyte, glucose is either stored as glycogen or metabolized to pyruvate (glycolysis) for eventual oxidation in the mitochondria to produce ATP(9). Glucose break down provides the adult heart with approximately 30% of its energy requirements(4).

1.1.2. Fatty acid utilization

Compared with glucose, FA is the preferred energy source for the heart, providing over 70% of the ATP demand for normal cardiac function(1,4). As the heart has limited capacity to synthesize and store FA, its delivery to the cardiomyocyte is required, and this occurs through multiple mechanisms(10). Albumin-bound FA can pass into the cardiomyocyte through passive diffusion across the plasma membrane in a bidirectional manner(11). However, as an inhibitor of carrier-mediated processes blocked cardiac FA uptake by 60-80%, it was proposed that FA transport required carrier proteins(12,13). Until now, three FA transporters have been identified; plasma membrane fatty acid-binding protein ($FABP_{PM}$), fatty acid translocase (FAT/CD36), and

fatty acid-transport protein (FATP)(14,15). In addition to albumin-bound FA, cardiac lipoprotein lipase (LPL) also contributes towards the provision of FA to the heart, and does so by hydrolyzing circulating lipoprotein triglyceride (TG) to release FA(16). As the molar concentration of FA in lipoprotein-TG is ~10-fold larger than FA bound to albumin, LPL mediated hydrolysis of circulating lipoproteins to FA is suggested to be the principal source of FA for cardiac utilization(17). Nevertheless, it should be noted that other studies have reported higher extraction rates for albumin-bound FA than TG FA, and turnover rate of albumin bound FA (the number molecules that circulate over a given amount of time) is much higher than that of circulating VLDL(18).

1.2. Lipoprotein lipase

1.2.1. Synthesis, activation and degradation

LPL is a pivotal enzyme in the catabolism of triglyceride-rich lipoproteins(19). It is widely expressed in various tissues, including adipose tissue, heart, adrenals, kidneys, spleen, lungs, and skeletal muscle(19-21). This enzyme hydrolyzes plasma lipoproteins at the vascular endothelium, where it is present bound to heparan sulfate proteoglycans (HSPGs)(10,19) (Fig. 1-1). Although the functional location of LPL is at the capillary endothelial cell surface, the endothelial cell does not express LPL mRNA(22). In the heart, LPL mRNA is only detected in cardiomyocytes(16), and suggests that this enzyme is synthesized and processed in cardiomyocyte before it translocates to the vascular endothelium.

Within the myocyte, LPL transcription is from the 8p22 chromosome in the nucleus(23). Following this, the LPL mRNA is translated as an inactive, monomeric proenzyme in the rough endoplasmic reticulum (ER), followed by enzyme activation through multiple steps(24,25). In the ER, the inactive monomer undergoes glycosylation, and several post-translational processes

to be dimerized(25). During glycosylation, mannose rich oligosaccharides are added to the arginine residues of the LPL peptide(25,26). The lipid-linked oligosaccharide helps to retain nascent LPL in the ER for further modification by glucosidase and α-mannosidase(27,28). These enzymes remove three terminal glucose and one mannose residue from the LPL polypeptide(25). The mannose rich LPL then moves to the Golgi for further processing(25,29). The Golgi consists of three compartments: cis-Golgi (for receiving proteins), medial-Golgi (for processing), and trans-Golgi (for sorting and eventual transport of proteins)(30). Once LPL enters the cis-Golgi, three mannoses are removed, whereas in the medial-Golgi, two additional mannoses are deleted by mannosidase(25,30,31). In medial and trans-Golgi, N-acetylglucosamine is added onto the LPL protein by transferase(25,30-32). Following processing in the trans-Golgi, the sorted LPL has two destinations: either delivery into lysosomes for degradation or movement towards the cell surface for secretion(25,30) (Fig. 1-2). Degradation is usually a fate for misfolded or misassembled proteins(33). However, interestingly, 80% of newly synthesized LPL in adipocyte is degraded in lysosomes(27,34,35). As lysosomal degradation of proteins also requires ATP(35), it would appear that synthesis and degradation of LPL in adipose tissue is an inefficient process. Transfer of LPL towards the cell surface is an important mechanism which determines the eventual ability of this enzyme to hydrolyze lipoprotein triglyceride.

1.2.2. Transfer from Golgi to cell surface

The precise mechanisms by which sorted LPL vesicles transport to the cell surface remains unclear. However, several suggestions have been proposed for this enzyme transfer. For example, actin cytoskeleton rearrangement is widely believed to play an important role in intracellular protein transport(36,37), and has also been implicated in cardiomyocyte LPL

secretion(38,39). Interestingly, cytochalasin D (an actin polymerization inhibitor) appreciably reduces cell surface LPL activity(38,39). At present, the process by which actin filaments promote selective LPL vesicular movement is unknown, but likely involves distinct sets of actin-binding proteins(40). For actin rearrangement, several actin-binding proteins are responsible for assembly and disassembly of actin filaments(41-44). For example, cofilin alters the fibrilar actin (F-actin) structure by interacting with actin to cause its disassembly and prevent its repolymerization(42,43,45). Phosphorylation at serine (Ser) 3 on cofilin reduces its activity and increases actin polymerization(45). Indeed, Rho kinase (ROCK) signals promote actin cytoskeleton rearrangement through this cofilin phosphorylation(45). In addition to cofilin, heat shock protein 25 (Hsp25) has also been shown to bind the actin monomer preventing actin polymerization(44). Under stress conditions, and phosphorylation of Hsp25, actin monomers are released and undergo polymerization(46). ATP is not necessary for this process, but in its presence, the actin structure is more stable(47). Another suggested mechanism for LPL transfer to the cell surface involves phosphorylation and activation of AMP-activated protein kinase (AMPK)(48,49). Following metabolic stresses associated with energy depletion (as seen following diabetes), the demand for intracellular ATP promotes activation of AMPK(49,50) and increases in cardiac LPL. Interestingly, inhibition of AMPK using 9-β-D-arabinofuranoside (Ara-A), or activation of AMPK using oligomycin, significantly alters cardiac LPL activity in the absence of any change in LPL mRNA or protein(49). AMPK control of LPL could be related to the actin cytoskeleton, and recently a novel relationship between AMPK and the actin cytoskeleton has been described in skeletal muscle(51). AMPK activation is known to facilitate p38 mitogen activated protein kinase (p38 MAPK) activation through its interaction with transforming growth factor β-activated protein kinase 1-binding protein 1 (TAB1)(52).

Phosphorylation of Hsp25 is the end result of this increased p38 MAPK activation(53), resulting in release of actin monomer from Hsp25 to self-associate to form fibrillar actin(46).

1.3. Stress kinases

AMPK is a heterotrimeric complex of catalytic α, and regulatory β and γ subunits, with multiple isoforms(54,55). Until recently, two α isoforms (α1, α2), two β isoforms (β1, β2), and three γ isoforms (γ1, γ2 and γ3) have been identified(56). In the heart, the AMPK complex contains α2, β2, γ1, and γ2(57,58). The α subunit N-terminus contains the catalytic domain whereas its C-terminus has binding sites for β and γ subunits(59), and several phosphorylation residues including threonine (Thr) 172, Thr 258 and Ser 485(60). The β subunit contains an anchor domain that connects α and γ subunits, and a glycogen-binding domain that acts as glycogen sensor(61). The γ subunit has an AMP binding domain for allosteric activation(62). Metabolic energy demand increases ATP turnover with AMP and ADP formation(63). Following ATP depletion, AMP binds to γ subunits to active AMPK allosterically(62,63). This initial stimulation makes AMPK an easy substrate to be phosphorylated by upstream kinases such as LKB1(64,65). Following this, and phosphorylation of the AMPK α subunit at Thr 172, there is a 50-100 times increase in AMPK activity(66). In this way, by responding to low ATP levels, AMPK activation can modulate various signals that replenish intracellular ATP; it enhances glucose uptake, FA oxidation, and glycolysis or downregulates gluconeogenesis, glycogen, lipid and protein synthesis(67,68).

A stress-activated serine/threonine protein kinase, p38 MAPK belongs to the MAP kinase super family(69). Until now, four isoforms of p38 MAPKα, β, γ and δ have identified(70,71). p38α and β are expressed in most tissues, whereas p38γ and δ have specific tissue expression, predominantly in lung and testis(72,73). A variety of extracellular signals including pro-

inflammatory cytokines and osmotic and oxidative stress can activate p38 MAPK through its upstream kinases including several MAPK Kinases (MKK3, MKK4 or MKK6) or AMPK(74-76). Once phosphorylated, p38 MAPK can regulate a wide range of downstream-signals that includes transcription, apoptosis, cytokine production, cell differentiation and cytoskeletal reorganization(77-79). Through these mechanisms, p38 MAPK activation has been implicated in inflammatory disease, cancer, cardiovascular disease and diabetes(80-83).

In addition to these stress kinases (AMPK and p38 MAPK), the protein kinase C (PKC) family of serine/threonine-specific proteins is also suggested to control LPL(84,85). In this regard, pharmacological inhibition of PKC has been shown to decrease LPL activity by attenuating LPL vesicular trafficking(84). More recently, an important role of PKCμ (also referred to as protein kinase D, PKD) in vesicle formation(86) has been described, and could be implicated in LPL movement.

1.4. Protein kinase D

1.4.1. Overview

PKC isoforms have been classified based on structural differences and activation requirements; Ca^{2+} dependent (PKCα, β1, β2, and γ), Ca^{2+} independent (PKCε, δ, η, and θ), and atypical PKCs (PKCζ and λ)(87). Recently, a new member of this PKC family was identified, and was initially named atypical PKCμ(88). Similar to the other PKC isoforms, it is a serine/threonine-specific kinase whose regulatory domain is stimulated by diacylglycerol (DAG)(87,88). However, its catalytic sequence is highly homologous to calcium/calmodulin-dependent protein kinase (CAMK) and myosin light chain kinase(88,89). However, although its structure and substrate specificity makes PKD a part of the CAMK family, it is not included in this group as it cannot be activated by calcium/calmodulin(89). Therefore, this hybrid enzyme was called protein kinase

D, and was classified as a new group within the PKC family(88). Mammalian PKD consists of three members, and these include PKD1 (PKCμ), PKD2 and PKD3 (PKCν) isoforms(90-92). During development, PKD1 and PKD3 show widespread distribution, especially in the brain, heart and skeletal muscle(93). Although PKD2 also shows widespread distribution in various tissues during development, its total expression is limited(93,94). In adulthood, the expression of PKD is constrained(93).

1.4.2. Structure

The N-terminus of PKD contains a hydrophobic region, two cysteine-rich domains (Cys1 and Cys2), and a pleckstrin homology (PH) domain(95). Within PKD, the cysteine-rich domains have been shown to have a critical role in recruiting and binding PKD to the Golgi whereas the PH domain has an inhibitory effect on the catalytic domain(96,97). Although the PH domain is known to bind phosphoinositides, PKD is unable to generate PI3-kinase signals(98,99). The C-terminal catalytic domain has several residues that can be phosphorylated, and these include Ser 744, Ser 748 and Ser 916(100,101). Phosphorylation of these residues leads to activation of PKD(100). In addition, PKD1 and PKD2 contain a PDZ-binding motif at their C-terminus, allowing proteins to anchor to the actin cytoskeleton(102) (Fig. 1-3).

1.4.3. Regulation

When PKD is inactive, its two-cysteine and PH residues on the regulatory domain inhibit the catalytic domain(86,103). Following initial activation through phosphorylation of Ser 744 and 748, the catalytic domain is uncovered from these inhibitory residues, leading to full activation(86,104). The exact mechanism by which this process occurred remained largely undiscovered. However, a recent study has suggested a mechanism for PKD activation that involves A-kinase anchoring protein (AKAP)(105). AKAPs are a family of scaffolding proteins

that normally target protein kinase A (PKA), and other signaling enzymes(106). Interestingly, AKAP is also known to interact with PKD, with the AKAP anchored PKD complex negatively regulating PKD activity(105). However, on recruitment of an upstream kinase like PKCη to the anchoring protein, PKD activation is made possible through phosphorylation of Ser 2737 on AKAP by PKA(105). This phosphorylation dissociates PKD from AKAP, releasing PKD into the cytoplasm(105). Once released, PKD can be stimulated by a number of signals. In most cases, PKD activation is mediated by DAG dependent signals through dual pathways(95,107,108). DAG can stimulate PKD directly by binding to its Cys1 domain(95). Indirect stimulation includes activation of various PKC isoforms (PKCθ, ε, η, δ) by DAG which in turn can phosphorylate Ser 744 and Ser 748 within the activation loop of PKD(95,109). Interestingly, several G-protein coupled receptor (GPCR) agonists, growth factors and lysophosphatidic acid (LPA) are known to activate PKD through DAG associated PKC activation(107,108,110). Besides DAG and PKC related signals, PKD can also be stimulated by various pathophysiological conditions that effect Ser 744/748 phosphorylation(100,111). For example, following oxidative stress, the sarcoma (Src)-mediated phosphorylation at tyrosine (Tyr) 95 residue within the PKD-regulatory domain facilitates its binding to PKCδ, which in turn phosphorylates Ser 744/748 in the activation loop of PKD(111). In addition to Ser 744/748 on the activation loop, Ser 916 has also been identified as an autophosphorylation site for PKD(96,100). As constitutively active forms of PKD (such as PH domain deleted or S744E/S748E-substituted mutants) display Ser 916 phosphorylation under resting conditions, phosphorylation at Ser 916 is viewed as an autocatalytic reaction(100). In fact, despite the numerous phosphorylation sites on PKD, phosphorylation of Ser 916 is the one that most closely

mirrors PKD activity(96). It should be noted that genotoxic agents have also been shown to activate PKD via a caspase-3-mediated proteolytic cleavage without phosphorylation(112).

Once activated, PKD shuttles to the nucleus, Golgi or cell surface membranes. The nuclear accumulation of PKD requires its Cys2 domain in conjunction with importin, while its nuclear export requires its PH domain(113-115). Further analysis of point mutations demonstrated that loss of PKD3 kinase activity prevented its nuclear import(116). These results indicate that the catalytic activity of PKD3 may also regulate its nuclear import(116). The cysteine rich motifs of PKD also regulate its interaction with Golgi and cell surface. While the proline 155 in Cys1 domain on PKD is necessary for its recruitment to Golgi, the Cys2 motif is responsible for cell surface translocation(89,117).

Once localized in different subcellular compartments, PKD carries out its various cellular responses and functions. In the cytosol, PKD downregulates c-Jun N-terminal kinase (JNK) activity by phosphorylating c-Jun, whereas it upregulates ERK1/2 by phosphorylating the Ras-binding protein RIN1(118,119). At this location, it is also known to impair cardiac myofilament Ca^{2+} sensitivity by phosphorylation of troponin I(120). In Golgi, PKD regulates transport carriers including ceramide transport (CERT)(121). Activated PKD phosphorylates Ser 132 on CERT, decreasing the affinity of CERT for Golgi membranes thereby reducing ceramide transfer activity(121). As ceramide has been described as a lipotoxic molecule known to induce cardiac injury, activation of PKD may induce cardiac dysfunction through its regulation of CERT(121,122). PKD has also been reported to regulate neurotensin, a gut peptide that plays an important role in gastrointestinal secretion(123). Additionally, with oxidative stress, p38δ MAPK activation in pancreatic β cells is known to phosphorylate PKD at Ser 397/401, reduce PKD activation and decrease insulin secretion(124). Interestingly, p38δ MAPK deficient β cells

are known to increase insulin secretion on PKD activation(124). In the nucleus, activated PKD can phosphorylate class IIa histone deacetylase (HDAC) that is a known repressor of myocyte enhancer factor 2 (MEF2)(125). Phosphorylation of HDACs promotes its interaction with 14-3-3, exporting the complex from the nucleus to facilitate MEF-2 gene transcription, which is implicated in cardiac hypertrophy(125,126). Recently, PKD has also been reported to phosphorylate Ser 258 of the activator protein (AP) 2α(127). AP2α negatively regulates expression of the ATP-binding cassette transporter A (ABCA) 1, which is known to increase high-density lipoprotein (HDL) biogenesis(127,128). Following knockdown of PKD, there was a decrease in AP2α activity, increased ABCA1 expression and higher plasma HDL(127). Overall, through these regulatory mechanisms, PKD has been implicated in several diseases including cancer, asthma, cardiac hypertrophy and atherosclerosis, and thus could be an important pharmacological target(125,127,129).

1.4.4. Control of vesicle biology and LPL secretion

The mechanism by which PKD generates vesicles from the Golgi, and transports them to the cell surface is not clearly understood. However, several mechanisms have been proposed. For example, the cysteine domains on PKD have been shown to be essential for its recruitment to the Golgi, and its binding with high affinity(130). Mutations at the Ser 744/748 sites on the catalytic domain of PKD not only causes a loss in its basal activity, but also prevents its transport to the Golgi suggesting that phosphorylation of Ser 744/748 on its activation loop may have a critical role in recruiting PKD to Golgi(117). On binding to Golgi, the vesicle budding process could be initiated by the action of PKD on its substrate, phosphatidylinositol 4-kinase IIIβ (PI_4KIII-β), a known enhancer of vesicle fission(131). In addition to this interaction, a product of activation of PI_4KIII-β is phosphoinositide production, which can recruit other molecules involved in Golgi

carrier formation(131,132). Vesicles formed following activation of PI_4KIII-β predominantly move to the cell surface instead of the lysosome(131) (Fig. 1-4). Thus, PKD could be essential for LPL vesicle formation.

Following vesicle budding, and depending on its protein cargo, these structures are coated with specific adaptor proteins. Theses include COPI, COPII and clathrin(133-135). COPI coated vesicles are transported from Golgi to ER whereas COPII coated vesicles are moved from the ER into the Golgi(133,134). Clathrin trafficking is ubiquitous, transporting vesicles between Golgi, cell surface and endosomes(135). Given this function of clathrin, this adaptor protein could be involved in LPL transfer to the cell surface. At present, it is uncertain whether LPL vesicles are coated with clathrin. In pancreatic β-cells, PKD can accelerate insulin vesicle secretion and exocytosis by a clathrin independent mechanism, and non-clathrin-coated vesicles are produced following PKD stimulation in HeLa cells(136,137). Thus, it is likely that PKD related vesicle biogenesis is independent of clathrin coating, and requires further investigation.

Once coated, vesicle destination depends on the appropriate docking protein. One such protein involved in vesicle targeting is soluble NSF attachment protein receptor (SNARE)(138). SNAREs can be classified into two categories: vesicle SNARE (v-SNARE), which is incorporated into the membranes of transport vesicles, and target SNARE (t-SNARE), which is located in target membranes(138,139). Following specific interaction between these two SNAREs, vesicles are able to dock onto target membranes(138). At present, it is unclear as to what protein targets LPL vesicles to the cell surface. Recently, using yeast two-hybrid screening, vesicle associated membrane protein (VAMP, one of the v-SNAREs) was identified as a novel binding partner of PKD(140). Photo bleaching has also determined that PKD can also directly interact with VAMP, and this complex regulates vesicular movement for cell surface

docking(140). Once generated, the vesicle interacts with myosin motor, which translocates the complex along actin filaments(141). Structurally, the myosin motor has a conserved head but a tail which is highly variable, and able to interact with a large number of different cargoes(142). Currently, it is unclear which myosin motor is able to interact with LPL vesicles, to transport them to the cell surface. However, as PKD has a high affinity to bind PDZ protein through its PDZ-binding motifs, PDZ domain containing myosin motors are likely involved in this process(102,143).

1.5. Myocyte to endothelial cell transfer of LPL

To hydrolyze TG-rich lipoproteins, LPL translocation is essential from its site of synthesis (cardiomyocyte) to its site of action (endothelial lumen)(25,144). The mechanism for this translocation is not completely elucidated. However, a number of suggestions have been proposed to explain the transfer of LPL from the apical side of cardiomyocyte to the vascular lumen(145-147). One proposal for this vectorial movement is that LPL is transferred along a continuous network of HSPG in the interstitial space that extends from myocyte to endothelial cells(146). Another theory has implicated endothelial heparanase in this movement(147) (Fig. 1-5). Heparanase is synthesized as a latent 65 kDa enzyme and transferred from Golgi to lysosomes(148). In the endothelial lysosome, it undergoes proteolytic cleavage by cathepsin-L, and a 50 kDa polypeptide is formed that is ~200-fold more active than the 65 kDa parent compound(148,149). Within the acidic compartment of the lysosome, active heparanase is stored in a stable form (half-life ~30 h)(150). Mobilization by demand can occur, where the enzyme is either translocated to the nucleus to affect gene transcription, or secreted towards the cardiac cell surface to cleave heparan sulfate(151-153). The mechanism by which heparanase is secreted has not been completely elucidated. A previous report has suggested preferential

release from the basolateral side of endothelial cells towards the cardiomyocyte, where the enzyme can initiate cleavage of myocyte HSPG side chains(10). More recently, data from our lab suggests that following hyperglycemia, rapid secretion of heparanase occurs, and this process requires an intact microtubule and actin cytoskeleton(154). Following cardiac HSPG cleavage by heparanase, the oligosaccharide-bound LPL released into the interstitial space is then transported to and across the endothelial cell by a process that requires both HSPG and very low-density lipoprotein (VLDL) receptor(145,155). At the endothelial lumen, LPL hydrolyzes the TG-rich lipoproteins such as VLDL and chylomicrons, to release FA(10).

1.6. Regulation of LPL

Nutrition and hormonal factors have been shown to modulate LPL activity in various tissues. For example, during fasting, LPL activity is reduced in adipose but increased in cardiac tissue(25,156). This change reduces adipose TG storage but increases FA delivery to the heart to meet the increased demand of the heart for energy(10). The fasting associated changes in adipose LPL have been connected to a rapid increase in angiopoietin-like protein 4 (Angptl-4) mRNA and protein which converts LPL from a catalytically active dimer to an inactive monomer(157). Interestingly, on re-feeding or insulin treatment, Angptl-4 mRNA is rapidly turned over, and LPL activity is restored to control levels(158,159). Compared to adipose tissue, fasting increases cardiac LPL activity at the coronary vascular lumen without any corresponding changes in the levels of mRNA or total cardiac protein(10). As cardiac Angptl-4 mRNA expression level is minimal in the heart compared to adipose tissue, the increase enzyme following fasting does not appear to be influenced by this mechanism(160). We reported that the fasting induced increase in cardiac LPL is likely mediated by AMPK(49). Thus, inhibition of AMPK in fasted hearts using an inhibitor like Ara-A or insulin, markedly lowered the enhanced

luminal LPL activity, suggesting that AMPK has an important role in the redistribution of LPL from cardiomyocytes to endothelial cells(49).

Regarding hormonal regulation of LPL, insulin is known to increase LPL activity 3-fold in adipose tissue, but reduce it significantly in skeletal muscle(161). In adipose tissue, insulin regulates glucose trimming of the N-linked oligosaccharide on LPL, enabling it to transfer from ER to Golgi(31). Stress, anxiety, and hypoglycemia can cause excess production of catecholamines (epinephrine and norepinephrine), resulting in increased LPL activity in skeletal muscle and heart by mechanisms not yet determined(31). Other hormones like thyroid hormone and glucocorticoids (which impair insulin sensitivity), are also known to affect cardiac LPL activity (162).

In addition to hormonal regulation, LPL activity can also be modulated by many other factors. For example, apolipoprotein (apo) CII on lipoproteins activate LPL and enhances TG lipolysis, whereas binding of lipoproteins containing apo CIII or apo E is known to suppress LPL activity(163,164). High concentrations of FA are also known to influence LPL, either through a direct inhibition of enzyme activity or displacement of LPL from its HSPG binding site on vascular endothelial cells(165). These effects of FA are suggested to provide a negative feedback for LPL to prevent lipolysis and oversupply of FA(165). LPL can also be regulated by its recycling in endothelial cells(166). Following a drop of intracellular pH, the LPL-HSPG complex can be internalized into endothelial cells and stored in endocytotic vesicles (and not degraded)(166). This process allows the endothelium to maintain an auxiliary pool of LPL, which can then recycle to the apical side of endothelial cells when demand for LPL increases(166). Thus, low endothelial pH (like that anticipitated following diabetes) would be expected to reduce LPL degradation, allowing more enzyme to appear at the vascular lumen.

Interestingly, a decrease in pH from 7.3 to 6.6 is also known to activate AMPK *in vitro* and during ischemia(167,168).

1.7. Pathological roles of LPL

Given that LPL is a central enzyme in lipid metabolism, it has been directly or indirectly implicated in several pathophysiological conditions such as hypertriglyceridaemia, obesity, and atherosclerosis(169,170). Deficiency in LPL or its cofactor apo CII, or inhibition of LPL by overexpression of apo CIII leads to a substantial hypertriglyceridemia(171-173). This condition may induce severe abdominal pain, yellow skin lumps, and enlarged liver and spleen(174). Atherosclerosis is a condition in which the artery wall thickens due to accumulation of lipids, and it is the underlying cause for vascular disease, heart attack and stroke(169). It starts from initial damage to the endothelium, which increases adhesive molecules, thereby causing uptake of monocytes(169). Monocyte-derived macrophage engulf oxidized low density lipoprotein (LDL) to develop foam cells(169). Unfortunately, these cells are unable to process the oxidized LDL, grow and then rupture, depositing a large amount of oxidized cholesterol in the artery wall(169). As LPL is expressed in both macrophages and macrophage-derived foam cells, LPL has been proposed to influence the development of atherosclerosis(169,175). It is suggested that LPL acts as a ligand, associating with lipoproteins to promote their binding to the LDL receptor-related protein, accelerating lipoprotein uptake(176). This function of LPL is largely a non-catalytic function of the enzyme(176). A similar role of LPL has also been described for the macrophage, permitting LDL uptake(169,176). Interestingly, decreased expression of LPL or macrophage selective LPL deficiency in animals protects the vascular wall against feeding of an atherogenic diet(177). It should be noted that LPL overexpression in adipose tissue prevents atherosclerosis by aiding in the clearance of circulating lipoprotein particles(178). Moreover,

several drugs which are known to increase LPL expression, have been found to reduce atherosclerosis(179). Thus, the role of LPL in atherosclerosis depends on its tissue expression(31).

1.8. Models of Diabetes

Despite insulin therapy, early metabolic changes may predispose the diabetic heart to accelerated damage when exposed to conditions of dyslipidemia, atherosclerosis, and hypertension(180). Examination of these initial metabolic changes have been problematic given the limited availability of animal models. We have used two animal models to successfully indentify acute changes in cardiac metabolism. For my thesis, I have only focused on models of Type 1 diabetes. Diazoxide (DZ, 100 mg/kg), a selective K^{+}_{ATP} channel opener, was used to rapidly decrease insulin secretion from β-cells(181). On injection with DZ, a rapid decline in serum insulin occurred within 1 h and was associated with a robust increase in plasma glucose that reached a maximum level after 2 h(181). The reduction in insulin was also characterized by significant and rapid increases in plasma FA and TG(181). Streptozotocin (STZ), a selective β-cell toxin, was also utilized to reduce plasma insulin and induce hyperglycemia(182). When using STZ, we varied the doses to obtain moderate (55 mg/kg, D-55) and severe (100 mg/kg, D-100) diabetes, and the animals were usually followed for 4 days after STZ administration(182). After treatment of STZ in D-55 animals, hyperglycemia develops within 24~48 h in concert with a ~50% reduction in plasma insulin in the absence of any change in plasma FA and TG(182). In D-100 animals, there is intense β-cell necrosis, loss of 98% of pancreatic insulin stores, and severely reduced plasma insulin(182). Compared to D-55, these D-100 animals show remarkable elevation of plasma FA and TG(182). It should be noted that although STZ and DZ may have pleiotropic cardiovascular effects, all the effects of diabetes on LPL can be reversed by insulin

suggesting that changes in LPL are a consequence of the disease, and not drug induced(162,181). In other studies, our lab has also reported the influence of insulin resistance, using dexamethasone, on cardiac LPL(162).

1.9. Cardiac LPL following diabetes

Following diabetes, the heart switches to using FA for energy supply in the presence of lower glucose utilization. Our lab was the first to report an increase in cardiac LPL following moderate diabetes(182). Thus, using retrograde perfusion of isolated D-55 hearts with heparin to displace coronary LPL, we demonstrated significantly elevated heparin-releasable (HR)-LPL activity(182). Mechanistically, we subsequently reported that the increase in LPL closely followed AMPK phosphorylation(48). We concluded that this increase in LPL can promote myocardial FA or TG accumulation. Under conditions of FA overload, the production of ceramide and reactive oxygen species (ROS) trigger the flux of calcium from endoplasmic reticulum to mitochondria, eventually resulting in release of cytochrome C into the cytosol and apoptotic cell death(183). When cardiac lipid droplet formation is overwhelming, there is up-regulation of peroxisome proliferator activated receptor α (PPARα) and myosin heavy chain β (MHC-β) which have been known to depress cardiac function(184,185). During severe diabetes (D-100), there is provision of FA through increased adipose tissue lipolysis resulting in elevated circulating plasma FA(182). Hepatic VLDL-TG secretion also increases in this situation(182). In the event of increased FA delivery by these mechanisms, we anticipated that LPL regulated FA supply would be limited to avoid oversupply of this potentially lethal substrate. Indeed, following severe diabetes, coronary HR-LPL activity was lower compared to control hearts(182).

1.10. Summary of previous findings from the supervisor's laboratory

Using retrograde perfusion of the heart with heparin to displace coronary LPL, we found significantly elevated luminal LPL activity following diabetes(10). We determined that the increased enzyme in the diabetic heart is: i) not the result of increased gene expression, ii) likely unrelated to an increase in the number of capillary endothelial HSPG binding sites, iii) acutely (hours) regulated by short-term changes in insulin levels, iv) largely independent of circulating blood glucose, and v) functionally relevant and capable of hydrolyzing lipoprotein-TG(10,186). More recently, we have been studying the contributions of the endothelial cell in enabling this increased enzyme at the vascular lumen(187). At the endothelial cell, we reported that TG and lipoprotein breakdown products like lysophosphatidylcholine (LPC), through their release of heparanase, enabled myocyte HSPG cleavage and transfer of LPL towards the coronary lumen(187).

1.11. Hypothesis and research objectives

Although cardiovascular disease is the leading cause of diabetes-related death, its etiology is still not understood. The earliest change that occurs in the diabetic heart is altered energy metabolism where, in the presence of lower glucose utilization, the heart switches to exclusively using FA for energy supply. It does this by increasing LPL at the coronary lumen. *My hypothesis is that in response to diabetes, LPL increase at the vascular lumen is facilitated by transfer of cardiomyocyte LPL to the endothelial cell.* This metabolic adaptation increases FA utilization and could promote cardiac injury.

The objectives of my research proposal were to:

1. Determine the mechanisms by which the actin cytoskeleton assists in enabling cardiomyocyte intracellular LPL transport.

2. Evaluate the process that controls cardiac LPL vesicular formation and secretion.
3. Resolve the intrinsic compensatory mechanisms that limit LPL derived FA under conditions of severe hyperlipidemia.

Figures

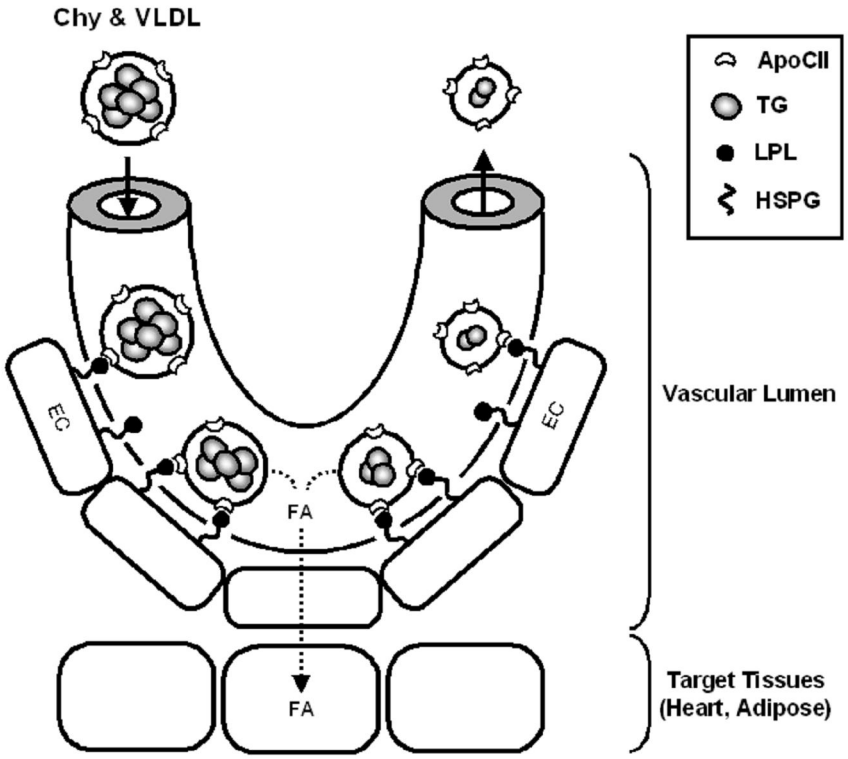

Fig. 1-1 Fatty acid (FA) provision to target tissues by lipoprotein lipase (LPL). Vascular endothelial-bound (to heparan sulfate proteoglycans, HSPGs) lipoprotein lipase (LPL) hydrolyzes circulating triglyceride-rich lipoproteins (chylomicrons, Chy; very low density lipoprotein, VLDL), to release fatty acids (FA). The apolipoprotein (Apo) CII on lipoproteins stimulates LPL activity, enhancing TG lipolysis and FA supply to target tissues. EC, endothelial cell.

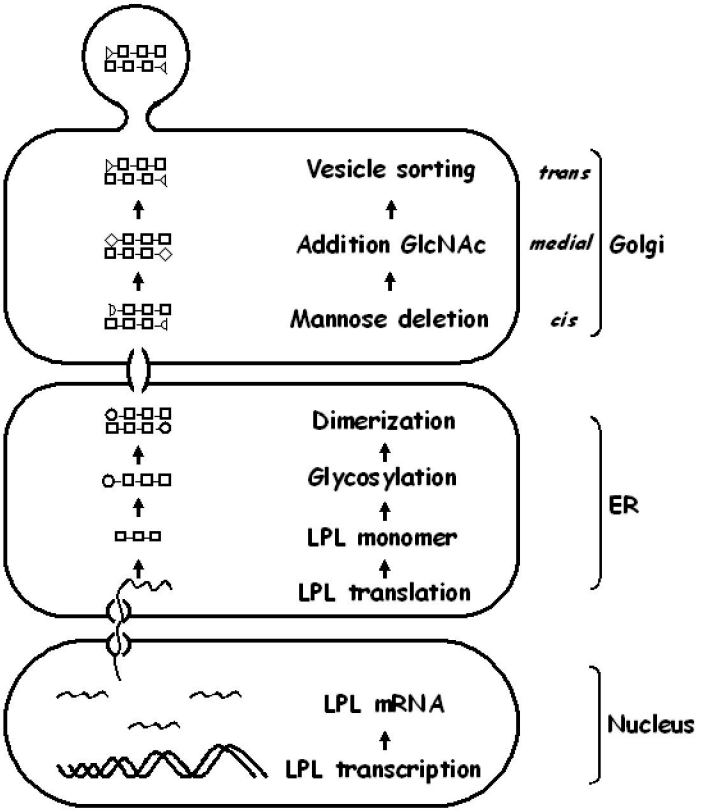

Fig. 1-2 LPL synthesis and processing. Following gene transcription, LPL mRNA is translated as inactive LPL proteins. The inactive monomer undergoes glycosylation, and several post-translational processes to be dimerized in the endoplasmic reticulum (ER). This dimerized LPL then moves to the Golgi for further processing. In the cis-Golgi, three mannoses are removed, whereas GlcNAc (N-acetylglucosamine) is added onto the LPL protein by transferase in the medial-Golgi. After additional processing in the trans-Golgi, the fully processed LPL is sorted in vesicles that are targeted either towards lysosomes (for degradation) or cell surface (for secretion).

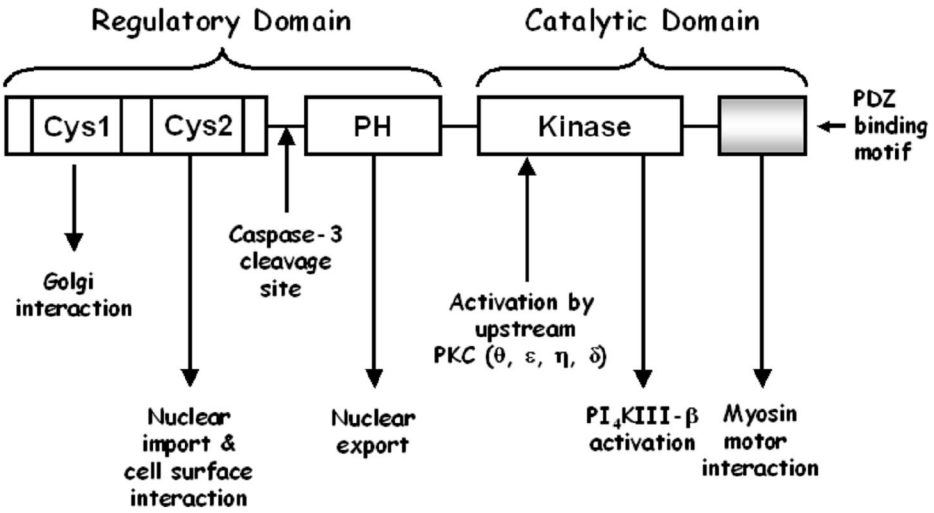

Fig. 1-3 PKD domains and functions. The N-terminus of PKD contains two cysteine-rich domains (Cys1 and Cys2), and a pleckstrin homology (PH) domain. The Cys1 has been shown to have a critical role in recruiting and binding PKD to Golgi, whereas Cys2 interacts with the cell surface and promotes its nuclear accumulation. The PH domain is responsible for nuclear export in addition to having an inhibitory effect on the catalytic domain. The C-terminal catalytic domain has several residues that can be phosphorylated, and these include Ser 744, Ser 748 and Ser 916. Phosphorylation of these residues by upstream PKCs leads to PKD activation. Once PKD is activated, its kinase domain initiates vesicle budding through interaction with phosphatidylinositol 4-kinase IIIβ (PI_4KIII-β) in trans-Golgi. In this situation, its PDZ-binding motif interacts with myosin motor allowing vesicle movement. There is a caspase-3 cleavage site present between cysteine-rich and PH domains.

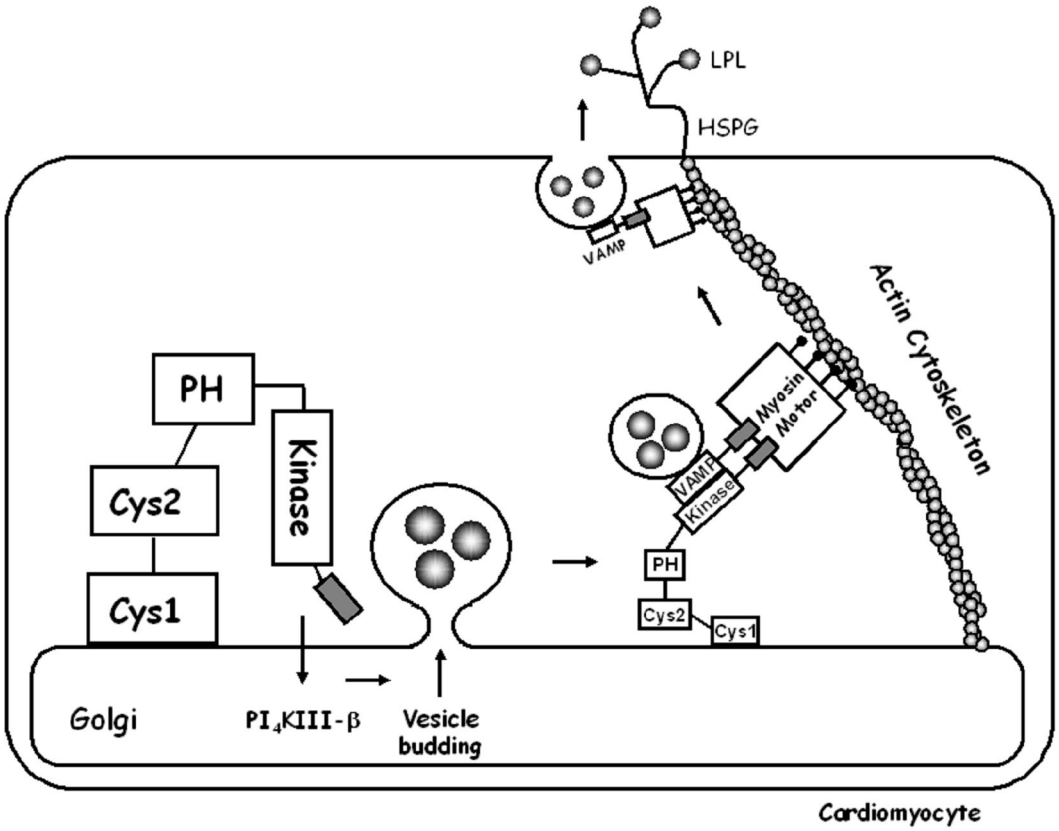

Fig. 1-4 PKD regulated formation of LPL vesicles and secretion. Once PKD is activated, it interacts with Golgi through its Cys1 domain to initiate LPL vesicle formation via stimulation of phosphatidylinositol 4-kinase IIIβ (PI_4KIII-β), a known enhancer of vesicle fission. Activated PKD also directly interacts with vesicle associated membrane protein (VAMP) and myosin motor; the complex can then move along the actin cytoskeleton, dock with the cell surface, and release LPL onto HSPG binding sites.

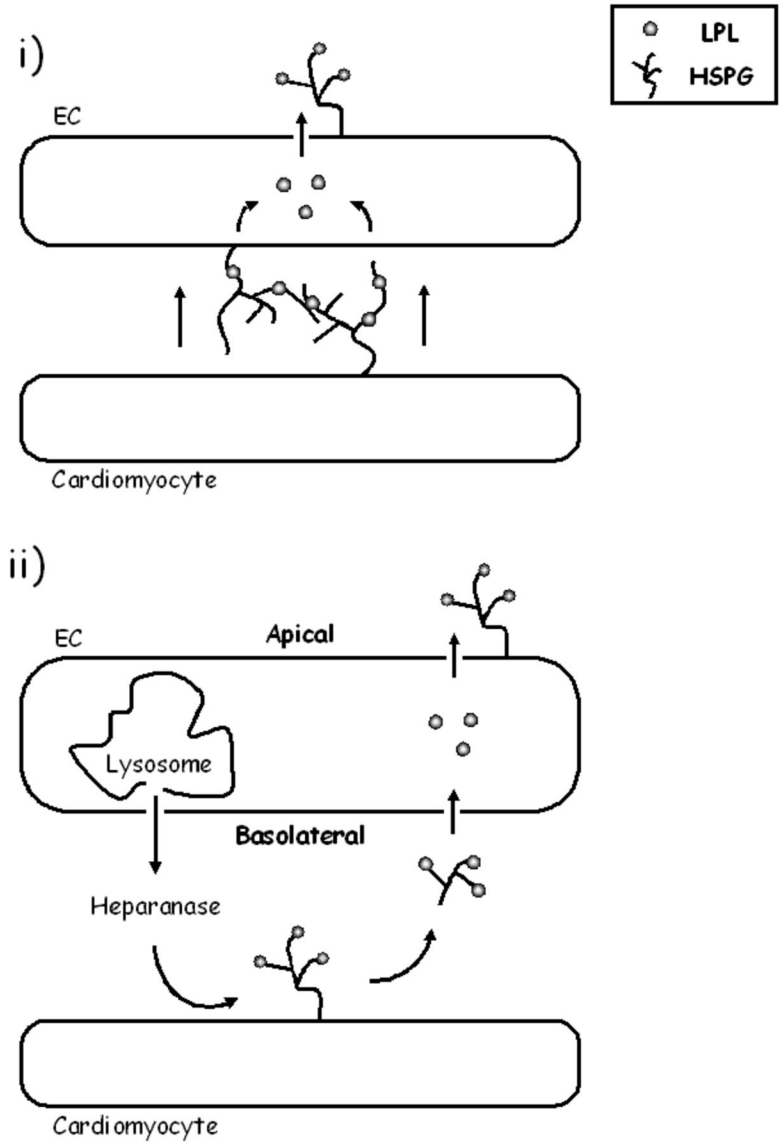

Fig. 1-5 Putative models for LPL mobilization from cardiomyocyte to vascular lumen. One proposed mechanism for LPL transfer is that the protein is moved along a continuous network of HSPG in the interstitial space that extends from the myocyte to endothelial cells (i). Another theory has implicated endothelial heparanase in this movement (ii). In the endothelial cell lysosomes, an active heparanase is stored in a stable form. Once it releases from the basolateral side of endothelial cells towards the cardiomyocyte, the enzyme can initiate cleavage of myocyte HSPG side chains. Following this, the oligosaccharide-bound LPL released into the interstitial space is then transported towards the apical side of endothelial cells to bind to luminal HSPG.

1.12. Bibliography

1. van der Vusse GJ, van Bilsen M, Glatz JF: Cardiac fatty acid uptake and transport in health and disease. *Cardiovasc Res* 45:279-293, 2000

2. van der Vusse GJ, de Groot MJ: Interrelationship between lactate and cardiac fatty acid metabolism. *Mol Cell Biochem* 116:11-17, 1992

3. Bassenge E, Wendt VE, Schollmeyer P, Bluemchen G, Gudbjarnason S, Bing RJ: Effect of Ketone Bodies on Cardiac Metabolism. *Am J Physiol* 208:162-168, 1965

4. Brownsey RW, Boone AN, Allard MF: Actions of insulin on the mammalian heart: metabolism, pathology and biochemical mechanisms. *Cardiovasc Res* 34:3-24, 1997

5. Kraegen EW, Sowden JA, Halstead MB, Clark PW, Rodnick KJ, Chisholm DJ, James DE: Glucose transporters and in vivo glucose uptake in skeletal and cardiac muscle: fasting, insulin stimulation and immunoisolation studies of GLUT1 and GLUT4. *Biochem J* 295 (Pt 1):287-293, 1993

6. Ciaraldi TP, Mudaliar S, Barzin A, Macievic JA, Edelman SV, Park KS, Henry RR: Skeletal muscle GLUT1 transporter protein expression and basal leg glucose uptake are reduced in type 2 diabetes. *J Clin Endocrinol Metab* 90:352-358, 2005

7. Ramm G, Slot JW, James DE, Stoorvogel W: Insulin recruits GLUT4 from specialized VAMP2-carrying vesicles as well as from the dynamic endosomal/trans-Golgi network in rat adipocytes. *Mol Biol Cell* 11:4079-4091, 2000

8. Till M, Kolter T, Eckel J: Molecular mechanisms of contraction-induced translocation of GLUT4 in isolated cardiomyocytes. *Am J Cardiol* 80:85A-89A, 1997

9. Bendjelid K, Canet E, Rayan E, Casali C, Revel D, Janier M: Role of glycolysis in the energy production for the non-mechanical myocardial work in isolated pig hearts. *Curr Med Res Opin* 19:51-58, 2003

10. Pulinilkunnil T, Rodrigues B: Cardiac lipoprotein lipase: metabolic basis for diabetic heart disease. *Cardiovasc Res* 69:329-340, 2006

11. Hamilton JA: Fatty acid transport: difficult or easy? *J Lipid Res* 39:467-481, 1998

12. Ring A, Pohl J, Volkl A, Stremmel W: Evidence for vesicles that mediate long-chain fatty acid uptake by human microvascular endothelial cells. *J Lipid Res* 43:2095-2104, 2002

13. Stremmel W: Fatty acid uptake by isolated rat heart myocytes represents a carrier-mediated transport process. *J Clin Invest* 81:844-852, 1988

14. Luiken JJ, Schaap FG, van Nieuwenhoven FA, van der Vusse GJ, Bonen A, Glatz JF: Cellular fatty acid transport in heart and skeletal muscle as facilitated by proteins. *Lipids* 34 Suppl:S169-175, 1999

15. Dutta-Roy AK: Cellular uptake of long-chain fatty acids: role of membrane-associated fatty-acid-binding/transport proteins. *Cell Mol Life Sci* 57:1360-1372, 2000

16. Blanchette-Mackie EJ, Masuno H, Dwyer NK, Olivecrona T, Scow RO: Lipoprotein lipase in myocytes and capillary endothelium of heart: immunocytochemical study. *Am J Physiol* 256:E818-828, 1989

17. Augustus AS, Kako Y, Yagyu H, Goldberg IJ: Routes of FA delivery to cardiac muscle: modulation of lipoprotein lipolysis alters uptake of TG-derived FA. *Am J Physiol Endocrinol Metab* 284:E331-339, 2003

18. Teusink B, Voshol PJ, Dahlmans VE, Rensen PC, Pijl H, Romijn JA, Havekes LM: Contribution of fatty acids released from lipolysis of plasma triglycerides to total plasma fatty acid flux and tissue-specific fatty acid uptake. *Diabetes* 52:614-620, 2003

19. Merkel M, Eckel RH, Goldberg IJ: Lipoprotein lipase: genetics, lipid uptake, and regulation. *J Lipid Res* 43:1997-2006, 2002

20. Ruge T, Neuger L, Sukonina V, Wu G, Barath S, Gupta J, Frankel B, Christophersen B, Nordstoga K, Olivecrona T, Olivecrona G: Lipoprotein lipase in the kidney: activity varies widely among animal species. *Am J Physiol Renal Physiol* 287:F1131-1139, 2004

21. Camps L, Reina M, Llobera M, Bengtsson-Olivecrona G, Olivecrona T, Vilaro S: Lipoprotein lipase in lungs, spleen, and liver: synthesis and distribution. *J Lipid Res* 32:1877-1888, 1991

22. Camps L, Reina M, Llobera M, Vilaro S, Olivecrona T: Lipoprotein lipase: cellular origin and functional distribution. *Am J Physiol* 258:C673-681, 1990

23. Sparkes RS, Zollman S, Klisak I, Kirchgessner TG, Komaromy MC, Mohandas T, Schotz MC, Lusis AJ: Human genes involved in lipolysis of plasma lipoproteins: mapping of loci for lipoprotein lipase to 8p22 and hepatic lipase to 15q21. *Genomics* 1:138-144, 1987

24. Previato L, Parrott CL, Santamarina-Fojo S, Brewer HB, Jr.: Transcriptional regulation of the human lipoprotein lipase gene in 3T3-L1 adipocytes. *J Biol Chem* 266:18958-18963, 1991

25. Braun JE, Severson DL: Regulation of the synthesis, processing and translocation of lipoprotein lipase. *Biochem J* 287 (Pt 2):337-347, 1992

26. Elbein AD: Glycosidase inhibitors: inhibitors of N-linked oligosaccharide processing. *Faseb J* 5:3055-3063, 1991

27. Vannier C, Ailhaud G: Biosynthesis of lipoprotein lipase in cultured mouse adipocytes. II. Processing, subunit assembly, and intracellular transport. *J Biol Chem* 264:13206-13216, 1989

28. Simsolo RB, Ong JM, Kern PA: Characterization of lipoprotein lipase activity, secretion, and degradation at different sites of post-translational processing in primary cultures of rat adipocytes. *J Lipid Res* 33:1777-1784, 1992

29. Busca R, Martinez M, Vilella E, Peinado J, Gelpi JL, Deeb S, Auwerx J, Reina M, Vilaro S: The carboxy-terminal region of human lipoprotein lipase is necessary for its exit from the endoplasmic reticulum. *J Lipid Res* 39:821-833, 1998

30. Ailhaud G: Cellular and secreted lipoprotein lipase revisited. *Clin Biochem* 23:343-347, 1990

31. Mead JR, Irvine SA, Ramji DP: Lipoprotein lipase: structure, function, regulation, and role in disease. *J Mol Med* 80:753-769, 2002

32. Hoogewerf AJ, Bensadoun A: Occurrence of sulfate in an asparagine-linked complex oligosaccharide of chicken adipose lipoprotein lipase. *J Biol Chem* 266:1048-1057, 1991

33. Rome LH, Hill DF: Lysosomal degradation of glycoproteins and glycosaminoglycans. Efflux and recycling of sulphate and N-acetylhexosamines. *Biochem J* 235:707-713, 1986

34. Cupp M, Bensadoun A, Melford K: Heparin decreases the degradation rate of lipoprotein lipase in adipocytes. *J Biol Chem* 262:6383-6388, 1987

35. Winchester B: Lysosomal metabolism of glycoproteins. *Glycobiology* 15:1R-15R, 2005

36. Stamnes M: Regulating the actin cytoskeleton during vesicular transport. *Curr Opin Cell Biol* 14:428-433, 2002

37. Manneville JB, Etienne-Manneville S, Skehel P, Carter T, Ogden D, Ferenczi M: Interaction of the actin cytoskeleton with microtubules regulates secretory organelle movement near the plasma membrane in human endothelial cells. *J Cell Sci* 116:3927-3938, 2003

38. Pulinilkunnil T, An D, Ghosh S, Qi D, Kewalramani G, Yuen G, Virk N, Abrahani A, Rodrigues B: Lysophosphatidic acid-mediated augmentation of cardiomyocyte lipoprotein lipase involves actin cytoskeleton reorganization. *Am J Physiol Heart Circ Physiol* 288:H2802-2810, 2005

39. Ewart HS, Severson DL: Insulin and dexamethasone stimulation of cardiac lipoprotein lipase activity involves the actin-based cytoskeleton. *Biochem J* 340 (Pt 2):485-490, 1999

40. Fath KR, Burgess DR: Golgi-derived vesicles from developing epithelial cells bind actin filaments and possess myosin-I as a cytoplasmically oriented peripheral membrane protein. *J Cell Biol* 120:117-127, 1993

41. Abe H, Obinata T: An actin-depolymerizing protein in embryonic chicken skeletal muscle: purification and characterization. *J Biochem* 106:172-180, 1989

42. Hotulainen P, Paunola E, Vartiainen MK, Lappalainen P: Actin-depolymerizing factor and cofilin-1 play overlapping roles in promoting rapid F-actin depolymerization in mammalian nonmuscle cells. *Mol Biol Cell* 16:649-664, 2005

43. Zhao R, Du L, Huang Y, Wu Y, Gunst SJ: Actin depolymerization factor/cofilin activation regulates actin polymerization and tension development in canine tracheal smooth muscle. *J Biol Chem* 283:36522-36531, 2008

44. Aufricht C, Ardito T, Thulin G, Kashgarian M, Siegel NJ, Van Why SK: Heat-shock protein 25 induction and redistribution during actin reorganization after renal ischemia. *Am J Physiol* 274:F215-222, 1998

45. Maciver SK, Hussey PJ: The ADF/cofilin family: actin-remodeling proteins. *Genome Biol* 3:reviews3007, 2002

46. Guay J, Lambert H, Gingras-Breton G, Lavoie JN, Huot J, Landry J: Regulation of actin filament dynamics by p38 map kinase-mediated phosphorylation of heat shock protein 27. *J Cell Sci* 110 (Pt 3):357-368, 1997

47. Pantaloni D, Hill TL, Carlier MF, Korn ED: A model for actin polymerization and the kinetic effects of ATP hydrolysis. *Proc Natl Acad Sci U S A* 82:7207-7211, 1985

48. An D, Kewalramani G, Qi D, Pulinilkunnil T, Ghosh S, Abrahani A, Wambolt R, Allard M, Innis SM, Rodrigues B: beta-Agonist stimulation produces changes in cardiac AMPK and coronary lumen LPL only during increased workload. *Am J Physiol Endocrinol Metab* 288:E1120-1127, 2005

49. An D, Pulinilkunnil T, Qi D, Ghosh S, Abrahani A, Rodrigues B: The metabolic "switch" AMPK regulates cardiac heparin-releasable lipoprotein lipase. *Am J Physiol Endocrinol Metab* 288:E246-253, 2005

50. Hayashi T, Hirshman MF, Fujii N, Habinowski SA, Witters LA, Goodyear LJ: Metabolic stress and altered glucose transport: activation of AMP-activated protein kinase as a unifying coupling mechanism. *Diabetes* 49:527-531, 2000

51. Lee YM, Lee JO, Jung JH, Kim JH, Park SH, Park JM, Kim EK, Suh PG, Kim HS: Retinoic acid leads to cytoskeletal rearrangement through AMPK-Rac1 and stimulates glucose uptake through AMPK-p38 MAPK in skeletal muscle cells. *J Biol Chem* 283:33969-33974, 2008

52. Li J, Miller EJ, Ninomiya-Tsuji J, Russell RR, 3rd, Young LH: AMP-activated protein kinase activates p38 mitogen-activated protein kinase by increasing recruitment of p38 MAPK to TAB1 in the ischemic heart. *Circ Res* 97:872-879, 2005

53. Davidson SM, Morange M: Hsp25 and the p38 MAPK pathway are involved in differentiation of cardiomyocytes. *Dev Biol* 218:146-160, 2000

54. Hardie DG, Scott JW, Pan DA, Hudson ER: Management of cellular energy by the AMP-activated protein kinase system. *FEBS Lett* 546:113-120, 2003

55. Carling D: The AMP-activated protein kinase cascade--a unifying system for energy control. *Trends Biochem Sci* 29:18-24, 2004

56. Stapleton D, Mitchelhill KI, Gao G, Widmer J, Michell BJ, Teh T, House CM, Fernandez CS, Cox T, Witters LA, Kemp BE: Mammalian AMP-activated protein kinase subfamily. *J Biol Chem* 271:611-614, 1996

57. Cheung PC, Salt IP, Davies SP, Hardie DG, Carling D: Characterization of AMP-activated protein kinase gamma-subunit isoforms and their role in AMP binding. *Biochem J* 346 Pt 3:659-669, 2000

58. Ahmad F, Arad M, Musi N, He H, Wolf C, Branco D, Perez-Atayde AR, Stapleton D, Bali D, Xing Y, Tian R, Goodyear LJ, Berul CI, Ingwall JS, Seidman CE, Seidman JG: Increased alpha2 subunit-associated AMPK activity and PRKAG2 cardiomyopathy. *Circulation* 112:3140-3148, 2005

59. Crute BE, Seefeld K, Gamble J, Kemp BE, Witters LA: Functional domains of the alpha1 catalytic subunit of the AMP-activated protein kinase. *J Biol Chem* 273:35347-35354, 1998

60. Woods A, Vertommen D, Neumann D, Turk R, Bayliss J, Schlattner U, Wallimann T, Carling D, Rider MH: Identification of phosphorylation sites in AMP-activated protein kinase (AMPK) for upstream AMPK kinases and study of their roles by site-directed mutagenesis. *J Biol Chem* 278:28434-28442, 2003

61. Hudson ER, Pan DA, James J, Lucocq JM, Hawley SA, Green KA, Baba O, Terashima T, Hardie DG: A novel domain in AMP-activated protein kinase causes glycogen storage bodies similar to those seen in hereditary cardiac arrhythmias. *Curr Biol* 13:861-866, 2003

62. Adams J, Chen ZP, Van Denderen BJ, Morton CJ, Parker MW, Witters LA, Stapleton D, Kemp BE: Intrasteric control of AMPK via the gamma1 subunit AMP allosteric regulatory site. *Protein Sci* 13:155-165, 2004

63. Towler MC, Hardie DG: AMP-activated protein kinase in metabolic control and insulin signaling. *Circ Res* 100:328-341, 2007

64. Shaw RJ, Kosmatka M, Bardeesy N, Hurley RL, Witters LA, DePinho RA, Cantley LC: The tumor suppressor LKB1 kinase directly activates AMP-activated kinase and regulates apoptosis in response to energy stress. *Proc Natl Acad Sci U S A* 101:3329-3335, 2004

65. Imai K, Inukai K, Ikegami Y, Awata T, Katayama S: LKB1, an upstream AMPK kinase, regulates glucose and lipid metabolism in cultured liver and muscle cells. *Biochem Biophys Res Commun* 351:595-601, 2006

66. Shackelford DB, Shaw RJ: The LKB1-AMPK pathway: metabolism and growth control in tumour suppression. *Nat Rev Cancer* 9:563-575, 2009

67. Steinberg GR: Role of the AMP-activated protein kinase in regulating fatty acid metabolism during exercise. *Appl Physiol Nutr Metab* 34:315-322, 2009

68. Bertrand L, Ginion A, Beauloye C, Hebert AD, Guigas B, Hue L, Vanoverschelde JL: AMPK activation restores the stimulation of glucose uptake in an in vitro model of insulin-resistant cardiomyocytes via the activation of protein kinase B. *Am J Physiol Heart Circ Physiol* 291:H239-250, 2006

69. Cuenda A, Rousseau S: p38 MAP-kinases pathway regulation, function and role in human diseases. *Biochim Biophys Acta* 1773:1358-1375, 2007

70. Cohen P: The search for physiological substrates of MAP and SAP kinases in mammalian cells. *Trends Cell Biol* 7:353-361, 1997

71. Enslen H, Brancho DM, Davis RJ: Molecular determinants that mediate selective activation of p38 MAP kinase isoforms. *Embo J* 19:1301-1311, 2000

72. Hu MC, Wang YP, Mikhail A, Qiu WR, Tan TH: Murine p38-delta mitogen-activated protein kinase, a developmentally regulated protein kinase that is activated by stress and proinflammatory cytokines. *J Biol Chem* 274:7095-7102, 1999

73. Li Z, Jiang Y, Ulevitch RJ, Han J: The primary structure of p38 gamma: a new member of p38 group of MAP kinases. *Biochem Biophys Res Commun* 228:334-340, 1996

74. Tanaka N, Kamanaka M, Enslen H, Dong C, Wysk M, Davis RJ, Flavell RA: Differential involvement of p38 mitogen-activated protein kinase kinases MKK3 and MKK6 in T-cell apoptosis. *EMBO Rep* 3:785-791, 2002

75. Winston BW, Chan ED, Johnson GL, Riches DW: Activation of p38mapk, MKK3, and MKK4 by TNF-alpha in mouse bone marrow-derived macrophages. *J Immunol* 159:4491-4497, 1997

76. Jacquet S, Zarrinpashneh E, Chavey A, Ginion A, Leclerc I, Viollet B, Rutter GA, Bertrand L, Marber MS: The relationship between p38 mitogen-activated protein kinase and AMP-activated protein kinase during myocardial ischemia. *Cardiovasc Res* 76:465-472, 2007

77. Okada T, Otani H, Wu Y, Kyoi S, Enoki C, Fujiwara H, Sumida T, Hattori R, Imamura H: Role of F-actin organization in p38 MAP kinase-mediated apoptosis and necrosis in neonatal rat cardiomyocytes subjected to simulated ischemia and reoxygenation. *Am J Physiol Heart Circ Physiol* 289:H2310-2318, 2005

78. Gaundar SS, Bradstock KF, Bendall LJ: p38MAPK inhibitors attenuate cytokine production by bone marrow stromal cells and reduce stroma-mediated proliferation of acute lymphoblastic leukemia cells. *Cell Cycle* 8:2975-2983, 2009

79. El Mchichi B, Hadji A, Vazquez A, Leca G: p38 MAPK and MSK1 mediate caspase-8 activation in manganese-induced mitochondria-dependent cell death. *Cell Death Differ* 14:1826-1836, 2007

80. Hollenbach E, Neumann M, Vieth M, Roessner A, Malfertheiner P, Naumann M: Inhibition of p38 MAP kinase- and RICK/NF-kappaB-signaling suppresses inflammatory bowel disease. *Faseb J* 18:1550-1552, 2004

81. Olson JM, Hallahan AR: p38 MAP kinase: a convergence point in cancer therapy. *Trends Mol Med* 10:125-129, 2004

82. Olzinski AR, McCafferty TA, Zhao SQ, Behm DJ, Eybye ME, Maniscalco K, Bentley R, Frazier KS, Milliner CM, Mirabile RC, Coatney RW, Willette RN: Hypertensive target organ damage is attenuated by a p38 MAPK inhibitor: role of systemic blood pressure and endothelial protection. *Cardiovasc Res* 66:170-178, 2005

83. Lim AK, Nikolic-Paterson DJ, Ma FY, Ozols E, Thomas MC, Flavell RA, Davis RJ, Tesch GH: Role of MKK3-p38 MAPK signalling in the development of type 2 diabetes and renal injury in obese db/db mice. *Diabetologia* 52:347-358, 2009

84. Ranganathan G, Kaakaji R, Kern PA: Role of protein kinase C in the translational regulation of lipoprotein lipase in adipocytes. *J Biol Chem* 274:9122-9127, 1999

85. Ranganathan G, Song W, Dean N, Monia B, Barger SW, Kern PA: Regulation of lipoprotein lipase by protein kinase C alpha in 3T3-F442A adipocytes. *J Biol Chem* 277:38669-38675, 2002

86. Ghanekar Y, Lowe M: Protein kinase D: activation for Golgi carrier formation. *Trends Cell Biol* 15:511-514, 2005

87. Ananthanarayanan B, Stahelin RV, Digman MA, Cho W: Activation mechanisms of conventional protein kinase C isoforms are determined by the ligand affinity and conformational flexibility of their C1 domains. *J Biol Chem* 278:46886-46894, 2003

88. Johannes FJ, Prestle J, Eis S, Oberhagemann P, Pfizenmaier K: PKCu is a novel, atypical member of the protein kinase C family. *J Biol Chem* 269:6140-6148, 1994

89. Rozengurt E, Rey O, Waldron RT: Protein kinase D signaling. *J Biol Chem* 280:13205-13208, 2005

90. Valverde AM, Sinnett-Smith J, Van Lint J, Rozengurt E: Molecular cloning and characterization of protein kinase D: a target for diacylglycerol and phorbol esters with a distinctive catalytic domain. *Proc Natl Acad Sci U S A* 91:8572-8576, 1994

91. Sturany S, Van Lint J, Muller F, Wilda M, Hameister H, Hocker M, Brey A, Gern U, Vandenheede J, Gress T, Adler G, Seufferlein T: Molecular cloning and characterization of the human protein kinase D2. A novel member of the protein kinase D family of serine threonine kinases. *J Biol Chem* 276:3310-3318, 2001

92. Hayashi A, Seki N, Hattori A, Kozuma S, Saito T: PKCnu, a new member of the protein kinase C family, composes a fourth subfamily with PKCmu. *Biochim Biophys Acta* 1450:99-106, 1999

93. Oster H, Abraham D, Leitges M: Expression of the protein kinase D (PKD) family during mouse embryogenesis. *Gene Expr Patterns* 6:400-408, 2006

94. Chauvet V, Qian F, Boute N, Cai Y, Phakdeekitacharoen B, Onuchic LF, Attie-Bitach T, Guicharnaud L, Devuyst O, Germino GG, Gubler MC: Expression of PKD1 and PKD2 transcripts and proteins in human embryo and during normal kidney development. *Am J Pathol* 160:973-983, 2002

95. Wang QJ: PKD at the crossroads of DAG and PKC signaling. *Trends Pharmacol Sci* 27:317-323, 2006

96. Iglesias T, Waldron RT, Rozengurt E: Identification of in vivo phosphorylation sites required for protein kinase D activation. *J Biol Chem* 273:27662-27667, 1998

97. Iglesias T, Rozengurt E: Protein kinase D activation by mutations within its pleckstrin homology domain. *J Biol Chem* 273:410-416, 1998

98. Hu Y, Liu Z, Ye K: Phosphoinositol lipids bind to phosphatidylinositol 3 (PI3)-kinase enhancer GTPase and mediate its stimulatory effect on PI3-kinase and Akt signalings. *Proc Natl Acad Sci U S A* 102:16853-16858, 2005

99. Stafford MJ, Watson SP, Pears CJ: PKD: a new protein kinase C-dependent pathway in platelets. *Blood* 101:1392-1399, 2003

100. Rybin VO, Guo J, Steinberg SF: Protein kinase D1 autophosphorylation via distinct mechanisms at Ser744/Ser748 and Ser916. *J Biol Chem* 284:2332-2343, 2009

101. Waldron RT, Rozengurt E: Protein kinase C phosphorylates protein kinase D activation loop Ser744 and Ser748 and releases autoinhibition by the pleckstrin homology domain. *J Biol Chem* 278:154-163, 2003

102. Sanchez-Ruiloba L, Cabrera-Poch N, Rodriguez-Martinez M, Lopez-Menendez C, Jean-Mairet RM, Higuero AM, Iglesias T: Protein kinase D intracellular localization and activity control kinase D-interacting substrate of 220-kDa traffic through a postsynaptic density-95/discs large/zonula occludens-1-binding motif. *J Biol Chem* 281:18888-18900, 2006

103. Iglesias T, Rozengurt E: Protein kinase D activation by deletion of its cysteine-rich motifs. *FEBS Lett* 454:53-56, 1999

104. Matthews SA, Rozengurt E, Cantrell D: Characterization of serine 916 as an in vivo autophosphorylation site for protein kinase D/Protein kinase Cmu. *J Biol Chem* 274:26543-26549, 1999

105. Carnegie GK, Smith FD, McConnachie G, Langeberg LK, Scott JD: AKAP-Lbc nucleates a protein kinase D activation scaffold. *Mol Cell* 15:889-899, 2004

106. Manni S, Mauban JH, Ward CW, Bond M: Phosphorylation of the cAMP-dependent protein kinase (PKA) regulatory subunit modulates PKA-AKAP interaction, substrate phosphorylation, and calcium signaling in cardiac cells. *J Biol Chem* 283:24145-24154, 2008

107. Kam Y, Exton JH: Role of phospholipase D in the activation of protein kinase D by lysophosphatidic acid. *Biochem Biophys Res Commun* 315:139-143, 2004

108. Chiu TT, Leung WY, Moyer MP, Strieter RM, Rozengurt E: Protein kinase D2 mediates lysophosphatidic acid-induced interleukin 8 production in nontransformed human colonic epithelial cells through NF-kappaB. *Am J Physiol Cell Physiol* 292:C767-777, 2007

109. Zugaza JL, Sinnett-Smith J, Van Lint J, Rozengurt E: Protein kinase D (PKD) activation in intact cells through a protein kinase C-dependent signal transduction pathway. *Embo J* 15:6220-6230, 1996

110. Rey O, Reeve JR, Jr., Zhukova E, Sinnett-Smith J, Rozengurt E: G protein-coupled receptor-mediated phosphorylation of the activation loop of protein kinase D: dependence on plasma membrane translocation and protein kinase Cepsilon. *J Biol Chem* 279:34361-34372, 2004

111. Doppler H, Storz P: A novel tyrosine phosphorylation site in protein kinase D contributes to oxidative stress-mediated activation. *J Biol Chem* 282:31873-31881, 2007

112. Endo K, Oki E, Biedermann V, Kojima H, Yoshida K, Johannes FJ, Kufe D, Datta R: Proteolytic cleavage and activation of protein kinase C [micro] by caspase-3 in the apoptotic response of cells to 1-beta -D-arabinofuranosylcytosine and other genotoxic agents. *J Biol Chem* 275:18476-18481, 2000

113. Rey O, Young SH, Cantrell D, Rozengurt E: Rapid protein kinase D translocation in response to G protein-coupled receptor activation. Dependence on protein kinase C. *J Biol Chem* 276:32616-32626, 2001

114. Rey O, Sinnett-Smith J, Zhukova E, Rozengurt E: Regulated nucleocytoplasmic transport of protein kinase D in response to G protein-coupled receptor activation. *J Biol Chem* 276:49228-49235, 2001

115. Rey O, Zhukova E, Sinnett-Smith J, Rozengurt E: Vasopressin-induced intracellular redistribution of protein kinase D in intestinal epithelial cells. *J Cell Physiol* 196:483-492, 2003

116. Rey O, Papazyan R, Waldron RT, Young SH, Lippincott-Schwartz J, Jacamo R, Rozengurt E: The nuclear import of protein kinase D3 requires its catalytic activity. *J Biol Chem* 281:5149-5157, 2006

117. Maeda Y, Beznoussenko GV, Van Lint J, Mironov AA, Malhotra V: Recruitment of protein kinase D to the trans-Golgi network via the first cysteine-rich domain. *Embo J* 20:5982-5990, 2001

118. Hurd C, Rozengurt E: Protein kinase D is sufficient to suppress EGF-induced c-Jun Ser 63 phosphorylation. *Biochem Biophys Res Commun* 282:404-408, 2001

119. Wong C, Jin ZG: Protein kinase C-dependent protein kinase D activation modulates ERK signal pathway and endothelial cell proliferation by vascular endothelial growth factor. *J Biol Chem* 280:33262-33269, 2005

120. Haworth RS, Cuello F, Herron TJ, Franzen G, Kentish JC, Gautel M, Avkiran M: Protein kinase D is a novel mediator of cardiac troponin I phosphorylation and regulates myofilament function. *Circ Res* 95:1091-1099, 2004

121. Fugmann T, Hausser A, Schoffler P, Schmid S, Pfizenmaier K, Olayioye MA: Regulation of secretory transport by protein kinase D-mediated phosphorylation of the ceramide transfer protein. *J Cell Biol* 178:15-22, 2007

122. Colligan PB, Relling DP, Ren J: Ceramide attenuates high glucose-induced cardiac contractile abnormalities in cultured adult rat ventricular myocytes. *Cell Mol Biol (Noisy-le-grand)* 48 Online Pub:OL251-257, 2002

123. Li J, O'Connor KL, Hellmich MR, Greeley GH, Jr., Townsend CM, Jr., Evers BM: The role of protein kinase D in neurotensin secretion mediated by protein kinase C-alpha/-delta and Rho/Rho kinase. *J Biol Chem* 279:28466-28474, 2004

124. Sumara G, Formentini I, Collins S, Sumara I, Windak R, Bodenmiller B, Ramracheya R, Caille D, Jiang H, Platt KA, Meda P, Aebersold R, Rorsman P, Ricci R: Regulation of PKD by the MAPK p38delta in insulin secretion and glucose homeostasis. *Cell* 136:235-248, 2009

125. Ha CH, Wang W, Jhun BS, Wong C, Hausser A, Pfizenmaier K, McKinsey TA, Olson EN, Jin ZG: Protein kinase D-dependent phosphorylation and nuclear export of histone deacetylase 5 mediates vascular endothelial growth factor-induced gene expression and angiogenesis. *J Biol Chem* 283:14590-14599, 2008

126. Grozinger CM, Schreiber SL: Regulation of histone deacetylase 4 and 5 and transcriptional activity by 14-3-3-dependent cellular localization. *Proc Natl Acad Sci U S A* 97:7835-7840, 2000

127. Iwamoto N, Abe-Dohmae S, Lu R, Yokoyama S: Involvement of protein kinase D in phosphorylation and increase of DNA binding of activator protein 2 alpha to downregulate ATP-binding cassette transporter A1. *Arterioscler Thromb Vasc Biol* 28:2282-2287, 2008

128. Iwamoto N, Abe-Dohmae S, Ayaori M, Tanaka N, Kusuhara M, Ohsuzu F, Yokoyama S: ATP-binding cassette transporter A1 gene transcription is downregulated by activator protein 2alpha. Doxazosin inhibits activator protein 2alpha and increases high-density lipoprotein biogenesis independent of alpha1-adrenoceptor blockade. *Circ Res* 101:156-165, 2007

129. Paolucci L, Rozengurt E: Protein kinase D in small cell lung cancer cells: rapid activation through protein kinase C. *Cancer Res* 59:572-577, 1999

130. Rey O, Rozengurt E: Protein kinase D interacts with Golgi via its cysteine-rich domain. *Biochem Biophys Res Commun* 287:21-26, 2001

131. Hausser A, Storz P, Martens S, Link G, Toker A, Pfizenmaier K: Protein kinase D regulates vesicular transport by phosphorylating and activating phosphatidylinositol-4 kinase IIIbeta at the Golgi complex. *Nat Cell Biol* 7:880-886, 2005

132. Nishikawa K, Toker A, Wong K, Marignani PA, Johannes FJ, Cantley LC: Association of protein kinase Cmu with type II phosphatidylinositol 4-kinase and type I phosphatidylinositol-4-phosphate 5-kinase. *J Biol Chem* 273:23126-23133, 1998

133. Barlowe C: COPII: a membrane coat that forms endoplasmic reticulum-derived vesicles. *FEBS Lett* 369:93-96, 1995

134. Wang Y, Wei JH, Bisel B, Tang D, Seemann J: Golgi cisternal unstacking stimulates COPI vesicle budding and protein transport. *PLoS One* 3:e1647, 2008

135. Carreno S, Engqvist-Goldstein AE, Zhang CX, McDonald KL, Drubin DG: Actin dynamics coupled to clathrin-coated vesicle formation at the trans-Golgi network. *J Cell Biol* 165:781-788, 2004

136. Orci L, Halban P, Amherdt M, Ravazzola M, Vassalli JD, Perrelet A: A clathrin-coated, Golgi-related compartment of the insulin secreting cell accumulates proinsulin in the presence of monensin. *Cell* 39:39-47, 1984

137. Bossard C, Bresson D, Polishchuk RS, Malhotra V: Dimeric PKD regulates membrane fission to form transport carriers at the TGN. *J Cell Biol* 179:1123-1131, 2007

138. Chamberlain LH, Gould GW: The vesicle- and target-SNARE proteins that mediate Glut4 vesicle fusion are localized in detergent-insoluble lipid rafts present on distinct intracellular membranes. *J Biol Chem* 277:49750-49754, 2002

139. Salem N, Faundez V, Horng JT, Kelly RB: A v-SNARE participates in synaptic vesicle formation mediated by the AP3 adaptor complex. *Nat Neurosci* 1:551-556, 1998

140. Lu G, Chen J, Espinoza LA, Garfield S, Toshiyuki S, Akiko H, Huppler A, Wang QJ: Protein kinase D 3 is localized in vesicular structures and interacts with vesicle-associated membrane protein 2. *Cell Signal* 19:867-879, 2007

141. DePina AS, Langford GM: Vesicle transport: the role of actin filaments and myosin motors. *Microsc Res Tech* 47:93-106, 1999

142. Karcher RL, Deacon SW, Gelfand VI: Motor-cargo interactions: the key to transport specificity. *Trends Cell Biol* 12:21-27, 2002

143. Furusawa T, Ikawa S, Yanai N, Obinata M: Isolation of a novel PDZ-containing myosin from hematopoietic supportive bone marrow stromal cell lines. *Biochem Biophys Res Commun* 270:67-75, 2000

144. Parthasarathy N, Goldberg IJ, Sivaram P, Mulloy B, Flory DM, Wagner WD: Oligosaccharide sequences of endothelial cell surface heparan sulfate proteoglycan with affinity for lipoprotein lipase. *J Biol Chem* 269:22391-22396, 1994

145. Saxena U, Klein MG, Goldberg IJ: Transport of lipoprotein lipase across endothelial cells. *Proc Natl Acad Sci U S A* 88:2254-2258, 1991

146. Scow RO, Blanchette-Mackie EJ: Endothelium, the dynamic interface in cardiac lipid transport. *Mol Cell Biochem* 116:181-191, 1992

147. Pillarisetti S, Paka L, Sasaki A, Vanni-Reyes T, Yin B, Parthasarathy N, Wagner WD, Goldberg IJ: Endothelial cell heparanase modulation of lipoprotein lipase activity. Evidence that heparan sulfate oligosaccharide is an extracellular chaperone. *J Biol Chem* 272:15753-15759, 1997

148. Cohen E, Atzmon R, Vlodavsky I, Ilan N: Heparanase processing by lysosomal/endosomal protein preparation. *FEBS Lett* 579:2334-2338, 2005

149. Vlodavsky I, Friedmann Y, Elkin M, Aingorn H, Atzmon R, Ishai-Michaeli R, Bitan M, Pappo O, Peretz T, Michal I, Spector L, Pecker I: Mammalian heparanase: gene cloning, expression and function in tumor progression and metastasis. *Nat Med* 5:793-802, 1999

150. Gingis-Velitski S, Zetser A, Kaplan V, Ben-Zaken O, Cohen E, Levy-Adam F, Bashenko Y, Flugelman MY, Vlodavsky I, Ilan N: Heparanase uptake is mediated by cell membrane heparan sulfate proteoglycans. *J Biol Chem* 279:44084-44092, 2004

151. Chen L, Sanderson RD: Heparanase regulates levels of syndecan-1 in the nucleus. *PLoS One* 4:e4947, 2009

152. Nobuhisa T, Naomoto Y, Okawa T, Takaoka M, Gunduz M, Motoki T, Nagatsuka H, Tsujigiwa H, Shirakawa Y, Yamatsuji T, Haisa M, Matsuoka J, Kurebayashi J, Nakajima M,

Taniguchi S, Sagara J, Dong J, Tanaka N: Translocation of heparanase into nucleus results in cell differentiation. *Cancer Sci* 98:535-540, 2007

153. Shafat I, Vlodavsky I, Ilan N: Characterization of mechanisms involved in secretion of active heparanase. *J Biol Chem* 281:23804-23811, 2006

154. Wang F, Kim MS, Puthanveetil P, Kewalramani G, Deppe S, Ghosh S, Abrahani A, Rodrigues B: Endothelial heparanase secretion after acute hypoinsulinemia is regulated by glucose and fatty acid. *Am J Physiol Heart Circ Physiol* 296:H1108-1116, 2009

155. Obunike JC, Lutz EP, Li Z, Paka L, Katopodis T, Strickland DK, Kozarsky KF, Pillarisetti S, Goldberg IJ: Transcytosis of lipoprotein lipase across cultured endothelial cells requires both heparan sulfate proteoglycans and the very low density lipoprotein receptor. *J Biol Chem* 276:8934-8941, 2001

156. Doolittle MH, Ben-Zeev O, Elovson J, Martin D, Kirchgessner TG: The response of lipoprotein lipase to feeding and fasting. Evidence for posttranslational regulation. *J Biol Chem* 265:4570-4577, 1990

157. Kersten S, Mandard S, Tan NS, Escher P, Metzger D, Chambon P, Gonzalez FJ, Desvergne B, Wahli W: Characterization of the fasting-induced adipose factor FIAF, a novel peroxisome proliferator-activated receptor target gene. *J Biol Chem* 275:28488-28493, 2000

158. Shan L, Yu XC, Liu Z, Hu Y, Sturgis LT, Miranda ML, Liu Q: The angiopoietin-like proteins ANGPTL3 and ANGPTL4 inhibit lipoprotein lipase activity through distinct mechanisms. *J Biol Chem* 284:1419-1424, 2009

159. Yamada T, Ozaki N, Kato Y, Miura Y, Oiso Y: Insulin downregulates angiopoietin-like protein 4 mRNA in 3T3-L1 adipocytes. *Biochem Biophys Res Commun* 347:1138-1144, 2006

160. Yu X, Burgess SC, Ge H, Wong KK, Nassem RH, Garry DJ, Sherry AD, Malloy CR, Berger JP, Li C: Inhibition of cardiac lipoprotein utilization by transgenic overexpression of Angptl4 in the heart. *Proc Natl Acad Sci U S A* 102:1767-1772, 2005

161. Sugden MC, Holness MJ, Howard RM: Changes in lipoprotein lipase activities in adipose tissue, heart and skeletal muscle during continuous or interrupted feeding. *Biochem J* 292 (Pt 1):113-119, 1993

162. Qi D, Pulinilkunnil T, An D, Ghosh S, Abrahani A, Pospisilik JA, Brownsey R, Wambolt R, Allard M, Rodrigues B: Single-dose dexamethasone induces whole-body insulin resistance and alters both cardiac fatty acid and carbohydrate metabolism. *Diabetes* 53:1790-1797, 2004

163. Jong MC, Rensen PC, Dahlmans VE, van der Boom H, van Berkel TJ, Havekes LM: Apolipoprotein C-III deficiency accelerates triglyceride hydrolysis by lipoprotein lipase in wild-type and apoE knockout mice. *J Lipid Res* 42:1578-1585, 2001

164. McIlhargey TL, Yang Y, Wong H, Hill JS: Identification of a lipoprotein lipase cofactor-binding site by chemical cross-linking and transfer of apolipoprotein C-II-responsive lipolysis from lipoprotein lipase to hepatic lipase. *J Biol Chem* 278:23027-23035, 2003

165. Saxena U, Witte LD, Goldberg IJ: Release of endothelial cell lipoprotein lipase by plasma lipoproteins and free fatty acids. *J Biol Chem* 264:4349-4355, 1989

166. Saxena U, Klein MG, Goldberg IJ: Metabolism of endothelial cell-bound lipoprotein lipase. Evidence for heparan sulfate proteoglycan-mediated internalization and recycling. *J Biol Chem* 265:12880-12886, 1990

167. Ponticos M, Lu QL, Morgan JE, Hardie DG, Partridge TA, Carling D: Dual regulation of the AMP-activated protein kinase provides a novel mechanism for the control of creatine kinase in skeletal muscle. *Embo J* 17:1688-1699, 1998

168. Liu Q, Docherty JC, Rendell JC, Clanachan AS, Lopaschuk GD: High levels of fatty acids delay the recovery of intracellular pH and cardiac efficiency in post-ischemic hearts by inhibiting glucose oxidation. *J Am Coll Cardiol* 39:718-725, 2002

169. Babaev VR, Fazio S, Gleaves LA, Carter KJ, Semenkovich CF, Linton MF: Macrophage lipoprotein lipase promotes foam cell formation and atherosclerosis in vivo. *J Clin Invest* 103:1697-1705, 1999

170. Kern PA: Potential role of TNFalpha and lipoprotein lipase as candidate genes for obesity. *J Nutr* 127:1917S-1922S, 1997

171. Julien P, Vohl MC, Gaudet D, Gagne C, Levesque G, Despres JP, Cadelis F, Brun LD, Nadeau A, Ven Murthy MR: Hyperinsulinemia and abdominal obesity affect the expression of hypertriglyceridemia in heterozygous familial lipoprotein lipase deficiency. *Diabetes* 46:2063-2068, 1997

172. Baggio G, Manzato E, Gabelli C, Fellin R, Martini S, Enzi GB, Verlato F, Baiocchi MR, Sprecher DL, Kashyap ML, et al.: Apolipoprotein C-II deficiency syndrome. Clinical features, lipoprotein characterization, lipase activity, and correction of hypertriglyceridemia after apolipoprotein C-II administration in two affected patients. *J Clin Invest* 77:520-527, 1986

173. Ito Y, Azrolan N, O'Connell A, Walsh A, Breslow JL: Hypertriglyceridemia as a result of human apo CIII gene expression in transgenic mice. *Science* 249:790-793, 1990

174. Sternowsky HJ, Gaertner U, Stahnke N, Kaukel E: Juvenile familial hypertriglyceridemia and growth retardation. Clinical and biochemical observations in three siblings. *Eur J Pediatr* 125:59-70, 1977

175. Renier G, Skamene E, DeSanctis JB, Radzioch D: High macrophage lipoprotein lipase expression and secretion are associated in inbred murine strains with susceptibility to atherosclerosis. *Arterioscler Thromb* 13:190-196, 1993

176. Medh JD, Bowen SL, Fry GL, Ruben S, Andracki M, Inoue I, Lalouel JM, Strickland DK, Chappell DA: Lipoprotein lipase binds to low density lipoprotein receptors and induces receptor-mediated catabolism of very low density lipoproteins in vitro. *J Biol Chem* 271:17073-17080, 1996

177. Semenkovich CF, Coleman T, Daugherty A: Effects of heterozygous lipoprotein lipase deficiency on diet-induced atherosclerosis in mice. *J Lipid Res* 39:1141-1151, 1998

178. Mead JR, Cryer A, Ramji DP: Lipoprotein lipase, a key role in atherosclerosis? *FEBS Lett* 462:1-6, 1999

179. Rauch U, Osende JI, Chesebro JH, Fuster V, Vorchheimer DA, Harris K, Harris P, Sandler DA, Fallon JT, Jayaraman S, Badimon JJ: Statins and cardiovascular diseases: the multiple effects of lipid-lowering therapy by statins. *Atherosclerosis* 153:181-189, 2000

180. Lteif AA, Mather KJ, Clark CM: Diabetes and heart disease an evidence-driven guide to risk factors management in diabetes. *Cardiol Rev* 11:262-274, 2003

181. Pulinilkunnil T, Qi D, Ghosh S, Cheung C, Yip P, Varghese J, Abrahani A, Brownsey R, Rodrigues B: Circulating triglyceride lipolysis facilitates lipoprotein lipase translocation from cardiomyocyte to myocardial endothelial lining. *Cardiovasc Res* 59:788-797, 2003

182. Rodrigues B, Cam MC, Jian K, Lim F, Sambandam N, Shepherd G: Differential effects of streptozotocin-induced diabetes on cardiac lipoprotein lipase activity. *Diabetes* 46:1346-1353, 1997

183. Borradaile NM, Schaffer JE: Lipotoxicity in the heart. *Curr Hypertens Rep* 7:412-417, 2005

184. Park TS, Hu Y, Noh HL, Drosatos K, Okajima K, Buchanan J, Tuinei J, Homma S, Jiang XC, Abel ED, Goldberg IJ: Ceramide is a cardiotoxin in lipotoxic cardiomyopathy. *J Lipid Res* 49:2101-2112, 2008

185. Sharma S, Adrogue JV, Golfman L, Uray I, Lemm J, Youker K, Noon GP, Frazier OH, Taegtmeyer H: Intramyocardial lipid accumulation in the failing human heart resembles the lipotoxic rat heart. *Faseb J* 18:1692-1700, 2004

186. Pulinilkunnil T, Abrahani A, Varghese J, Chan N, Tang I, Ghosh S, Kulpa J, Allard M, Brownsey R, Rodrigues B: Evidence for rapid "metabolic switching" through lipoprotein lipase occupation of endothelial-binding sites. *J Mol Cell Cardiol* 35:1093-1103, 2003

187. Pulinilkunnil T, An D, Yip P, Chan N, Qi D, Ghosh S, Abrahani A, Rodrigues B: Palmitoyl lysophosphatidylcholine mediated mobilization of LPL to the coronary luminal surface requires PKC activation. *J Mol Cell Cardiol* 37:931-938, 2004

2. Acute diabetes moderates trafficking of cardiac lipoprotein lipase through p38 MAPK dependent actin cytoskeleton organization[1]

2.1. Introduction

Heart disease is a leading cause of death in diabetic patients (1), with coronary vessel disease and atherosclerosis being primary reasons for the increased incidence of cardiovascular dysfunction (2). However, a predisposition to heart failure in patients with both Type 1 and Type 2 diabetes might also reflect the effects of underlying abnormalities in diastolic function that can be detected in asymptomatic patients with diabetes alone (3-5). These observations suggest a specific impairment of heart muscle, termed diabetic cardiomyopathy. As rodent models of chronic diabetes also display abnormalities in diastolic left ventricular function, with or without systolic left ventricular dysfunction (6), it can be proposed that the diabetic state can directly induce abnormalities in cardiac tissue independent of vascular defects. Several etiological factors have been put forward to explain the development of diabetic cardiomyopathy including an increased stiffness of the left ventricular wall associated with accumulation of connective tissue and insoluble collagen (7), and abnormalities of various proteins that regulate ion flux, specifically intracellular calcium (8). More recently, the view that diabetic cardiomyopathy could also occur as a consequence of metabolic alterations has been put forward (9).

During insulin resistance or diabetes, glucose utilization is compromised. This alteration, together with increased fatty acid (FA) supply, switches cardiac energy generation to utilization of FA. High FA uptake and metabolism not only augments accumulation of FA intermediates

[1]A version of this chapter has been published. **Kim, M.**, Kewalramani, G., Puthanveetil, P., Lee, V., Kumar, U., An, D., Abrahani, A, and Rodrigues, B. (2008) Acute diabetes moderates trafficking of cardiac lipoprotein lipase through p38 MAPK dependent actin cytoskeleton organization. **Diabetes** 57: 64-76.

and triglyceride (TG), but also increases oxygen demand and generation of reactive oxygen species, leading to cardiac damage. Interestingly, increasing FA uptake through overexpression of cardiac human lipoprotein lipase (LPL) (10) or fatty acid transport protein (11), or augmenting FA oxidation through overexpression of cardiac PPAR-α (12) or long-chain acyl CoA synthase (13), results in a cardiac phenotype resembles diabetic cardiomyopathy. Conversely, normalizing cardiac metabolism in diabetic animals reverses the development of cardiomyopathy (14). Taken together, these studies strongly support the role of altered metabolism in the development of diabetic cardiomyopathy.

LPL hydrolyzes triglyceride (TG) rich lipoproteins, thus regulating the supply of FA to meet the metabolic demands of different tissues. It is synthesized in myocytes and subsequently transported onto heparan sulfate proteoglycan (HSPG) binding sites on the myocyte cell surface (15). Through mechanisms that are not completely understood, LPL is then transported onto HSPG binding sites on the luminal surface of the capillary endothelium (16). At this location, the enzyme plays a crucial role in hydrolysis of TG rich lipoproteins to FA, which are transported to the heart and used either for energy production or for re-synthesis of TG. Recently, LPL-mediated hydrolysis of circulating TG was suggested to be the principal source of FA for cardiac utilization (17,18). In addition to its role as a lipolytic enzyme, LPL also mediates a non-catalytic bridging function that allows it to bind simultaneously to both lipoproteins and specific cell surface proteins, facilitating cellular uptake of lipoproteins (19).

AMP activated protein kinase (AMPK) plays a key role in the regulation of cardiac metabolism. Once activated, AMPK switches off energy consuming processes like protein synthesis, whereas ATP generating mechanisms, such as FA oxidation and glycolysis, are turned on (20). Additionally, results from our laboratory have demonstrated a strong correlation between activation of AMPK and increases in LPL activity (21). The objective of the present

study was to determine the mechanisms by which AMPK augments cardiac LPL. Our data demonstrates that stress kinases like AMPK and p38 mitogen-activated protein kinase (MAPK), through their control of heat shock protein (Hsp) and the actin cytoskeleton, act in unison to facilitate LPL translocation to the myocyte cell surface, and eventually to the coronary lumen. The ensuing alteration in cardiac FA metabolism could be translated into increased cardiovascular risk following diabetes.

2.2. Methods

2.2.1. Experimental animals

The investigation conforms to the guide for the care and use of laboratory animals published by the US National Institutes of Health and the University of British Columbia. Adult male Wistar rats (260-300 g) were obtained from the UBC Animal Care Unit and supplied with a standard laboratory diet (PMI Feeds, Richmond, VA), and water ad libitum. Diazoxide (DZ), a selective K^+_{ATP} channel opener, decreases insulin secretion and causes hyperglycemia (22,23). Although doses of 25 and 50 mg/kg increased plasma glucose, the extent and duration of hyperglycemia were not as substantial as that seen with 100 mg/kg, which caused a rapid decline in serum insulin within 1 h (23). DZ (100 mg/kg) was administered i.p., and animals were euthanized at various times. Subsequently, hearts were removed for measurement of coronary luminal LPL activity and Western blotting.

2.2.2. Plasma measurements

Control rats were injected with DZ at 10 AM (fed state). Following DZ, blood samples from the tail vein were collected over a period of 4 h, and blood glucose determined using a glucometer (AccuSoft) and glucose test strips (Accu-Chek Advantage, Roche). At varying intervals, blood was also acquired in heparinized glass capillary tubes. Blood samples were immediately centrifuged and plasma was collected and assayed. A diagnostic kit was used to measure non-esterified fatty acid (NEFA, Wako).

2.2.3. Isolated heart perfusion

Rats were anesthetized with 65 mg/kg sodium pentobarbital i.p., the thoracic cavity opened, and the heart carefully excised. Following cannulation of the aorta, hearts were secured by tying below the innominate artery and perfused retrogradely by the nonrecirculating Langendorff technique with Krebs-Henseleit buffer containing 10 mM glucose (pH 7.4). Perfusion fluid was

continuously gassed with 95% O_2/5% CO_2. The rate of coronary flow (7-8 ml/min) was controlled by a peristaltic pump (24).

2.2.4. LPL activity and gene and protein expression

To measure coronary endothelium-bound LPL, the perfusion solution was changed to buffer containing fatty acid free BSA (1%) and heparin (5 U/ml). This concentration of heparin can maximally release cardiac LPL from its HSPG binding sites. The coronary effluent (perfusate that drips down to the apex of the heart) was collected in timed fractions (10 sec) over 5 min, and assayed for LPL activity by measuring the hydrolysis of a [^{3}H] triolein substrate emulsion (25). Retrograde perfusion of whole hearts with heparin results in a discharge of LPL that is rapid (within 0.5 to 1 min; suggested to represent LPL located at or near the endothelial cell surface) followed by a prolonged slow release (that is considered to originate from the myocyte cell surface) (24). As we were primarily concerned with examining regulation of LPL at coronary lumen, only peak LPL activities are illustrated. LPL activity is expressed as nanomoles oleate released per hour per milliliter. LPL gene expression was measured using RT-PCR (26), and protein expression was determined using the 5D2 monoclonal mouse anti-bovine LPL (generously provided by Dr. J. Brunzell, University of Washington, Seattle, WA) ([27; 28]).

2.2.5. Western blotting

Western blot was carried out as described previously (21). Briefly, ventricles (50 mg) or plated myocytes (0.4 x 10^6) were homogenized in ice-cold lysis buffer. After centrifugation at 5,000 g for 20 min, the protein content of the supernatant was quantified using a Bradford protein assay. Samples were diluted, boiled with sample loading dye, and 50 μg used in SDS-polyacrylamide gel electrophoresis. After blotting, membranes were blocked in 5% skim milk in Tris-buffered saline containing 0.1% Tween-20. Membranes were incubated with rabbit AMPK-α, phospho-

AMPK (Thr-172), p38 MAPK, phospho-p38 MAPK (Thr180/Tyr182), Hsp25, and phospho-Hsp25 (S86) antibodies, and subsequently with secondary goat anti-rabbit HRP-conjugated antibody. Reaction products were visualized using an ECL® detection kit, and quantified by densitometry.

2.2.6. Isolated cardiac myocytes

Ventricular calcium-tolerant myocytes were prepared by a previously described procedure (23,28). Briefly, myocytes were made calcium-tolerant by successive exposure to increasing concentrations of calcium. Our method of isolation yields a highly enriched population of calcium-tolerant myocardial cells that are rod-shaped in the presence of 1 mM Ca^{2+} with clear cross striations. Intolerant cells are intact but hypercontract into vesiculated spheres. Yield of myocytes (cell number, ~4.8 x 10^6) was determined microscopically using an improved Neubauer haemocytometer. Myocyte viability (generally between 75-85%) was assessed as the percentage of elongated cells with clear cross striations that excluded 0.2% trypan blue. To examine the influence 5-aminoimidazole-4-carboxamide-1-ß -D-ribofuranoside (AICAR, an AMPK activator) and the serine protease thrombin (to activate p38 MAPK) on LPL activity, cardiomyocytes were plated on laminin-coated 6-well culture plates (to a density of 200,000 cells/well). Cells were maintained using Media-199, and incubated at 37°C under an atmosphere of 95% O_2/5% CO_2 for 16 hours. Subsequently, and where indicated, AICAR (2 mM) or thrombin (0.05 U/ml) was added to the culture medium. Following the indicated times, myocyte basal LPL activity released into the medium was measured. To release surface-bound LPL activity, heparin (8 U/mL; 1 min) was added to the culture plates, aliquots of cell medium removed, separated by centrifugation, and assayed for LPL activity. In separate experiments, following incubation of plated myocytes (0.4 x 10^6 cells in a 60 x 15 mm tissue culture dish) with AICAR or thrombin, myocyte cell lysates were also used for Western blotting. In addition,

myocytes were: a) pre-incubated with a p38 MAPK inhibitor (SB202190, 20 μM) for 60 min prior to addition of either AICAR or thrombin (at the indicated times) and LPL activity and phospho-Hsp25 determined, or b) incubated with 0.5-1.5 mM albumin bound palmitic acid (1:2) for 15 mins prior to Western blotting for AMPK.

2.2.7. Nuclear localization of p38 MAPK

Following DZ, heart tissue was homogenized whereas after incubation of myocytes with thrombin, cells were scraped and washed twice with 0.5 ml PBS. Subsequently, samples were lysed in ice-cold buffer A (10 mM HEPES pH 7.9, 10 mM KCl, 0.1 mM EDTA, 0.1 mM EGTA 1 mM DTT, 0.5 mM PMSF and 0.5 % NP40) for 15 min. After centrifugation (13,000 rpm, 3 min, 4°C), the supernatant (cytosolic fraction) was separated, and the pellet vigorously vortexed with buffer B (20 mM HEPES pH 7.9, 0.42 M NaCl, 1 mM EDTA, 1 mM EGTA, 1 mM DTT, 1 mM PMSF) for 10 min. Following centrifugation (13,000 rpm, 10 min, 4°C), the supernatant (nuclear fraction) was quantified using a Bradford protein assay, and used for Western blotting to determine nuclear localization of p38 MAPK. Using an antibody against Histone H3 as a nuclear marker, we show good purity of nuclear fractions (data not shown).

2.2.8. Filamentous (F) and globular (G) actin

F-actin/G-actin ratio in the whole heart was determined using an in vivo assay kit. Briefly, hearts from control and DZ animals were isolated and lysed. Lysates were homogenized and centrifuged at 2000 rpm for 5 min. Total actin content of the supernatant was centrifuged at 100,000 g for 1 hr at 37°C to isolate F-actin (pellet) and G-actin (supernatant). The pellets were re-suspended to same volume as the G-actin fraction using ice-cold Milli-Q water plus 10 μM cytochalasin D, and left on ice for 1 hr to dissociate F-actin. The ratio of F-actin/G-actin was determined using western blotting and densitometry.

F-actin and G-actin was also determined in isolated cardiomyocytes using immunofluorescence. Briefly, myocytes were plated on laminin coated cover glass slides and rinsed with PBS. Following incubation with thrombin or SB202190 at the indicated times, myocytes were fixed for 10 min with 4% paraformaldehyde in PBS, permeabilized with 0.1% Triton X-100 in PBS for 3 min, treated with PBS containing 1% BSA for 20 minutes, and finally rinsed with PBS. Cells were double stained with DNAaseI AlexaFluor®594 and Rhodamine®488 Phalloidin to colocalize monomeric globular actin (red, G actin), and polymerized filamentous actin (green, F actin) (29). The unbound fluorescent probe was rinsed with PBS buffer and slides were visualized and photographed by using a Leica fluorescent microscope (Wetzlar, Postfach, Germany). The effects of AICAR in myocytes were also determined in the presence or absence of 1 μM cytochalasin D (CTD; an actin polymerization inhibitor) (30).

2.2.9. Silencing of p38 MAPK by siRNA

SiRNA transfection of p38 MAPK in cardiomyocytes was carried out using a kit from Santa Cruz. Briefly, in 6-well culture plates, 0.1 x 10^6 cells were plated and subsequently exposed to the siRNA (or scrambled, Scr) solution for 8h at 37°C in a CO_2 incubator. Following this, the media was changed to Media 199 and the cells incubated for another 18h. Subsequently, AICAR (2 mM) was added to the culture medium for 2h, and LPL (released by heparin), p38 MAPK and Hsp25 (using Western blotting) were determined.

2.2.10. Materials

[^{3}H]triolein was purchased from Amersham Canada. Heparin sodium injection (Hapalean; 1000 USP U/ml) was obtained from Organon Teknika. The F-actin/G-actin in vivo assay kit was obtained from Cytoskeleton Inc., Denver, CO. Total AMPK-α, Phospho-AMPK-α, p38 MAPK,

phospho-p38 MAPK, GAPDH, and Histone H3 antibodies were obtained from Cell Signaling (Danvers, MA). Hsp25 and phospho-Hsp25 antibodies were obtained from GeneTex®, Inc. (San Antonio, TX). SB202190 was purchased from Sigma-Aldrich. ECL® detection kit was obtained from Amersham. A diagnostic kit was used to measure non-esterified fatty acid (NEFA, Wako). All other chemicals were obtained from Sigma Chemical.

2.2.11 Statistical analysis

Values are means ± SE. Wherever appropriate, one-way ANOVA followed by the Bonferroni test was used to determine differences between group mean values. The level of statistical significance was set at $P < 0.05$.

2.3. Results

2.3.1. Acute diabetes increases LPL at the vascular lumen

Following DZ, blood glucose levels increased, and were significantly higher at 1 and 4 h after administration (Fig. 2-1A). Another characteristic feature associated with hyperglycemia, such as polydipsia, was also observed in DZ treated animals. Retrograde perfusion of hearts with heparin resulted in release of LPL into the coronary perfusate. Compared to control rat hearts, there was a substantial increase in LPL activity (~400%, Fig. 2-1B) at the vascular lumen following 4 h of DZ. This change in LPL activity was independent of shifts in mRNA (data not shown), suggesting a posttranscriptional increase in myocyte LPL. In addition, as no change in whole heart LPL protein was observed (data not shown), it is likely that the increase in LPL activity at the coronary lumen is simply due to transport of enzyme from myocytes to the endothelial cell. We have previously reported that control of LPL by DZ is dependent on its lowering of insulin rather than its direct effects on the heart or blood pressure (23).

2.3.2. Influence of fatty acids on cardiac AMPK phosphorylation

Previous studies from our lab have reported significantly higher AMPK phosphorylation in hearts from moderately diabetic STZ animals (31). In the present study, following DZ, an approximately 6-fold increase of cardiac AMPK phosphorylation was observed after 15 min (Fig. 2-2A). With time, despite persistence of hyperglycemia, AMPK phosphorylation in hearts from DZ treated animals declined, and reached basal levels within 4 h (Fig. 2-2A). As AMPK activation is prevented in severe STZ diabetes with its attendant enlargement of plasma and heart lipids (31), we measured changes in plasma FA to resolve whether a relationship exists between AMPK and FA in DZ treated animals. Interestingly, with time, the reduction in AMPK activation corresponded to a significant and rapid increase of FA that peaked at 60 min, and remained high until 4 h (Fig. 2-2B). When control myocytes were incubated with appropriate

concentrations of palmitic acid, concentrations that varied from 0.5-0.8 mM activated cardiac AMPK (Fig. 2-2C). However, with high concentrations of palmitic acid (that resembled the peak circulating concentrations seen with DZ), activation of AMPK was absent (Fig. 2-2C), suggesting that *in vivo* and *in vitro*, FA has dual effects on AMPK activation.

2.3.3. Diazoxide stimulates cardiac actin polymerization

P38 MAPK, a downstream target of AMPK (32), is suggested to regulate actin polymerization through its phosphorylation of heat shock protein 25. In turn, the actin cytoskeleton has been implicated in managing myocyte LPL secretion (33). Estimation of cardiac cytosolic p38 MAPK phosphorylation showed a similar pattern to that seen with activation of AMPK; rapid activation followed by a decline to control levels within 4 h (Fig. 2-3A). Once phosphorylated, p38 MAPK relocates to the nucleus (34). Separation of the nuclear fraction revealed that concurrent to the decline in cytosolic p38 MAPK phosphorylation, nuclear p38 MAPK phosphorylation increased (Fig. 2-3A, inset). Phosphorylation of Hsp25 also intensified (Fig. 2-3B). However, this increase was time dependent, reaching a maximum around 60 min and remaining elevated for the next 3 h. To determine whether Hsp25 phosphorylation elicits F-actin polymerization, we quantitated F-actin and G-actin cellular fractions using Western blot. In the resting cardiomyocyte, the proportion of polymerized F-actin is consistently higher than G-actin (90:10), and is predominantly localized along the cell periphery. Additionally, an increase in F-to-G actin ratio indicates actin polymerization. DZ increased the F/G actin ratio (Fig. 2-3C). Interestingly, the increase in F-actin polymerization closely mirrored the enlargement of LPL activity at 4 h after DZ (Fig. 2-1B).

2.3.4. Promotion of AMPK phosphorylation in isolated control myocytes activates p38 MAPK and Hsp25 and recruits LPL to the cardiomyocyte cell surface

To directly turn on AMPK, control myocytes were incubated for different times and with varying concentrations of AICAR. AICAR up to 1 mM was incapable of phosphorylating cardiac AMPK (data not shown). Interestingly, increasing the concentration to 2 mM activated AMPK phosphorylation in a pattern similar to that seen with acute diabetes; rapid activation followed by a decline to control levels with time (Fig. 2-4A). Comparable to acute diabetes induced with DZ, the activation of AMPK was temporally related to phosphorylation of p38 MAPK (Fig. 2-4B), and subsequently Hsp25 (Fig. 2-4C). We evaluated whether AICAR can augment LPL in myocytes, and Table 2-1 illustrates both basal and heparin releasable LPL activity. Incubation of myocytes with AICAR had no effect on basal LPL activity. Interestingly, 2 mM AICAR appreciably enhanced heparin releasable activity in the medium. This increase occurred in the absence of any change in LPL mRNA or protein in cardiomyocyte lysates (data not shown).

We hypothesized that inhibition of Hsp25 phosphorylation should decrease cardiomyocyte LPL activity. In the absence of specific inhibitors of Hsp25, we used SB202190, an inhibitor of p38 MAPK. Incubation of control myocytes for 1 hour with SB202190 decreased Hsp25 phosphorylation that is produced by AICAR (Fig. 2-5A). More importantly, the robust increase in heparin-releasable LPL activity induced by AICAR was also reduced by pre-incubation of myocytes with SB202190 (Fig. 2-5B). To investigate the involvement of the actin cytoskeleton in AICAR-mediated augmentation of myocyte LPL, myocytes were pretreated with an actin polymerization inhibitor, CTD, before incubation with AICAR. CTD reduced the effect of AICAR to increase myocyte HR-LPL without any effect on basal activity (control-3417 ± 181; AICAR-5305 ± 223; AICAR+CTD-2163 ± 178, $nmol \cdot h^{-1} \cdot 10^{-6}$ cells, $P<0.05$).

2.3.5. Directly increasing p38 MAPK activity also enlarges the cardiomyocyte cell surface LPL pool

To activate p38 MAPK in the absence of AMPK phosphorylation, we used thrombin. As predicted, control myocytes in the presence of the serine protease thrombin did not display any change in AMPK phosphorylation (Fig. 2-6A, inset). Nevertheless, thrombin rapidly (within 5 min) phosphorylated cytosolic p38 MAPK, which was followed by a decline to control levels within 30 min. Comparable to diabetes, the decline in cytosolic p38 MAPK phosphorylation corresponded to an activation of nuclear p38 MAPK (Fig. 2-6B), Hsp25 phosphorylation (Fig. 2-6C), F-actin polymerization (Fig. 2-8), and enhanced heparin releasable activity (Fig. 2-7B). Pre-incubation of control myocytes for 1 hour with SB202190 prevented all of these effects induced by thrombin (Fig. 2-7 and 2-8).

2.3.6. Silencing of p38 MAPK prevents cardiomyocyte LPL recruitment observed with AICAR

To confirm the relationship between p38 MAPK and LPL, we used short interfering RNA to silence p38 MAPK expression in isolated cardiomyocytes. We first validated successful p38 MAPK inhibition using Western blotting (Fig. 2-9, inset). Interestingly, in myocytes in which p38 MAPK was silenced, heparin releasable LPL activity was reduced (control+heparin-2308 ± 150; p38 MAPK silenced control+heparin-1142 ± 167, $nmol \cdot h^{-1} \cdot 10^{-6}$ cells, $P<0.05$). Cardiomyocytes were next exposed to AICAR and Hsp25 and LPL activity determined. In myocytes in which p38 MAPK was silenced, AICAR had no influence on total p38 MAPK which remained low (Fig. 2-9A) and was unable to phosphorylate Hsp25 (Fig. 2-9B) or increase LPL activity (Fig. 2-9C).

2.4. Discussion

The major source of FA for myocardial energy utilization is LPL mediated hydrolysis of TG-rich lipoproteins at the vascular endothelium (17). Despite this essential role of LPL at the coronary luminal surface, endothelial cells do not manufacture LPL. In the heart, the enzyme is synthesized in the underlying myocytes (35) before it is translocated to the luminal side of the coronary vessel wall with the help of heparan sulfate oligosaccharides acting as extracellular chaperones (16;36). Within the myocyte, we (30) and others (33) have reported actin cytoskeleton reorganization as an important means by which LPL is secreted onto plasma membrane HSPG binding sites. In this study, for the first time, we demonstrate that following diabetes, it is the phosphorylation of AMPK, p38 MAPK, and Hsp25 that causes actin cytoskeleton rearrangement to facilitate LPL translocation to the myocyte cell surface, and eventually to the coronary lumen.

AMPK is the switch that regulates cellular energy metabolism (37). Changes in intracellular AMP/ATP levels promote Threonine (Thr^{172}) phosphorylation and activation of AMPK, an important regulator of both carbohydrate and lipid metabolism (38,39). Thus, in heart and skeletal muscle, phosphorylated AMPK stimulates glucose uptake by inducing GLUT4 recruitment to the plasma membrane (40,41) and subsequent glycolysis through activation of 6-phosphofructo-2-kinase (42). AMPK control of FA utilization includes its effect on FA delivery to cardiomyocytes through its regulation of CD36 (43), and its role in facilitating FA oxidation through its effect on acetyl-CoA carboxylase (ACC) (44). Recently, we have also demonstrated that following AMPK activation after overnight fasting (with its attendant hypoinsulinemia), heparin-releasable LPL activity is amplified providing an additional mechanism whereby cellular energy is regulated (21). In the present study, we report that acute diabetes increases cardiac LPL activity within four hours. This augmentation in LPL activity was preceded by a rapid and

intense phosphorylation in AMPK, that was not sustainable, and declined to control levels at 4 hours. The early increase in AMPK may well be a product of either metabolic stress associated with a decrease in insulin, or a direct activation by circulating FFA. Interestingly, in studies using L6 skeletal muscle, FA's have been demonstrated to allosterically activate AMPK without changing energy charge (45). Despite the prevailing hyperglycemia following increasing durations of DZ, the decrease of AMPK activation to control levels is likely a consequence of the excessive amount of both circulating and LPL derived FA. This idea was strengthened by our experiment using isolated myocytes incubated with high concentrations of palmitate. In addition, moderate diabetes significantly increases cardiac AMPK and ACC phosphorylation, whereas in severe diabetes, with the addition of augmented plasma and heart lipids, AMPK activation is prevented (31). Recently, high FA or TG, through their formation of ceramide, has been shown to activate protein phosphatase 2A leading to dephosphorylation of AMPK (46).

Given the observation that when LPL activity was the highest, AMPK phosphorylation had returned to normal, we considered the possibility that the early activation of AMPK may have turned on other downstream signals. One downstream target of AMPK is p38 MAPK, and there was coincident activation of both AMPK and p38 MAPK following injection of DZ. Other studies have demonstrated that AMPK activates p38 MAPK through its interaction with transforming growth factor-β-activated protein kinase 1-binding protein 1 (32). Cytosolic activation of p38 MAPK results in its transfer to the nucleus, and gene activation through a number of transcription factors (47). In the nucleus, p38 MAPK can also activate MAPKAP kinase 2, which is then exported to phosphorylate Hsp25. Our studies in the heart confirmed that cytosolic activation of p38 MAPK was followed by its nuclear translocation. More importantly, with increasing duration of hyperglycemia, phosphorylation of Hsp25 progressively increased. Hsp25 is known to inhibit actin polymerization, and its phosphorylation results in a decline of

this inhibitory function (48). In this setting, actin monomers are released from the phosphorylated Hsp25 to self-associate to form fibrillar actin. Since the increase in myocyte LPL activity at 4 hours corresponded to an enlargement in the F-actin/G-actin ratio, our data suggest that AMPK and p38 MAPK, through their control of Hsp25 and the actin cytoskeleton, act in unison to facilitate LPL translocation to the myocyte cell surface.

To eliminate the possibility that the above changes are: a) an outcome of a direct cardio toxic effect of DZ, and b) a result of the myriad metabolic and hormonal changes that arise during diabetes, we used compounds to directly stimulate AMPK and p38 MAPK. AICAR is a cell permeable activator of AMPK (49). In neonatal myocytes, 0.5-1 mM AICAR is required to stimulate AMPK activity (50), whereas a concentration of up to 2 mM is essential for AMPK phosphorylation in adult myocytes (51). In the present study, 2 mM AICAR activated AMPK in a manner comparable to that seen with DZ. Prompt activation followed by a reduction to control levels. At present, the mechanism for this decrease in cardiomyocyte AMPK phosphorylation with time is unknown (given the absence of FA in the myocyte incubation medium). An increase in energy charge due to amplification in glucose uptake, and the limited demand for energy in these non-beating quiescent myocytes are potential explanations. Similar to DZ, there was a close relationship between AMPK activation, p38 MAPK and Hsp25 phosphorylation, and the increase in cardiomyocyte heparin releasable LPL activity after exposure to AICAR. A different approach used thrombin to activate p38 MAPK. It should be noted that the more traditional methods to activate p38 MAPK includes sorbitol and anisomycin; however, sorbitol is also known to activate AMPK (52), whereas anisomycin is shown to cause insulin resistance (53). Thrombin, without affecting AMPK phosphorylation, had a robust effect to provoke cardiomyocyte p38 MAPK, likely through PAR-4 receptor and c-Src tyrosine kinase activation (54). More importantly, p38 MAPK phosphorylation was followed by nuclear translocation,

phosphorylation of Hsp25, actin cytoskeleton reorganization and an increase in cell surface LPL activity. As the p38 MAPK inhibitor SB202190 and siRNA mediated inhibition of p38 MAPK blocked the effects of thrombin and AICAR respectively on Hsp25 and LPL activity, our data suggest that F-actin polymerization produced by activation of p38 MAPK is an important means by which vesicle transport of LPL is made possible.

In summary, we propose that in addition to its direct role in promoting FA oxidation, AMPK recruitment of LPL to the cardiomyocyte cell surface could represent an immediate compensatory response by the heart to guarantee FA supply when glucose utilization is compromised. The mechanism underlying this process embraces p38 MAPK activation, and an increase in actin cytoskeleton polymerization (Fig. 2-10). Interestingly, the actin cytoskeleton also plays a key role in promoting insulin-induced GLUT 4 translocation. At present, the process of LPL vesicular movement along the actin filament network is unknown, and merits further investigation. Understanding this mechanism could lead to strategies that overcome contractile dysfunction following diabetes. This is because changes in cardiac LPL activity may predispose people with diabetes to premature death from cardiac disease. In mice, both cardiac specific overexpression [with its attendant lipid deposition, muscle fiber degeneration, and proliferation of mitochondria and peroxisomes, (55)], and knockout [associated with cardiac interstitial and perivascular fibrosis (56)] of LPL have been implicated in cardiac dysfunction.

2.5. Limitations of study

One limitation of this study is the lack of mouse models supporting the role of AMPK/p38 MAPK in regulating LPL recruitment to the cardiomyocyte cell surface. Transgenic mice overexpressing MAPK kinase 6 and MKP-1 are available, and could potentially be used in future studies. However, it should be noted that endothelium-bound heparin-releasable LPL activity was unchanged in both Type 1 and Type 2 diabetic mouse hearts (57). This could be a consequence of genetic adaptation, or the excessive heart rate in control animals (~600 beats/min), permitting prior translocation of LPL from the cardiomyocyte to the coronary lumen to saturate all of the LPL HSPG binding sites.

Notwithstanding the extensive and effective use of isolated cardiomyocytes in this study, the question of whether studies with an isolated cell are truly representative of the situation in the intact heart must always be paramount. It has been argued that short-term culture of isolated cardiomyocytes may be an important experimental approach, so that the cells have time to "rest and repair" after the trauma of isolation procedures that involve exposure to low-calcium concentrations and collagenase. Also, the preparation of cardiomyocytes from diseased hearts must be subject to the qualification that the isolated cells may not be representative because of selection bias for viable cells from the healthy portions of the myocardium. Finally, it should be the isolated myocytes are quiescent and do not beat against an after load.

Tables and figures

Table 2-1. Effect of AICAR on cardiomyocyte LPL activity

(min) / LPL activity (nmol/hr/10^6cells)	AICAR				
	0	30	60	90	120
-Heparin	1678 ± 94	1724 ± 32	1825 ± 164	1832 ± 73	1798 ± 92
+Heparin	2215 ± 85	2305 ± 48	3725 ± 256	5624 ± 75*	5782 ± 115*

Myocytes were prepared as described in the methods. AICAR (2 mM) was added to the culture medium, and myocytes kept for 30-120 minutes. Following the indicated times, myocyte basal LPL activity released into the medium was measured. To release surface-bound LPL activity, heparin (8 U/ml; 1min) was added to the culture plates, aliquots of cell medium removed, separated by centrifugation, and assayed for LPL activity. Results are the mean ± SEM of 3 rats in each group. *Significantly different from control, $P<0.05$.

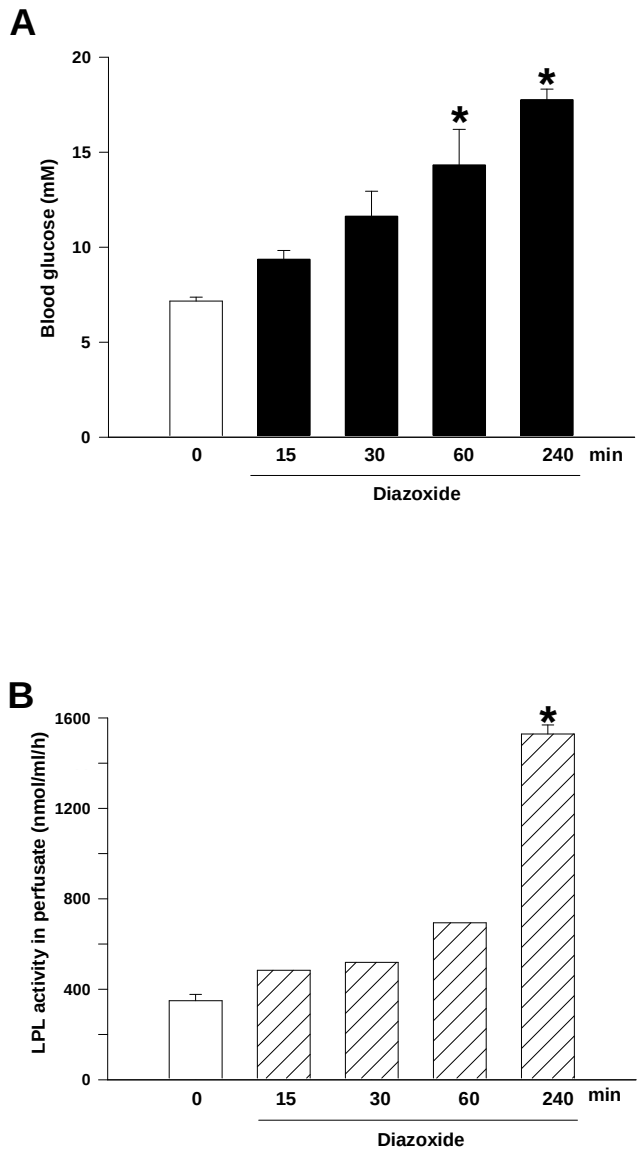

Fig. 2-1 *Blood glucose and LPL activity subsequent to Diazoxide (DZ).* Animals were treated with DZ (100 mg/kg, i.p.), and blood samples collected over a period of 4 h. Blood glucose was determined using a glucometer and glucose test strips (A). Results are the means ± SE of 3 rats in each group. At the indicated times, hearts from control and DZ treated animals were also isolated and perfused in the non-recirculating retrograde mode. Thereafter, coronary luminal LPL was released with heparin (5 U/ml). Coronary effluents were collected (for 10 s) over 5 mins, but only peak LPL activities are illustrated. LPL activity was assayed using radiolabeled triolein. The lower panel (B) illustrates peak heparin-releasable LPL activity released after varying durations of DZ (0-240 min). Results are the means ± SE of 3 rats in the 0 and 240 min group. In the other groups, only a representative value is indicated. *Significantly different from untreated control (0 min), $P < 0.05$.

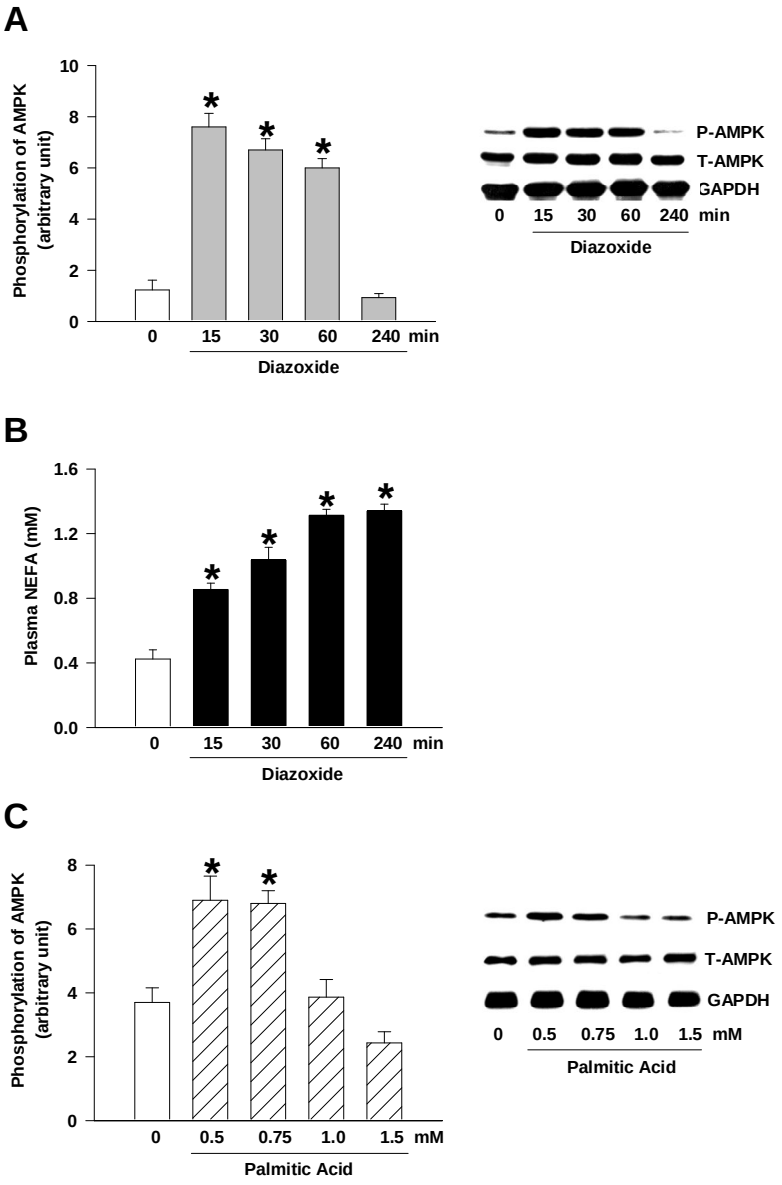

Fig. 2-2 *Alterations in AMPK phosphorylation in hearts isolated from Diazoxide treated animals or control myocytes treated with fatty acids.* Following DZ for different intervals, total or phosphorylated AMPK-α was determined immediately upon removal of the heart using Western blotting (A). Total and phospho-AMPK-α were measured using rabbit AMPK-α or phospho-AMPK (Thr-172) antibodies respectively. Blood samples were also collected over a period of 4-h after administration of DZ. After centrifugation, plasma was separated for determination of NEFA (B). Panel C represents total and phospho-AMPK-α following incubation of plated myocytes (0.4 x 10^6 cells) with 0.5-1.5 mM albumin bound palmitic acid (1:2). Data are means±SE of 3 rats in each group. *Significantly different from control (0 min), $P<0.05$.

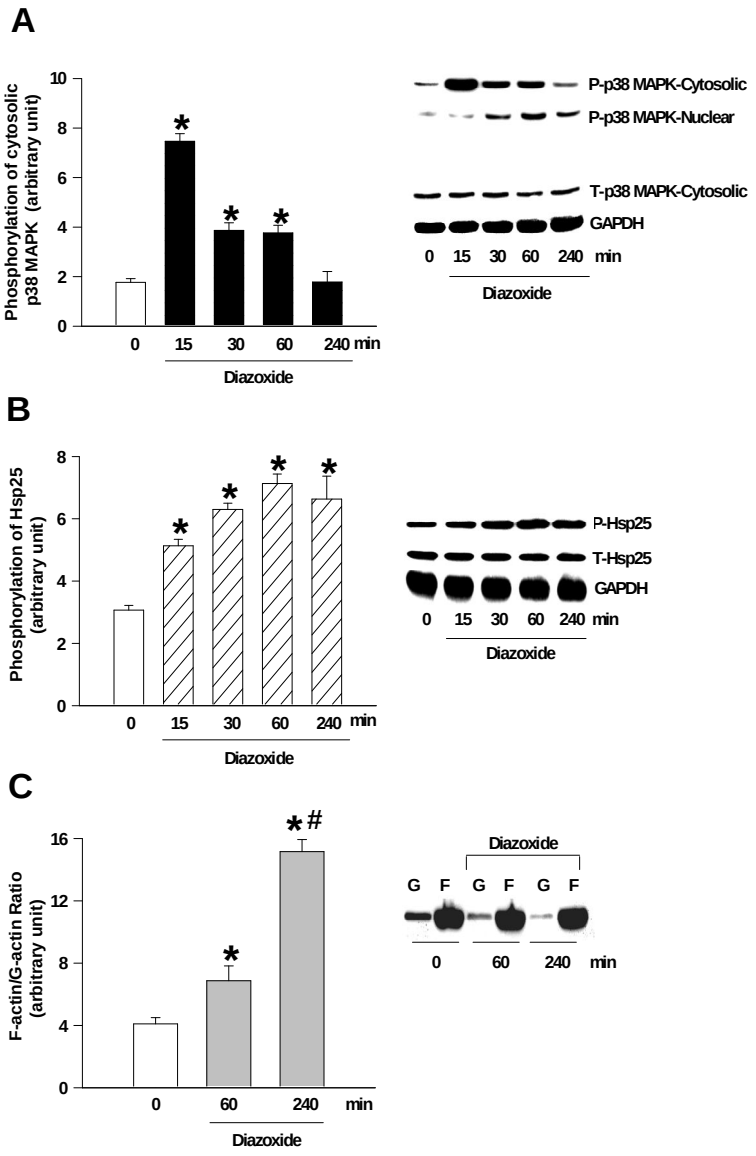

Fig. 2-3 *Time dependent changes in phosphorylation of p38 MAPK and Hsp25 and actin polymerization following DZ.* Cytosolic and nuclear p38 MAPK were evaluated using rabbit p38 MAPK or phospho-p38 MAPK (Thr180/Tyr182) antibodies (A). Total or phosphorylated Hsp25 were also determined immediately upon removal of the heart using rabbit Hsp25 or phospho-Hsp25 (S86) antibodies, and Western blotting (B). Data are means±SE of 3 different hearts in each group. *Significantly different from control, $P<0.05$. Cardiac actin rearrangement following DZ was determined using a G-actin/F-actin in vivo assay kit (C). Total actin was centrifuged to isolate F-actin (pellet) and G-actin (supernatant). The ratio of F-actin/G-actin was determined using western blotting and densitometry. An increase in F-to-G actin ratio was assumed to represent polymerization of actin filaments. Data are means±SE of 3 different hearts in each group. *Significantly different from control (0 min), #Significantly different from DZ (60 min), $P<0.05$.

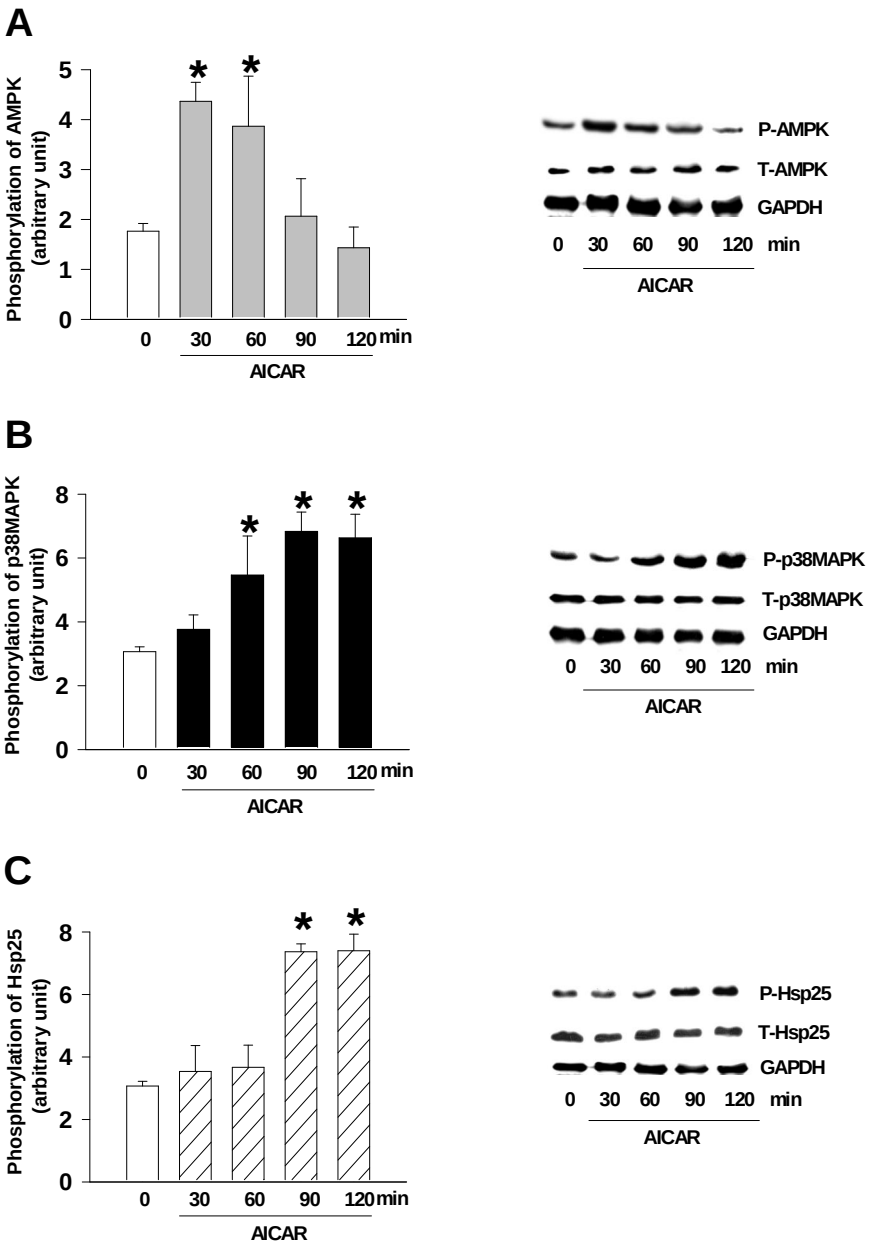

Fig. 2-4 *Consequence of AMPK activation using AICAR.* Cardiomyocytes were plated on laminin-coated culture plates. Cells were maintained using Media-199, and incubated at 37°C under an atmosphere of 95% O_2/5% CO_2 for 16 hours. Subsequently, 5-aminoimidazole-4-carboxamide-1-ß -D-ribofuranoside (2 mM) was added to the culture medium. At the indicated times, protein was extracted to determine AMPK (A), p38 (B), and Hsp25 (C) (both total and phosphorylated) using Western Blotting. Data are means ± SE; n=3 myocyte preparations from different animals. *Significantly different from control (0 min), $P < 0.05$.

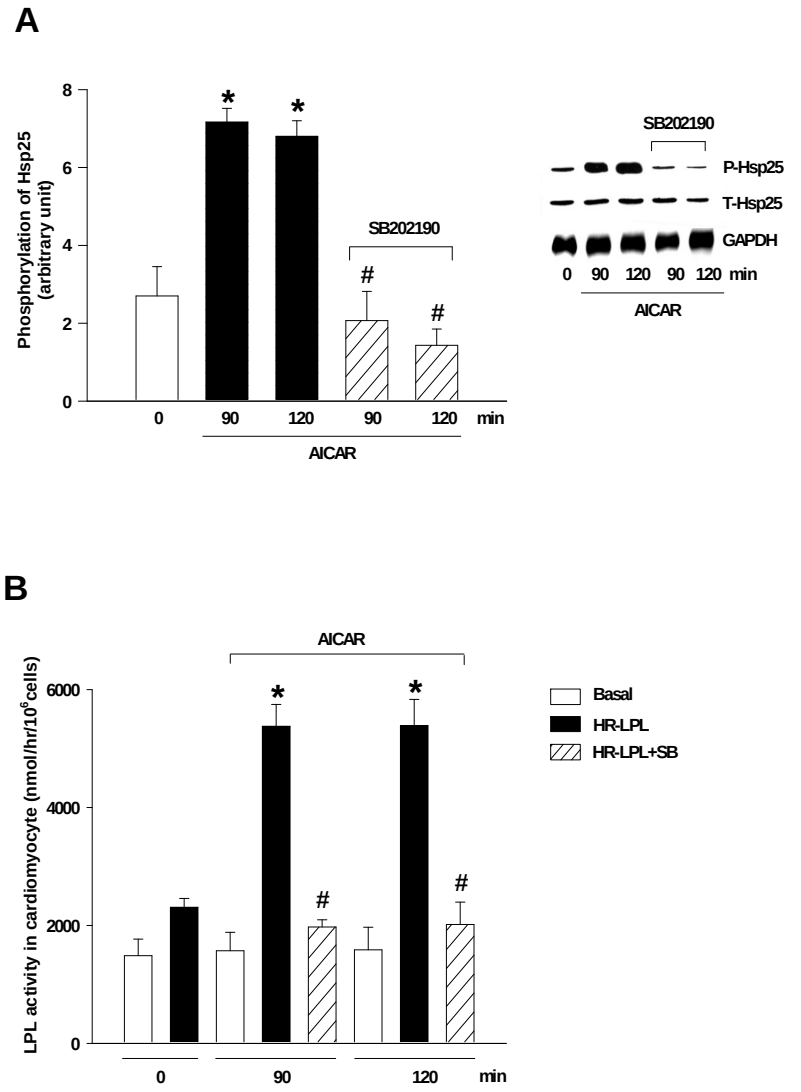

Fig. 2-5 *Effect of inhibiting p38 MAPK on AICAR induced phosphorylation of Hsp25 and increase in heparin-releasable LPL activity*. Cardiomyocytes were pre-incubated in the absence or presence of a p38 MAPK inhibitor (SB202190, 20 μM) added to the culture medium for 60 min. Subsequently, the myocytes were exposed to AICAR (2 mM). At the indicated times (90 and 120 min), protein was extracted to determine Hsp25 (both total and phosphorylated) using Western Blotting (A). Myocyte LPL activity was also measured after incubations with both SB202190 (pre-incubation for 60 min) and AICAR (90 and 120 min). To release surface-bound LPL activity, heparin (8 U/mL; 1 min) was added to the culture plates, aliquots of cell medium removed, separated by centrifugation, and assayed for LPL activity (B). Data are means ± SE; n=3 myocyte preparations from different animals. *Significantly different from control (0 min), #Significantly different from AICAR alone, $P < 0.05$.

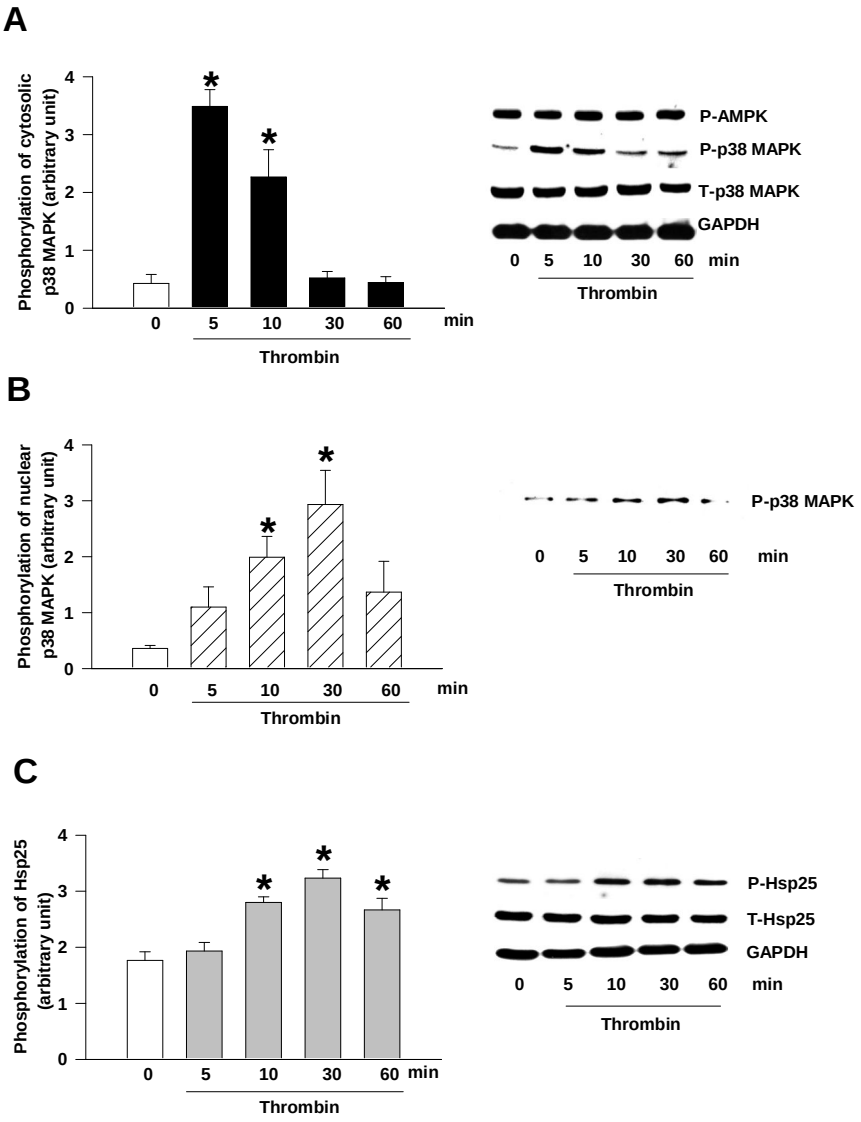

Fig. 2-6 *p38 MAPK and Hsp25 phosphorylation following incubation of cardiomyocytes with thrombin.* Cardiomyocytes were incubated with thrombin (0.05 U/ml) added to the culture medium, and myocytes kept for 0-60 minutes. At the indicated times, cytosolic (A) and nuclear (B) protein was extracted to determine p38 MAPK. Total and phosphorylated Hsp25 were also determined at the indicated times using Western Blotting (C). Cytosolic phospho-AMPK-α was also determined after incubation with thrombin (A, inset). Data are means ± SE; n=3 myocyte preparations from different animals. *Significantly different from control, $P < 0.05$.

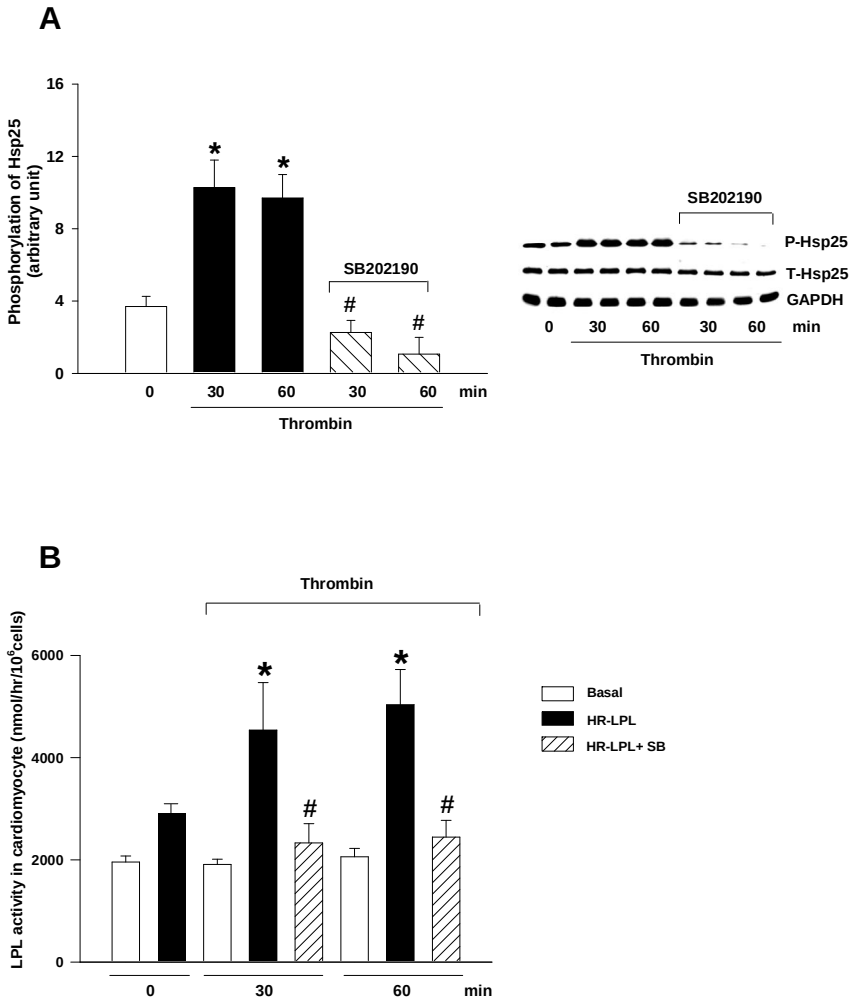

Fig. 2-7 *Effect of thrombin on Hsp25 phosphorylation and heparin-releasable LPL activity in cardiomyocytes.* Myocytes were prepared as described in the methods. Thrombin (0.05 U/ml) was added to the culture medium, and myocytes kept for 30 and 60 minutes. Following the indicated times, protein was extracted to determine Hsp25 (both total and phosphorylated) using Western Blotting (A). Myocyte basal LPL activity released into the medium was also measured following incubation with thrombin (30 and 60 min). To release surface-bound LPL activity, heparin (8 U/mL; 1 min) was added to the culture plates, aliquots of cell medium removed, separated by centrifugation, and assayed for LPL activity (B). Myocytes were also pre-incubated with a p38 MAPK inhibitor (SB202190, 20 μM) for 60 min prior to addition of thrombin (30 and 60 min) and subsequent determination of Hsp25 (A) and LPL activity (B). Data are means ± SE; n=3 myocyte preparations from different animals. *Significantly different from control (0 min), #Significantly different from thrombin alone, $P<0.05$.

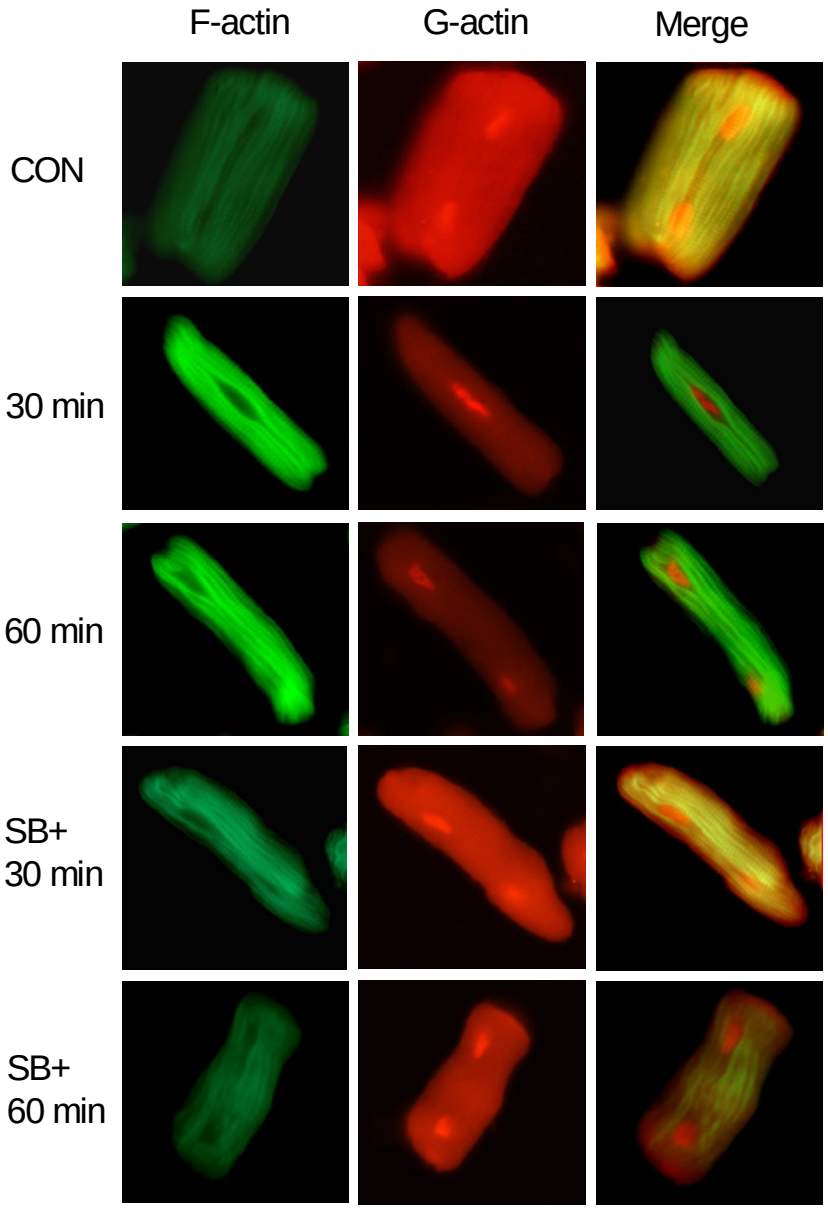

Fig. 2-8 *Myocyte actin rearrangement following thrombin.* Thrombin (0.05 U/ml) was added to plated myocytes, and the cells kept for 30 and 60 minutes. Myocytes were fixed, permeabilized and double stained with DNAaseI AlexaFluor®594 and Rhodamine®488 Phalloidin to colocalize monomeric globular actin (red, G-actin), and polymerized filamentous actin (green, F-actin). The merged image of F-actin and G-actin is described in the third panel. Myocytes were also pre-incubated with a p38 MAPK inhibitor (SB202190, 20 μM) for 60 min prior to addition of thrombin (30 and 60 min) and subsequent determination of F-actin and G-actin. Data is from a representative experiment done twice.

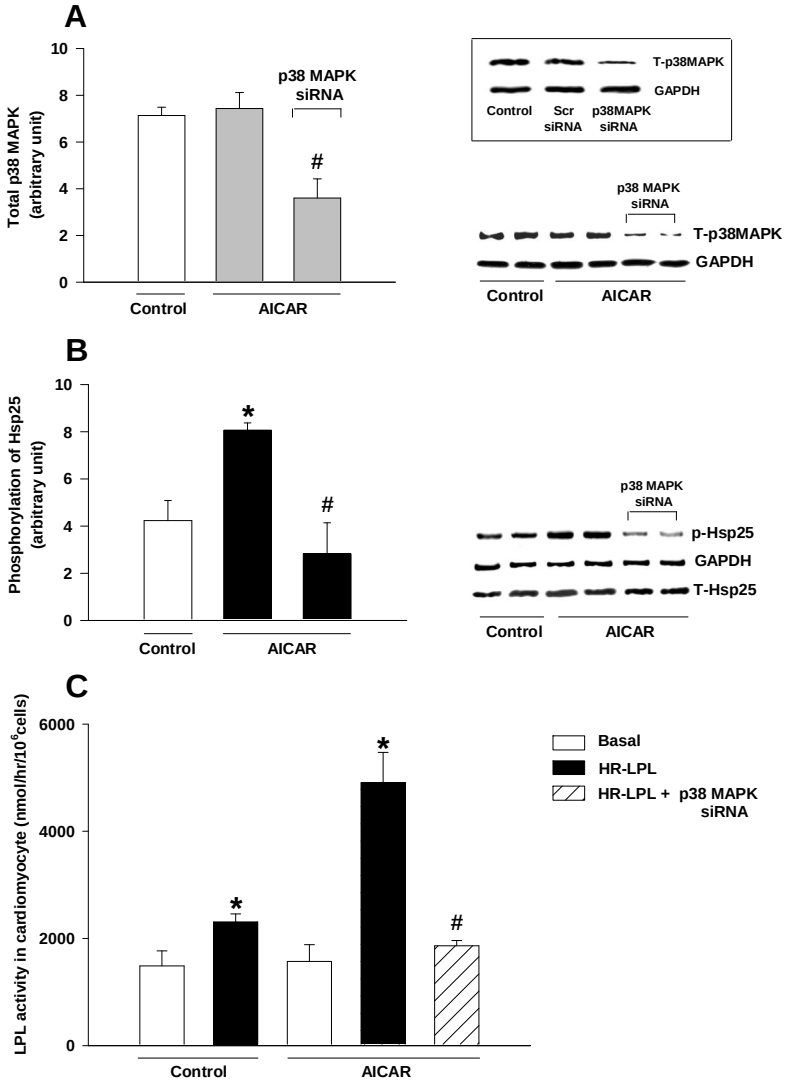

Fig. 2-9 *Silencing of p38 MAPK by siRNA*. siRNA transfection of p38 MAPK in cardiomyocytes was carried out using a kit from Santa Cruz. Plated myocytes were exposed to the siRNA (or scrambled, Scr). The inset depicts transfection efficiency. After this, AICAR (2 mM) was added to the culture medium for 2h and p38 MAPK (A), Hsp25 (B), and LPL activity (C) were evaluated. Data are means ± SE; n=3 myocyte preparations from different animals. *Significantly different from control, #Significantly different from AICAR treated control, $P<0.05$.

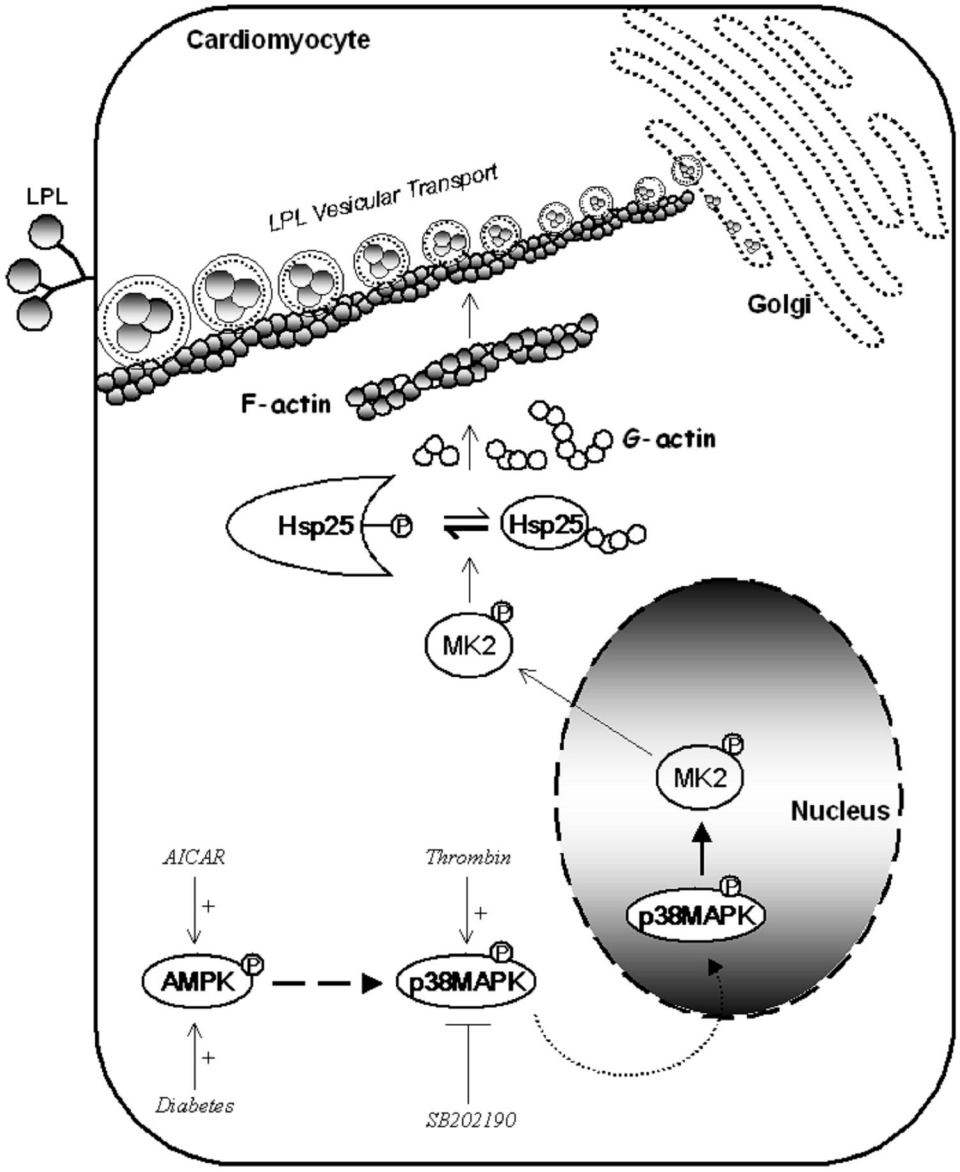

Fig. 2-10 *AMPK recruitment of LPL to the cardiomyocyte cell surface.* Following diabetes and activation of AMPK, p38 MAPK is phosphorylated and transferred to the nucleus to activate MAPKAP kinase 2, which is then exported to phosphorylate Hsp25. Actin monomers are released from the phosphorylated Hsp25 to self-associate to form fibrillar actin. Vesicles containing LPL then move along the actin filament network, and eventually bind to heparan sulfate proteoglycans on the plasma membrane. From here, LPL is transported onto HSPG binding sites on the luminal surface of the capillary endothelium.

2.6. Bibliography

1. Stamler J, Vaccaro O, Neaton JD, Wentworth D (1993) Diabetes, other risk factors, and 12-yr cardiovascular mortality for men screened in the Multiple Risk Factor Intervention Trial. Diabetes Care 16:434-444

2. Wilson PW (2001) Diabetes mellitus and coronary heart disease. Endocrinol Metab Clin North Am 30:857-881

3. Bertoni AG, Tsai A, Kasper EK, Brancati FL (2003) Diabetes and idiopathic cardiomyopathy: a nationwide case-control study. Diabetes Care 26:2791-2795

4. Diamant M, Lamb HJ, Groeneveld Y, Endert EL, Smit JW, Bax JJ, Romijn JA, de Roos A, Radder JK (2003) Diastolic dysfunction is associated with altered myocardial metabolism in asymptomatic normotensive patients with well-controlled type 2 diabetes mellitus. J Am Coll Cardiol 42:328-335

5. Fein FS (1990) Diabetic cardiomyopathy. Diabetes Care 13:1169-1179

6. Fang ZY, Prins JB, Marwick TH (2004) Diabetic cardiomyopathy: evidence, mechanisms, and therapeutic implications. Endocr Rev 25:543-567

7. Rodrigues B, Cam MC, McNeill JH (1995) Myocardial substrate metabolism: implications for diabetic cardiomyopathy. J Mol Cell Cardiol 27:169-179

8. Golfman LS, Takeda N, Dhalla NS (1996) Cardiac membrane Ca(2+)-transport in alloxan-induced diabetes in rats. Diabetes Res Clin Pract 31 Suppl:S73-77

9. Lopaschuk GD (2002) Metabolic abnormalities in the diabetic heart. Heart Fail Rev 7:149-159

10. Yagyu H, Chen G, Yokoyama M, Hirata K, Augustus A, Kako Y, Seo T, Hu Y, Lutz EP, Merkel M, Bensadoun A, Homma S, Goldberg IJ (2003) Lipoprotein lipase (LpL) on the surface of cardiomyocytes increases lipid uptake and produces a cardiomyopathy. J Clin Invest 111:419-426

11. Chiu HC, Kovacs A, Blanton RM, Han X, Courtois M, Weinheimer CJ, Yamada KA, Brunet S, Xu H, Nerbonne JM, Welch MJ, Fettig NM, Sharp TL, Sambandam N, Olson KM, Ory DS, Schaffer JE (2005) Transgenic expression of fatty acid transport protein 1 in the heart causes lipotoxic cardiomyopathy. Circ Res 96:225-233

12. Finck BN, Lehman JJ, Leone TC, Welch MJ, Bennett MJ, Kovacs A, Han X, Gross RW, Kozak R, Lopaschuk GD, Kelly DP (2002) The cardiac phenotype induced by PPARalpha overexpression mimics that caused by diabetes mellitus. J Clin Invest 109:121-130

13. Chiu HC, Kovacs A, Ford DA, Hsu FF, Garcia R, Herrero P, Saffitz JE, Schaffer JE (2001) A novel mouse model of lipotoxic cardiomyopathy. J Clin Invest 107:813-822

14. Belke DD, Larsen TS, Gibbs EM, Severson DL (2000) Altered metabolism causes cardiac dysfunction in perfused hearts from diabetic (db/db) mice. Am J Physiol Endocrinol Metab 279:E1104-1113

15. Eckel RH (1989) Lipoprotein lipase. A multifunctional enzyme relevant to common metabolic diseases. N Engl J Med 320:1060-1068

16. Pillarisetti S, Paka L, Sasaki A, Vanni-Reyes T, Yin B, Parthasarathy N, Wagner WD, Goldberg IJ (1997) Endothelial cell heparanase modulation of lipoprotein lipase activity. Evidence that heparan sulfate oligosaccharide is an extracellular chaperone. J Biol Chem 272:15753-15759

17. Augustus AS, Kako Y, Yagyu H, Goldberg IJ (2003) Routes of FA delivery to cardiac muscle: modulation of lipoprotein lipolysis alters uptake of TG-derived FA. Am J Physiol Endocrinol Metab 284:E331-339

18. Teusink B, Voshol PJ, Dahlmans VE, Rensen PC, Pijl H, Romijn JA, Havekes LM (2003) Contribution of fatty acids released from lipolysis of plasma triglycerides to total plasma fatty acid flux and tissue-specific fatty acid uptake. Diabetes 52:614-620

19. Mulder M, Lombardi P, Jansen H, van Berkel TJ, Frants RR, Havekes LM (1993) Low density lipoprotein receptor internalizes low density and very low density lipoproteins that are bound to heparan sulfate proteoglycans via lipoprotein lipase. J Biol Chem 268:9369-9375

20. Hardie DG (2003) Minireview: the AMP-activated protein kinase cascade: the key sensor of cellular energy status. Endocrinology 144:5179-5183

21. An D, Pulinilkunnil T, Qi D, Ghosh S, Abrahani A, Rodrigues B (2005) The metabolic "switch" AMPK regulates cardiac heparin-releasable lipoprotein lipase. Am J Physiol Endocrinol Metab 288:E246-253

22. Foy JM, Furman BL (1973) Effect of single dose administration of diuretics on the blood sugar of alloxan-diabetic mice or mice made hyperglycaemic by the acute administration of diazoxide. Br J Pharmacol 47:124-132

23. Pulinilkunnil T, Qi D, Ghosh S, Cheung C, Yip P, Varghese J, Abrahani A, Brownsey R, Rodrigues B (2003) Circulating triglyceride lipolysis facilitates lipoprotein lipase translocation from cardiomyocyte to myocardial endothelial lining. Cardiovasc Res 59:788-797

24. Rodrigues B, Cam MC, Jian K, Lim F, Sambandam N, Shepherd G (1997) Differential effects of streptozotocin-induced diabetes on cardiac lipoprotein lipase activity. Diabetes 46:1346-1353

25. Sambandam N, Abrahani MA, St Pierre E, Al-Atar O, Cam MC, Rodrigues B (1999) Localization of lipoprotein lipase in the diabetic heart: regulation by acute changes in insulin. Arterioscler Thromb Vasc Biol 19:1526-1534

26. Qi D, Kuo KH, Abrahani A, An D, Qi Y, Heung J, Kewalramani G, Pulinilkunnil T, Ghosh S, Innis SM, Rodrigues B (2006) Acute intralipid infusion reduces cardiac luminal lipoprotein lipase but recruits additional enzyme from cardiomyocytes. Cardiovasc Res 72:124-133

27. Qi D, Pulinilkunnil T, An D, Ghosh S, Abrahani A, Pospisilik JA, Brownsey R, Wambolt R, Allard M, Rodrigues B (2004) Single-dose dexamethasone induces whole-body insulin resistance and alters both cardiac fatty acid and carbohydrate metabolism. Diabetes 53:1790-1797

28. Pulinilkunnil T, Abrahani A, Varghese J, Chan N, Tang I, Ghosh S, Kulpa J, Allard M, Brownsey R, Rodrigues B (2003) Evidence for rapid "metabolic switching" through lipoprotein lipase occupation of endothelial-binding sites. J Mol Cell Cardiol 35:1093-1103

29. Haugland RP, You W, Paragas VB, Wells KS, DuBose DA (1994) Simultaneous visualization of G- and F-actin in endothelial cells. J Histochem Cytochem 42:345-350

30. Pulinilkunnil T, An D, Ghosh S, Qi D, Kewalramani G, Yuen G, Virk N, Abrahani A, Rodrigues B (2005) Lysophosphatidic acid-mediated augmentation of cardiomyocyte lipoprotein lipase involves actin cytoskeleton reorganization. Am J Physiol Heart Circ Physiol 288:H2802-2810

31. Kewalramani G, An D, Kim MS, Ghosh S, Qi D, Abrahani A, Pulinilkunnil T, Sharma V, Wambolt RB, Allard MF, Innis SM, Rodrigues B (2007) AMPK control of myocardial fatty acid metabolism fluctuates with the intensity of insulin-deficient diabetes. J Mol Cell Cardiol 42:333-342

32. Li J, Miller EJ, Ninomiya-Tsuji J, Russell RR, 3rd, Young LH (2005) AMP-activated protein kinase activates p38 mitogen-activated protein kinase by increasing recruitment of p38 MAPK to TAB1 in the ischemic heart. Circ Res 97:872-879

33. Ewart HS, Severson DL (1999) Insulin and dexamethasone stimulation of cardiac lipoprotein lipase activity involves the actin-based cytoskeleton. Biochem J 340 (Pt 2):485-490

34. Zheng C, Lin Z, Zhao ZJ, Yang Y, Niu H, Shen X (2006) MAPK-activated protein kinase-2 (MK2)-mediated formation and phosphorylation-regulated dissociation of the signal complex consisting of p38, MK2, Akt, and Hsp27. J Biol Chem 281:37215-37226

35. Camps L, Reina M, Llobera M, Vilaro S, Olivecrona T (1990) Lipoprotein lipase: cellular origin and functional distribution. Am J Physiol 258:C673-681

36. Otarod JK, Goldberg IJ (2004) Lipoprotein lipase and its role in regulation of plasma lipoproteins and cardiac risk. Curr Atheroscler Rep 6:335-342

37. Hardie DG, Hawley SA (2001) AMP-activated protein kinase: the energy charge hypothesis revisited. Bioessays 23:1112-1119

38. Hardie DG, Carling D (1997) The AMP-activated protein kinase--fuel gauge of the mammalian cell? Eur J Biochem 246:259-273

39. Hong SP, Leiper FC, Woods A, Carling D, Carlson M (2003) Activation of yeast Snf1 and mammalian AMP-activated protein kinase by upstream kinases. Proc Natl Acad Sci U S A 100:8839-8843

40. Hayashi T, Hirshman MF, Fujii N, Habinowski SA, Witters LA, Goodyear LJ (2000) Metabolic stress and altered glucose transport: activation of AMP-activated protein kinase as a unifying coupling mechanism. Diabetes 49:527-531

41. Russell RR, 3rd, Bergeron R, Shulman GI, Young LH (1999) Translocation of myocardial GLUT-4 and increased glucose uptake through activation of AMPK by AICAR. Am J Physiol 277:H643-649

42. Marsin AS, Bertrand L, Rider MH, Deprez J, Beauloye C, Vincent MF, Van den Berghe G, Carling D, Hue L (2000) Phosphorylation and activation of heart PFK-2 by AMPK has a role in the stimulation of glycolysis during ischaemia. Curr Biol 10:1247-1255

43. Luiken JJ, Coort SL, Willems J, Coumans WA, Bonen A, van der Vusse GJ, Glatz JF (2003) Contraction-induced fatty acid translocase/CD36 translocation in rat cardiac myocytes is mediated through AMP-activated protein kinase signaling. Diabetes 52:1627-1634

44. Kudo N, Barr AJ, Barr RL, Desai S, Lopaschuk GD (1995) High rates of fatty acid oxidation during reperfusion of ischemic hearts are associated with a decrease in malonyl-CoA levels due to an increase in 5'-AMP-activated protein kinase inhibition of acetyl-CoA carboxylase. J Biol Chem 270:17513-17520

45. Watt MJ, Steinberg GR, Chen ZP, Kemp BE, Febbraio MA (2006) Fatty acids stimulate AMP-activated protein kinase and enhance fatty acid oxidation in L6 myotubes. J Physiol 574:139-147

46. Wu Y, Song P, Xu J, Zhang M, Zou MH (2007) Activation of protein phosphatase 2A by palmitate inhibits AMP-activated protein kinase. J Biol Chem 282:9777-9788

47. Tan Y, Rouse J, Zhang A, Cariati S, Cohen P, Comb MJ (1996) FGF and stress regulate CREB and ATF-1 via a pathway involving p38 MAP kinase and MAPKAP kinase-2. Embo J 15:4629-4642

48. Dai T, Natarajan R, Nast CC, LaPage J, Chuang P, Sim J, Tong L, Chamberlin M, Wang S, Adler SG (2006) Glucose and diabetes: effects on podocyte and glomerular p38MAPK, heat shock protein 25, and actin cytoskeleton. Kidney Int 69:806-814

49. Corton JM, Gillespie JG, Hawley SA, Hardie DG (1995) 5-aminoimidazole-4-carboxamide ribonucleoside. A specific method for activating AMP-activated protein kinase in intact cells? Eur J Biochem 229:558-565

50. Chan AY, Soltys CL, Young ME, Proud CG, Dyck JR (2004) Activation of AMP-activated protein kinase inhibits protein synthesis associated with hypertrophy in the cardiac myocyte. J Biol Chem 279:32771-32779

51. Chabowski A, Momken I, Coort SL, Calles-Escandon J, Tandon NN, Glatz JF, Luiken JJ, Bonen A (2006) Prolonged AMPK activation increases the expression of fatty acid transporters in cardiac myocytes and perfused hearts. Mol Cell Biochem 288:201-212

52. Smith JL, Patil PB, Fisher JS (2005) AICAR and hyperosmotic stress increase insulin-stimulated glucose transport. J Appl Physiol 99:877-883

53. Hilder TL, Baer LA, Fuller PM, Fuller CA, Grindeland RE, Wade CE, Graves LM (2005) Insulin-independent pathways mediating glucose uptake in hindlimb-suspended skeletal muscle. J Appl Physiol 99:2181-2188

54. Kanda Y, Watanabe Y (2005) Thrombin-induced glucose transport via Src-p38 MAPK pathway in vascular smooth muscle cells. Br J Pharmacol 146:60-67

55. Levak-Frank S, Radner H, Walsh A, Stollberger R, Knipping G, Hoefler G, Sattler W, Weinstock PH, Breslow JL, Zechner R (1995) Muscle-specific overexpression of lipoprotein lipase causes a severe myopathy characterized by proliferation of mitochondria and peroxisomes in transgenic mice. J Clin Invest 96:976-986

56. Augustus AS, Buchanan J, Park TS, Hirata K, Noh HL, Sun J, Homma S, D'Armiento J, Abel ED, Goldberg IJ (2006) Loss of lipoprotein lipase-derived fatty acids leads to increased cardiac glucose metabolism and heart dysfunction. J Biol Chem 281:8716-8723

57. Neitzel AS, Carley AN, Severson DL (2003) Chylomicron and palmitate metabolism by perfused hearts from diabetic mice. Am J Physiol Endocrinol Metab 284:E357-365

3. Protein kinase D is a key regulator of cardiomyocyte lipoprotein lipase secretion following diabetes[2]

3.1. Introduction

Cardiac muscle has a high demand for energy and uses multiple substrates, including fatty acid (FA), carbohydrate, amino acids and ketones(1). Among these substrates, carbohydrate and FA are the major sources from which the heart derives most of its energy. In a normal heart, while glucose and lactate account for approximately 30% of energy provided to the cardiac muscle, 70% of ATP generation is through FA oxidation(2). FA delivery and utilization by the heart involves: i) release from adipose tissue and transport to the heart after complexing with albumin(3), ii) provision through breakdown of endogenous cardiac triglyceride (TG) stores(4), iii) internalization of whole lipoproteins(5), and iv) hydrolysis of circulating TG-rich lipoproteins to FA by lipoprotein lipase (LPL) positioned at the endothelial surface of the coronary lumen(6). The molar concentration of FA bound to albumin is ~10-fold less than that of FA in lipoprotein-TG(7) and LPL-mediated hydrolysis of circulating TG-rich lipoproteins to FA is suggested to be the principal source of FA for cardiac utilization(8).

Coronary endothelial cells do not synthesize LPL(9). In the heart, this enzyme is produced in cardiomyocytes and subsequently secreted onto heparan sulphate proteoglycan (HSPG) binding sites on the myocyte cell surface(10). From here, LPL is transported onto comparable binding sites on the luminal surface of endothelial cells(11). Electron microscopy using immunogold-labeling established that, in the heart, 78% of total LPL is present in cardiac myocytes, 3-6% in

[2]A version of this chapter has been published. **Kim, M.**, Wang, F., Puthanveetil, P., Kewalramani, G., Hosseini-Beheshti, E., Ng, N., Wang, Y., Kumar, U., Innis, S., Proud, C.G., Abrahani, A., and Rodrigues, B. (2008) Protein kinase D is a key regulator of cardiomyocyte lipoprotein lipase secretion after diabetes. **Circ. Res.** 103: 252-260.

the interstitial space, and 18% at the coronary endothelium(12).

The earliest change that occurs in the diabetic heart is altered energy metabolism where in the presence of lower glucose utilization, the heart switches to exclusively using FA for energy supply(13). It does this by increasing its LPL activity at the coronary lumen(8). We have examined LPL biology in the diabetic heart and have determined that the augmented activity(14) is: i) not the result of increased gene expression(14), ii) unrelated to an increase in the number of capillary endothelial HSPG binding sites(14), iii) acutely (hours) regulated by short-term changes in insulin(15), and iv) functionally relevant and capable of hydrolyzing lipoprotein-TG(16). More recently, we have examined the contributions of the endothelial cell and the cardiomyocyte in enabling this increased enzyme at the vascular lumen. At the endothelial cell, we reported that TG(17) and lipoprotein breakdown products like lysophosphatidylcholine(18), likely through their release of heparanase, enabled myocyte HSPG cleavage and transfer of LPL towards the coronary lumen. Within the myocyte, recruitment of LPL to the cell surface was controlled by stress kinases like AMPK and p38 MAPK that allowed for actin cytoskeleton polymerization and provision of a network that facilitated LPL movement(19). In the present study, we determined the mechanism that controls cardiac LPL vesicular trafficking following diabetes. Our data suggests that protein kinase D (PKD) activation is essential for LPL vesicle formation and its movement to the cardiomyocyte plasma membrane, for eventual translocation to the coronary vascular lumen.

3.2. Methods

3.2.1. Experimental animals

The investigation conforms to the guide for the care and use of laboratory animals published by the US NIH and the University of British Columbia. Adult male Wistar rats (260-300 g) were injected with diazoxide (DZ). This agent, either through selective K^+ATP channel opening(20; 21) or inhibitory effects on aerobic energy generation(22), decreases insulin secretion and causes hyperglycemia. DZ (100 mg/kg) was administered i.p., and animals were euthanized at 1 and 4 h after injection. Subsequently, hearts were removed for measurement of coronary luminal LPL activity, immunoprecipitation, immunofluorescence, and Western Blot. To inhibit PKD(23), some rats were injected with rottlerin (10 μM), 40 mins prior to administration of DZ. To validate our results using DZ, rats were made diabetic with streptozotocin (STZ, 55 mg/kg i.v.)(24). Animals were kept for 1 (acute) or 7 (chronic) days after STZ, at which time they were killed and hearts removed for measurement of LPL activity and PKD.

3.2.2. Isolated heart perfusion

Rats were anesthetized with 65 mg/kg sodium pentobarbital i.p. and the heart carefully excised. Following cannulation of aorta, hearts were perfused retrogradely with Krebs-Henseleit buffer(19). The rate of coronary flow (7-8 ml/min) was controlled by a peristaltic pump(24). To measure coronary endothelium-bound LPL, the perfusion solution was changed to buffer containing heparin (5 U/ml). The coronary effluent was collected in timed fractions (10 sec) over 5 min, and assayed for LPL activity by measuring the hydrolysis of a [^{3}H]triolein substrate emulsion(15).

3.2.3. Isolated cardiac myocytes

Ventricular calcium-tolerant myocytes were prepared as described previously(14; 21). To examine the influence of high glucose and FA or phorbol 12-myristate 13-acetate {PMA; a protein kinase C activator(25)} on cardiomyocytes, cells were plated on laminin-coated 6-well culture plates (to a density of 200,000 cells/well). Cells were maintained using Media-199, and incubated at 37°C under an atmosphere of 95% O_2/5% CO_2 for 16 hours. Subsequently and where indicated, 20 mM glucose and 1.5 mM albumin bound palmitic (PA) or oleic (OA) acid (molar ratio 1:2; 1-2 h) or 1 μM PMA (15 min) were added to the culture medium. BSA-FA solutions were prepared by first dissolving the FA in ethanol and then adding appropriate amounts to media to obtain the required molar ratio of BSA to FA. In some experiments, 20 mM mannitol was used as osmolarity control. Following the indicated times, cells were used either for Western Blot, immunoprecipitation, immunofluorescence or measurement of basal and heparin-releasable (heparin 8 U/mL; 1 min) LPL activity. To determine translocation of PKD, myocytes were homogenized in ice-cold buffer A (20 mM Tris-HCl, 2 mM EDTA, 5 mM EGTA, 50 mM 2-mercaptoethanol, 25 μg leupeptin, and 4 μg aprotinin, pH 7.5) and centrifuged for 1 h at 35000 rpm; the supernatant was used as the cytosolic fraction. The pellet was resuspended in buffer B (1% NP-40, 0.1% SDS, 0.5% deoxycholic acid and 5 mM EGTA, pH 7.5), sonicated for 30 s, and centrifuged at 35000 rpm for 1 h; the supernatant was used as the membrane fraction(26).

3.2.4. Adenoviral gene transfer

Cardiomyocytes were infected with recombinant adenovirus vectors carrying wild-type (WT) PKCδ and dominant-negative (DN) PKCδ (K376A), as described previously(27). Mock

infection as a control was performed using LacZ. Infected cells were incubated for a further 36 h before treatment in the absence or presence of high glucose and PA (2 h).

3.2.5. Western blotting

Western blot was carried out as described previously(28). Briefly, ventricular tissue (50 mg) or plated myocytes (0.4 x 10^6) were homogenized in ice-cold lysis buffer. Samples were diluted, boiled with sample loading dye, and 50 μg used in SDS-polyacrylamide gel electrophoresis. After blotting, membranes were blocked in 5% skim milk in Tris-buffered saline containing 0.1% Tween-20. Membranes were incubated with rabbit Hsp25, phospho-Hsp25 (S86), PKCδ, phospho-PKCδ (ser-643), PKD, and phospho-PKD (ser-744/748) antibodies, and subsequently with secondary goat anti-rabbit HRP-conjugated antibody. Reaction products were visualized using an ECL® detection kit, and quantified by densitometry.

3.2.6. Immunoprecipitation

Following DZ or treatment of plated cardiomyocytes with PMA (1 μM), lysates were immunoprecipitated using PKCδ or PKD antibodies overnight at 4°C. The immunocomplex was pulled down with protein A/G-sepharose for 1 h, and then heated for 5 min at 95°C. The immunocomplex was separated into two equal portions, each of which was immunoblotted with anti-Hsp25 and PKCδ or phospho-PKCδ and PKD.

3.2.7. Immunofluorescence

Heart-Hearts were placed in 10% formalin for 24 h. After formalin fixation and paraffin embedding, 3-μm sections were cut on silane-coated glass slides. Immunostaining was carried out as described before(18). Slides were incubated with chicken anti-bovine LPL antibody (1:400 dilution) overnight. After being washed with TBS, slides were incubated with biotinylated rabbit anti-chicken IgG (1:150 dilution; Chemicon) and streptavidin-conjugated Cy3

fluorescent probe (1:1,000 dilution) for 1 h. Slides were visualized using a fluorescent microscope.

Cardiomyocyte-Following incubation with high glucose and PA or PMA at the indicated times, myocytes were fixed for 10 min with 4% paraformaldehyde in PBS, permeabilized with 0.1% Triton X-100 in PBS for 3 min, treated with PBS containing 1% BSA for 20 minutes, and finally rinsed with PBS. Cells were incubated with rabbit polyclonal PKD and goat polyclonal vesicle associated membrane protein (VAMP) or chicken anti-bovine LPL antibody followed by incubation with secondary antibodies [goat anti-rabbit IgG-FITC, donkey anti-goat IgG-TR, streptavidin-conjugated Cy3 fluorescent probe] to localize PKD (green), VAMP (red), and LPL (red) respectively. Slides were visualized using a Zeiss Pascal confocal microscope.

3.2.8. Silencing of PKD and Hsp25 by siRNA

SiRNA transfection in cardiomyocytes was carried out using a kit from Santa Cruz(19). Briefly, in 6-well culture plates, 0.1 x 10^6 cells were plated and subsequently exposed to the siRNA (or scrambled, Scr) solution for 8 h at 37°C in a CO_2 incubator. Following this, the media was changed to Media 199 and the cells incubated for another 18 h. Subsequently, high glucose and PA or PMA were added to the culture medium, and LPL activity (released by heparin) and immunofluorescence, and PKD, Hsp25 and PKCδ (using Western Blot and immunoprecipitation) were determined.

3.2.9. Separation and measurement of cardiac diacylglycerol

Total cardiac lipids were extracted and solubilized in chloroform:methanol:acetone:hexane (4:6:1:1 v/v/v/v). Separation of 1,2-DAG was achieved using HPLC (Waters 2690 Alliance HPLC, Milford, MA) as described previously(29).

3.2.10. Plasma measurements

Following DZ, blood samples from the tail vein were collected over a period of 4 h, and blood glucose determined using a glucometer (AccuSoft) and glucose test strips (Accu-Chek Advantage). At varying intervals, blood was also acquired in heparinized glass capillary tubes. Blood samples were immediately centrifuged and plasma was collected and assayed for non-esterified fatty acid using a diagnostic kit (Wako).

3.2.11. Materials

[^{3}H]triolein and the ECL® detection kit were purchased from Amersham Canada. Heparin sodium injection (Hapalean; 1000 USP U/ml) was obtained from Organon Teknika. PKCδ, phospho-PKCδ (ser-643) and PKD antibodies were obtained from Santa Cruz biothechnology, Inc. (Delaware Avenue, CA). Hsp25 and phospho-Hsp25 antibodies were obtained from GeneTex®, Inc. (San Antonio, TX). Phospho-PKD (ser-744/748) and GAPDH were obtained from Cell Signaling (Danvers, MA). Rottlerin was purchased from Calbiochem. All other chemicals were obtained from Sigma Chemical.

3.2.12. Statistical analysis

Values are means ± SE. Wherever appropriate, one-way ANOVA followed by the Bonferroni test was used to determine differences between group mean values. The level of statistical significance was set at $P < 0.05$.

3.3. Results

3.3.1. Characterization of the model of acute diabetes induced with diazoxide

Subsequent to injection of DZ, blood glucose levels increased, and were significantly higher after 1 and 4 h (Table 3-1). Changes in plasma parameters with DZ also included significant and rapid increases in FA (Table 3-1). Other characteristics normally associated with hyperglycemia, such as polydipsia, was also observed in DZ treated animals. Retrograde perfusion of hearts with heparin resulted in release of LPL into the coronary perfusate. Compared to control rat hearts, there was a substantial increase in LPL activity at the vascular lumen following 1 and 4 h of DZ (Table 3-1). We have previously shown that this change in LPL activity was independent of shifts in mRNA(14), and was dependent on its lowering of insulin rather than its direct effects on the heart or blood pressure(21). Incubation of cardiomyocytes with DZ (1 mg/ml; calculated concentration *in vivo*) had no influence on heparin releasable LPL activity (Appendix Fig. A-1).

3.3.2. Mechanism of activation of PKD in hearts from animals with hyperglycemia

Recently, we have determined that diabetes increases the phosphorylation of Hsp25(19). In the present study, we duplicated this result (Fig. 3-1A) and additionally show that Hsp25 phosphorylation enables PKCδ to dissociate from Hsp25 (Fig. 3-1B). As Hsp25 binds directly to ser-643 of PKCδ, its separation permits PKCδ phosphorylation (Fig. 3-1C), with an associated increase in its activity(30). PKCδ has been suggested to regulate PKD activity in intestinal epithelial cells(23). Interestingly, in addition to PKCδ phosphorylation, DZ also augmented PKD phosphorylation at 1 and 4 h after injection (Fig. 3-1E). This increase in PKD phosphorylation paralleled a robust attachment of phospho-PKCδ to PKD (Fig. 3-1D). Injection of STZ precipitated overt hyperglycemia (Table 3-1). Compared to control hearts, LPL activity increased at the vascular lumen following 1 and 7 days of STZ (Fig. 3-1F). As observed with

DZ, this increase in LPL activity with STZ diabetes closely paralleled activation of PKD (Fig. 3-1G).

3.3.3. Role of PKD in diabetes induced augmentation of LPL activity

PKD assists in protein transport from the golgi to plasma membrane(31). We hypothesized that following DZ, activation of PKD facilitates LPL vesicular movement to the cardiomyocyte cell surface and eventually to the vascular lumen, and that its inhibition should reduce LPL activity at this location. In the absence of specific inhibitors of PKD, we used rottlerin, an inhibitor of PKCδ. Treatment of rottlerin for 1 h decreased PKD phosphorylation that is produced following DZ (Fig. 3-2A). More importantly, the remarkable increase in LPL immunofluroscence (Fig. 3-2B) or activity (Fig. 3-2C) at the vascular lumen following 4 h of DZ was also reduced by preincubation with rottlerin.

3.3.4. Simulation of diabetes promotes LPL trafficking to the cardiomyocyte plasma membrane

We duplicated the hyperglycemia and hyperlipidemia observed following DZ by incubating control myocytes with high glucose and palmitic acid (Glu+PA). 20 mM glucose with 1.5 mM PA increased the phosphorylation of Hsp25 (Fig. 3-3A), PKCδ (Fig. 3-3B) and PKD (Fig. 3-3C) in a pattern similar to that seen with diabetes induced by DZ. Once activated, PKD regulates formation of trans-golgi vesicles and facilitates their movement to the plasma membrane with help of vesicle associated membrane protein (VAMP)(32). High Glu+PA brought about both PKD and VAMP translocation, as measured by Western blotting and confocal microscopy (Fig. 3-4A and 3-4B). Interestingly, this milieu also augmented cardiomyocyte cell surface heparin releasable LPL activity (Fig. 3-4C) and protein (Fig. 3-5B, middle panel). Independently, high glucose or PA (Appendix Fig. A-2), and mannitol with PA (Fig. 3-4C) had no effect on cardiomyocyte LPL trafficking. Additionally, high glucose in the presence of physiologically

relevant concentrations of PA (0.5 mM) did not change heparin releasable LPL activity, which only increased with 1 and 1.5 mM PA (Appendix Fig. A-2). Finally, unlike PA, oleic acid (1.5 mM) in the presence of high glucose had no influence in increasing heparin releasable LPL activity (Appendix Fig. A-3).

3.3.5. Silencing of PKD prevents cardiomyocyte LPL recruitment observed with high Glu+PA

To confirm the relationship between PKD and LPL, we used siRNA to silence PKD expression in isolated cardiomyocytes. We first validated successful PKD inhibition using Western blotting (Fig. 3-5A, inset). In myocytes in which PKD was silenced, high Glu+PA had no influence on total PKD, which remained low in the PKD knockdown cells (Fig. 3-5A). Interestingly, in myocytes in which PKD was silenced, high Glu+PA was incapable of increasing LPL immunofluorescence (Fig. 3-5B) and activity (Fig. 3-5C) at the cardiomyocyte cell surface.

3.3.6. Hsp25 impedes the action PMA to phosphorylate PKCδ

As high Glu+PA induced a 1.4-fold increase in DAG (Con-2241±146, Glu+FA-3136±360 ng/10^6 cells; $P<0.05$), that is known to activate PKCδ, we incubated control myocytes with PMA, a DAG mimetic. Under our conditions, PMA was unable to phosphorylate PKCδ (Fig. 3-6B). We hypothesized that as Hsp25 masks the catalytic site of PKCδ(33), silencing of Hsp25 would permit PMA to promote phosphorylation of PKCδ. We validated successful Hsp25 inhibition using Western blotting (Fig. 3-6A, inset). In myocytes in which Hsp25 was silenced, PMA had no influence on total Hsp25, which remained low in the Hsp25 knockdown cells (Fig. 3-6A). Surprisingly, in these cells, PKCδ phosphorylation increased (Fig. 3-6B) with an associated amplification in its interaction with PKD (Fig. 3-6C). As predicted, in myocytes in which Hsp25 was silenced, PMA was now able to induce significant phosphorylation of PKCδ (Fig. 3-6B).

More importantly, in the presence of PMA, Hsp25 knockdown cells demonstrated a strong interaction between PKCδ and PKD (Fig. 3-6C).

3.3.7. Directly activating PKD enlarges the cardiomyocyte cell surface LPL pool

Given the relationship between PKD and LPL movement, we determined PKD phosphorylation in Hsp25 silenced myocytes. Simply knocking down Hsp25 augmented PKD phosphorylation (Fig. 3-7A), accelerated its translocation to the plasma membrane (Fig. 3-7B), and enlarged LPL immunofluorescence (Fig. 3-7B) and activity at the cardiomyocyte cell surface (Fig. 3-7C). In these cells, PMA brought about an even greater phosphorylation and translocation of PKD (Fig. 3-7A and 3-7B) with associated enlargement in LPL immunofluorescence (Fig. 3-7B) and activity (Fig. 3-7C).

3.3.8. PKD phosphorylation requires prior activation of PKCδ

PKCδ expression increased following infection with adenoviral vectors encoding WT and DN PKCδ (Fig. 3-8A). We have previously reported that overexpression of the DN PKCδ does not increase its activity(27). In PKCδ DN myocytes, high glucose and PA failed to increase phospho PKD (Fig. 3-8A) and completely abrogated the increase in heparin releasable LPL activity (Fig. 3-8B).

3.4. Discussion

During diabetes, when cardiac glucose uptake, glycolysis and pyruvate oxidation are impaired, the heart rapidly adapts to using FA exclusively for ATP generation(34). This change occurs not only as a consequence of increased FA supply (due to an increased release of FA from adipose tissue and hydrolysis of TG-rich lipoproteins by LPL), but also through an intrinsic adaptation/maladaptation to elevated FA that includes an augmented FA oxidation and expression of genes that control utilization of this substrate(35). Using retrograde perfusion of the heart with heparin to displace coronary LPL, we found significantly elevated luminal LPL activity following diabetes(14; 16; 21; 24). We determined that the increased enzyme at the vascular lumen is a consequence of transfer of enzyme from the cardiomyocyte cell surface to the apical side of the endothelial cell. Within the myocyte, recruitment of LPL to the cell surface was controlled by stress kinases like AMPK(28) and p38 MAPK that allowed for actin cytoskeleton polymerization, providing the cardiomyocyte with an infrastructure to facilitate LPL movement(19). In the present study, our data demonstrate that following diabetes induced by DZ or STZ, a cytosolic serine-threonine kinase, PKC-μ, otherwise known as PKD, is a key modulator of LPL vesicular trafficking within the cardiomyocyte.

Heat shock proteins (Hsps), also called stress proteins, are molecular chaperones that assist in protein folding, proper protein conformation, and targeting of proteins to degradative pathways(36; 37). Additionally, these stress proteins have been implicated in inhibiting cell death by multiple mechanisms including a direct interaction with cytochrome C and protein kinase C(33; 38). Recently, we have shown that Hsp can also affect cardiac metabolism by controlling the movement of cardiac LPL(19). Following diabetes, activation of cardiac AMPK and p38 MAPK, by a host of likely mechanisms {including the direct effects of FA(19), nitric

oxide mediated cytotoxicity(39) and augmentation of superoxide radicals(39; 40), and altered substrate utilization(34)}, facilitated Hsp25 phosphorylation. This allowed actin monomers to be released from Hsp25 to self-associate to form fibrillar actin, an infrastructure that allows LPL to traffic to the cardiomyocyte surface(19). In the current study, we tested whether Hsp25 can also affect PKD, an important kinase that regulates fission of vesicles from the golgi membrane(31). We demonstrate that with phosphorylation of Hsp25, its association with PKCδ is reduced, enabling PKCδ phosphorylation and activation. As PKCs (δ, ε, θ, η) can directly associate with the pleckstrin homology domain of PKD, allowing for its phosphorylation and activation(41), we determined the interaction between PKCδ and PKD. Interestingly, following DZ and phosphorylation of PKCδ, its interaction with PKD increased, facilitating phosphorylation and activation of the later kinase. As the increase in luminal LPL activity was closely associated to the robust phosphorylation of PKD, and as rottlerin, a PKCδ inhibitor prevented PKD phosphorylation and the subsequent increase in LPL, our data suggest that following diabetes, PKD is a key player responsible for fission of LPL vesicles for eventual transport to the cardiomyocyte cell surface. It should be noted that other studies have also reported an important contribution of PKCs towards LPL secretion in macrophages and adipocytes(42-44).

Diabetes is known to activate a number of PKC isoforms(45; 46). We attempted to activate PKC by duplicating the plasma concentrations of glucose and FA observed after DZ, and study its influence on cardiac LPL. Control myocytes were incubated with 20 mM glucose and 1.5 mM PA. Although high glucose or PA by themselves had no influence on myocyte LPL, their combination induced a robust increase in myocyte cell surface LPL activity. Given that in the presence of high glucose, unsaturated FA like oleic cid build up as TG whereas saturated FA like PA are diverted towards 1,2-DAG(47), whose downstream signaling includes activation of the

PKC super family of enzymes(46; 48), we measured levels of this lipid intermediate and report a 1.4 fold increase in myocytes treated with high Glu+PA. Interestingly, similar to DZ, the increase in LPL in myocytes treated with high Glu+PA closely mirrored the increase in phosphorylation of PKCδ and PKD. The zinc-finger domain of PKD is known to interact with trans-golgi membranes, allowing for fission of vesicles(31; 49). In addition, activation of PKD is also suggested to promote recruitment of VAMP(32), which helps with vesicle exocytosis and movement along the actin filament network to reach the cell surface. As silencing of PKD prevented the ability of high Glu+PA to increase cell surface LPL, our data suggest that by increasing DAG and promoting activation PKCδ, PKD is the eventual trigger that enables the cardiomyocyte LPL secretory pathway to turn on.

An alternate strategy to activate PKC is to use PMA, a DAG mimetic that is known to phosphorylate PKC(46; 50). Interestingly, in cardiomyocytes, we were unable to observe activation of PKCδ by PMA, an observation that was previously reported(50). In this setting, PMA was also unable to affect PKD. Given the observation that Hsp25 can prevent activation of PKCδ through a direct interaction(33), we knocked down Hsp25 using siRNA. In myocytes in which Hsp25 was silenced, PKCδ and PKD phosphorylation increased, and so did LPL activity. Interestingly, when these myocytes were now exposed to PMA, there was a further phosphorylation of PKCδ, an appreciable association between PKCδ and PKD, and a vigorous activation of PKD. As these cells also demonstrated an additional increase in cell surface LPL activity, and as a mutant form of PKCδ prevented PKD activation and increase in LPL activity observed with high glucose and palmitic acid, our data imply that following diabetes, PKD control of cardiomyocyte LPL activity requires dissociation of Hsp25 from PKCδ, activation of PKCδ by DAG, association between PKCδ and PKD, and vesicular transport of LPL.

In summary, following diabetes, when cardiac glucose utilization is impaired, the heart undergoes metabolic transformation wherein it switches energy production to exclusive β-oxidation of FA. One way by which this process is made possible is through amplification of coronary LPL, thereby allowing uninterrupted FA supply to the diabetic heart. Recruitment of LPL to the cardiomyocyte cell surface and eventually the vascular lumen could represent an immediate compensatory response by the heart to guarantee FA supply. The mechanism underlying this process embraces myocyte increase in actin cytoskeleton polymerization (through an AMPK/p38 MAPK pathway)(19) and PKD control of LPL vesicle formation and movement (Fig. 3-8C). Increasing FA uptake through overexpression of cardiac human LPL(51) or fatty acid transport protein(52), or augmenting FA oxidation through overexpression of cardiac PPAR-α(53) or long-chain acyl CoA synthase(54) results in a cardiac phenotype resembling diabetic cardiomyopathy. Thus, results from the present study could help in restricting or slowing cardiac LPL translocation and could lead to strategies that overcome contractile dysfunction following diabetes.

3.5. Limitations of the study

One limitation of this and other studies(4; 55-59) is that when examining the lipotoxic effects of palmitic acid on the heart, most studies have used *in vitro* incubations with 1-1.5 mM PA to duplicate the plasma concentration of total FFA observed with diabetes. Given that albumin-bound PA only makes up a fraction of the total plasma FFA, the concentration of PA used may be higher than the actual circulating amount bound to albumin. However, it should be noted that FA derived from the albumin bound fraction does not account for all of the FA provided to the heart. Thus, other physiologically relevant sources like hydrolysis of lipoproteins by cardiac LPL, which has a selective affinity towards palmitic acid containing lipoproteins (47.5% of total

fatty acids released)(60), also play some role in the provision of PA. This is particularly important as: i) LPL increases in the DZ diabetic heart, ii) the molar concentrations of FA in lipoproteins are approximately 10-fold higher than that of FA bound to albumin(7), and iii) circulating plasma TG concentrations increase following DZ. As intracellular TG and membrane phospholipids are also potential sources of PA, a true measure of the effects of PA and glucose on cardiac LPL would only be possible if all of these sources of PA are determined following diabetes induced by DZ.

Tables and figures

Table 3-1. General characteristics of the animals

	Control	DZ 1hr	DZ 4hr
Glucose (mM)	**6.9 ± 0.8**	**14.7 ± 1.2***	**17.5 ± 0.4***
FA (mM)	**0.43 ± 0.07**	**1.48 ± 0.08***	**1.5 ± 0.1***
LPL activity (nmol/ml/h)	**398 ± 59**	**712 ±43***	**1568 ± 89***

Values are means ± SE for 4 animals in each group. Animals were treated with diazoxide (DZ-1 and 4hr), blood samples collected, and plasma glucose and fatty acids (FA) determined. At the indicated times with DZ, hearts were also isolated and coronary luminal LPL released with heparin. Some animals were also made diabetic with sterptozotocin (STZ) and kept for 1 (plasma glucose 18.7 ± 1.1) and 7 (plasma glucose 19.6 ± 2) days. Although plasma FA was not measured following STZ, LPL activity in these animals is documented in Fig. 3-1. *Significantly different from untreated control, $P < 0.05$.

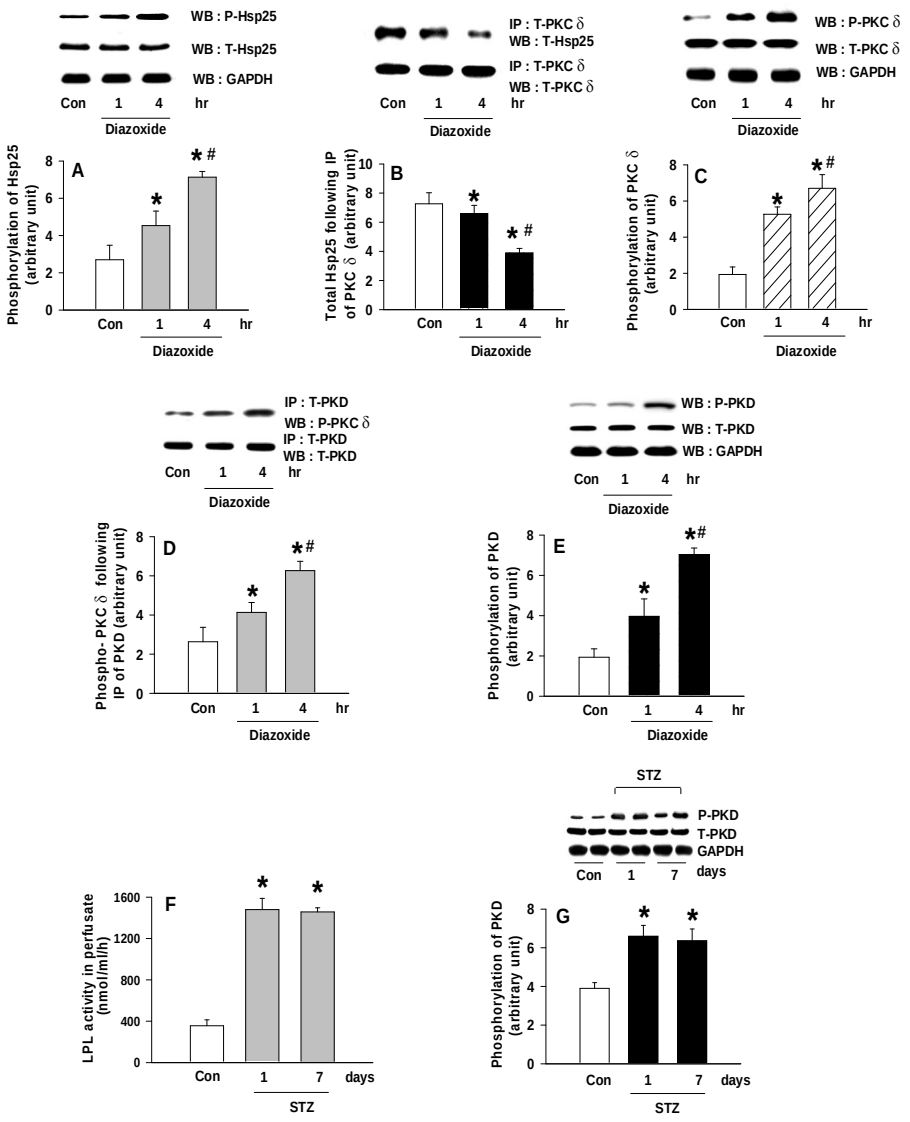

Fig. 3-1 *Acute diabetes elicits robust activation of cardiomyocyte PKD through dissociation of PKCδ from its complex with Hsp25*. Animals were treated with DZ, and at the indicated times, hearts from control and DZ treated animals were isolated. Thereafter, total or phosphorylated Hsp25 (A), PKCδ (C), and PKD (E) were determined using Western blotting. To examine the association between PKCδ and Hsp25, PKCδ was immunoprecipitated using a PKCδ antibody, the immunocomplex separated into two equal portions, and each portion immunoblotted with anti-Hsp25 or anti-PKCδ (to confirm that equal amount of PKCδ was immunoprecipitated) (B). The association between phospho-PKCδ and PKD was determined using a PKD antibody, the immunocomplex separated into two equal portions, and each portion immunoblotted with anti phospho-PKCδ or anti-PKD (D). Heparin-releasable LPL activity (F) and PKD (G) in hearts from animals made diabetic with streptozotocin (STZ) for 1 and 7 days is also illustrated. Results are the means ± SE of 3-5 rats in each group. *Significantly different from control; #Significantly different from DZ-1h, $P < 0.05$. WB-western blot; P-phosphorylated; T-total; IP-immunoprecipitation; Con-control.

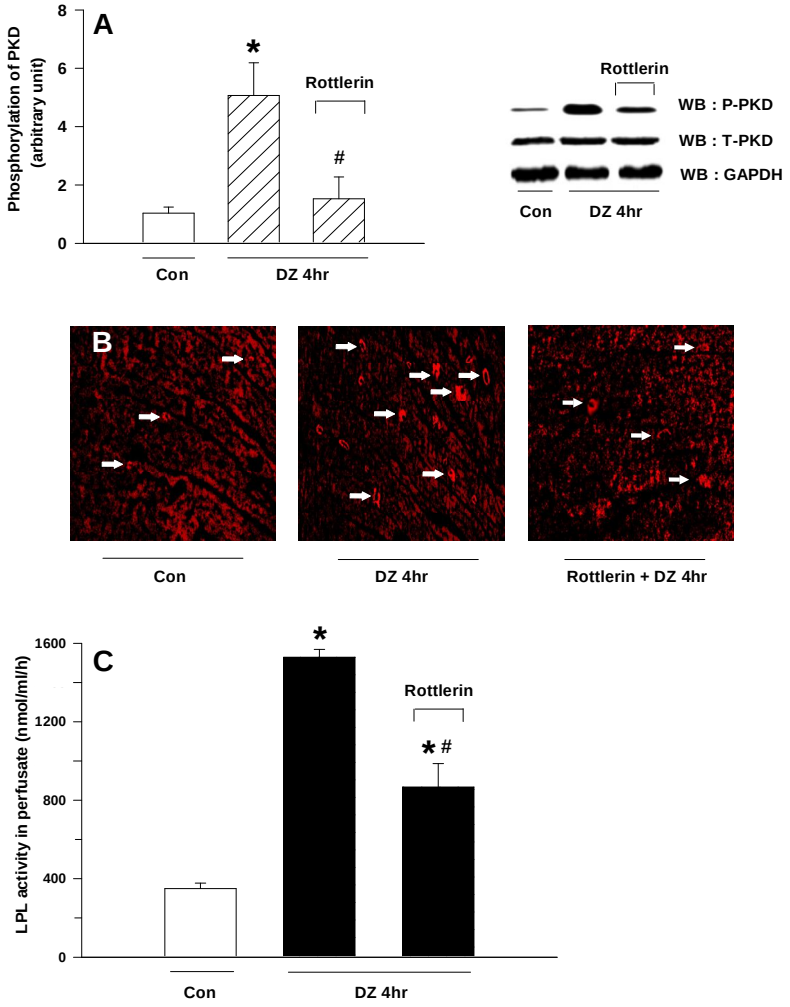

Fig. 3-2 *Inhibition of PKD phosphorylation reduces the diabetes induced augmentation of coronary LPL activity*. Animals were pretreated with rottlerin for 45 min prior to administration of diazoxide (DZ). Animals were killed 4 hr subsequent to DZ injection and hearts isolated for determination of PKD and LPL. Total and phosphorylated PKD were assessed using Western blotting (A). Fig. 3-2B is a representative photograph showing the effect of rottlerin on LPL immunofluorescence as visualized by fluorescent microscopy. Heart sections were fixed, incubated with the polyclonal chicken antibody against bovine LPL followed by incubations with biotinylated rabbit anti-chicken IgG and streptavidin-conjugated Cy3 fluorescent probe respectively. Majority of LPL in the DZ heart was present at the coronary lumen (arrows). To estimate this LPL, hearts were isolated and perfused in the nonrecirculating retrograde mode. Thereafter, coronary LPL was released with heparin. Coronary effluents were collected (for 10 s) at different time points over 10 mins (only the peak value is shown). LPL activity was assayed using radiolabeled triolein. Results are the means ± SE of 3-5 rats in each group. *Significantly different from control; #Significantly different from DZ alone, $P < 0.05$.

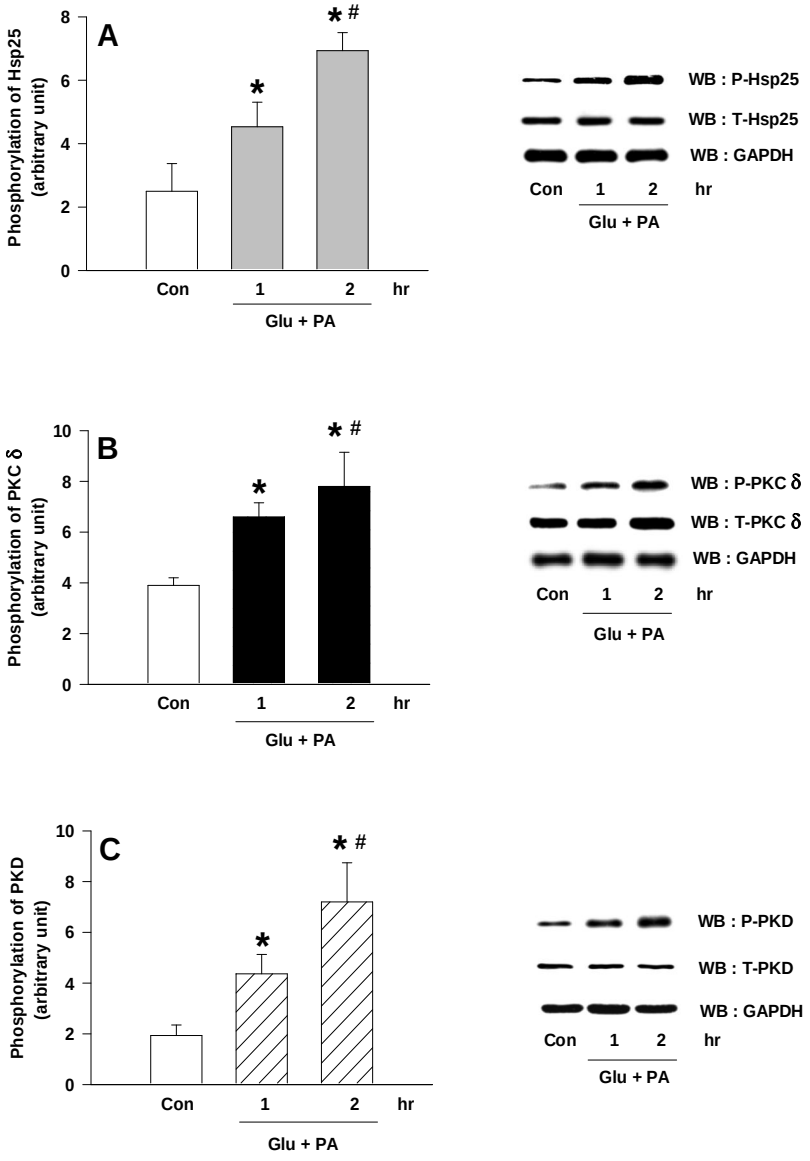

Fig. 3-3 *Mimicking diabetes in vitro using high glucose and fatty acid increases cardiomyocyte phosphorylation of Hsp25, PKCδ, and PKD.* Cardiomyocytes were plated on laminin-coated culture plates. Cells were maintained using Media-199, and incubated at 37°C under an atmosphere of 95% O_2/5% CO_2 for 16 hours. Subsequently, glucose (Glu, 20 mM) and palmitic acid (PA, 1.5 mM) were added to the culture medium. At the indicated times, protein was extracted to determine both total and phosphorylated Hsp25 (A), PKCδ (B), and PKD (C) using Western Blotting. Data are means ± SE. n=3 myocyte preparations from different animals. *Significantly different from Con; #Significantly different from Glu+PA-1h, $P < 0.05$.

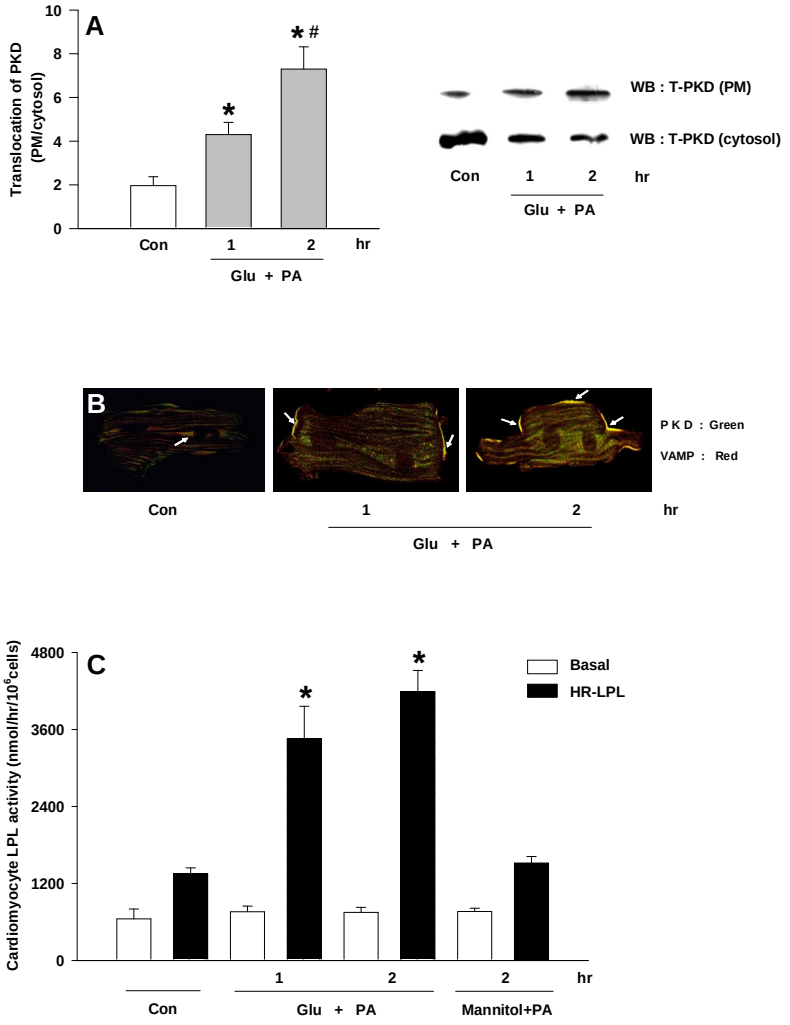

Fig. 3-4 *High glucose and fatty acid induced translocation of PKD is associated with increasing cardiomyocyte heparin-releasable LPL activity*. Following high glucose and palmitic acid added to the culture medium for 1 and 2 hr respectively, cardiomyocyte homogenates were prepared. Homogenates were subjected to cytosolic and membrane separation. Identification of total PKD protein was carried out using polyclonal rabbit PKD as the primary and goat anti-rabbit horseradish peroxidase as the secondary antibody (A). Representative photograph showing the effect of high glucose and PA on PKD immunofluorescence as visualized by a Zeiss Pascal confocal microscope (panel B). Cardiomyocytes were fixed, incubated with primary antibodies (rabbit polyclonal PKD and goat polyclonal VAMP) followed by incubation with secondary antibodies [goat anti-rabbit IgG-FITC (green) and donkey anti-goat IgG-TR (red)]. LPL activity in control and high glucose/mannitol and PA treated cardiomyocytes was determined by adding heparin (8 U/ml for 1 min) to the incubation medium, and the release of surface-bound LPL activity into the medium determined (C). Data are means ± SE. n=3 myocyte preparations from different animals. *Significantly different from Con; #Significantly different from Glu+PA-1h, $P < 0.05$.

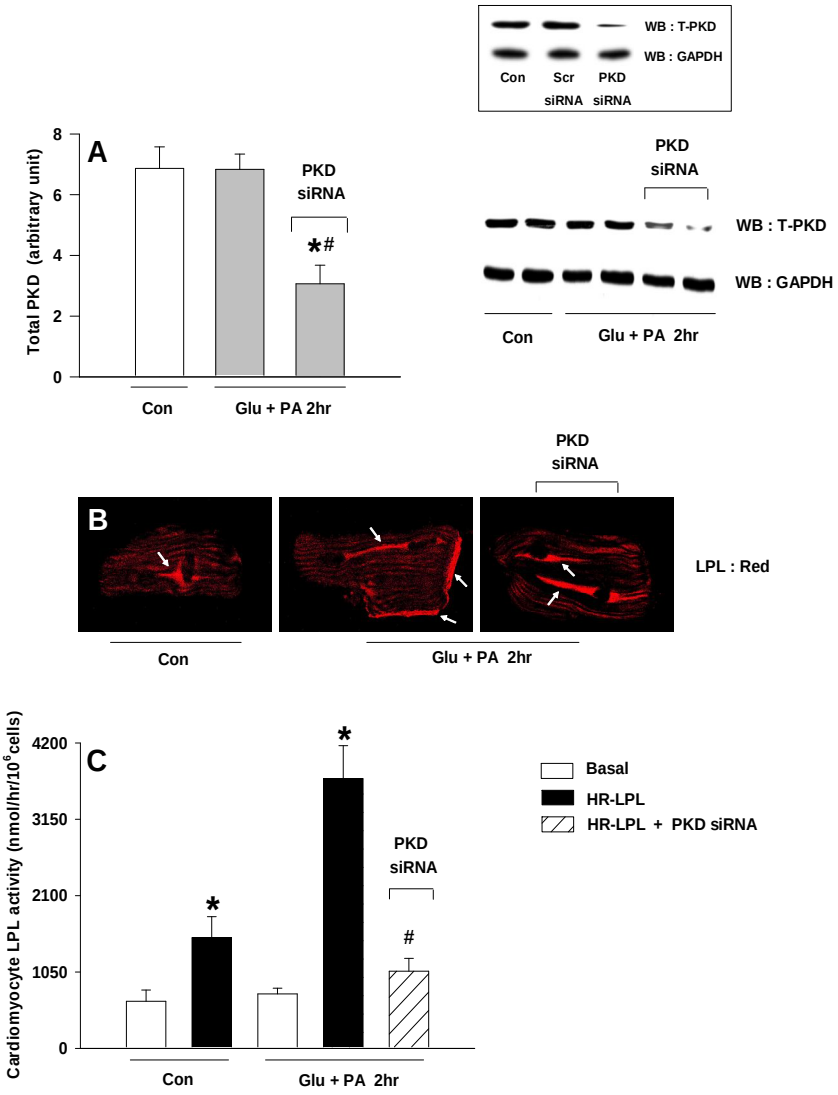

Fig. 3-5 *Silencing of PKD prevents cardiomyocyte LPL recruitment to the plasma membrane observed with high glucose and fatty acid.* siRNA transfection of PKD in cardiomyocytes was performed using a kit from Santa Cruz. Plated myocytes were exposed to the siRNA (or scrambled, Scr). The inset depicts transfection efficiency. After this, high glucose and palmitic acid were added to the culture medium for 2 hr and protein was extracted to confirm expression level of PKD (A). To determine the relationship between PKD and LPL, LPL immunofluorescence in myocytes from the different groups was visualized by a confocal microscope. Cardiomyocytes were fixed, incubated with the polyclonal chicken antibody against bovine LPL followed by incubations with biotinylated rabbit anti-chicken IgG and a streptavidin-conjugated Cy3 fluorescent probe (B). LPL activity was determined by adding heparin (8 U/ml) to the incubation medium, and the release of surface-bound LPL activity into the medium determined (C). Data are means ± SE. n=3 myocyte preparations from different animals. *Significantly different from Con; #Significantly different from Glu+PA-2h, $P < 0.05$.

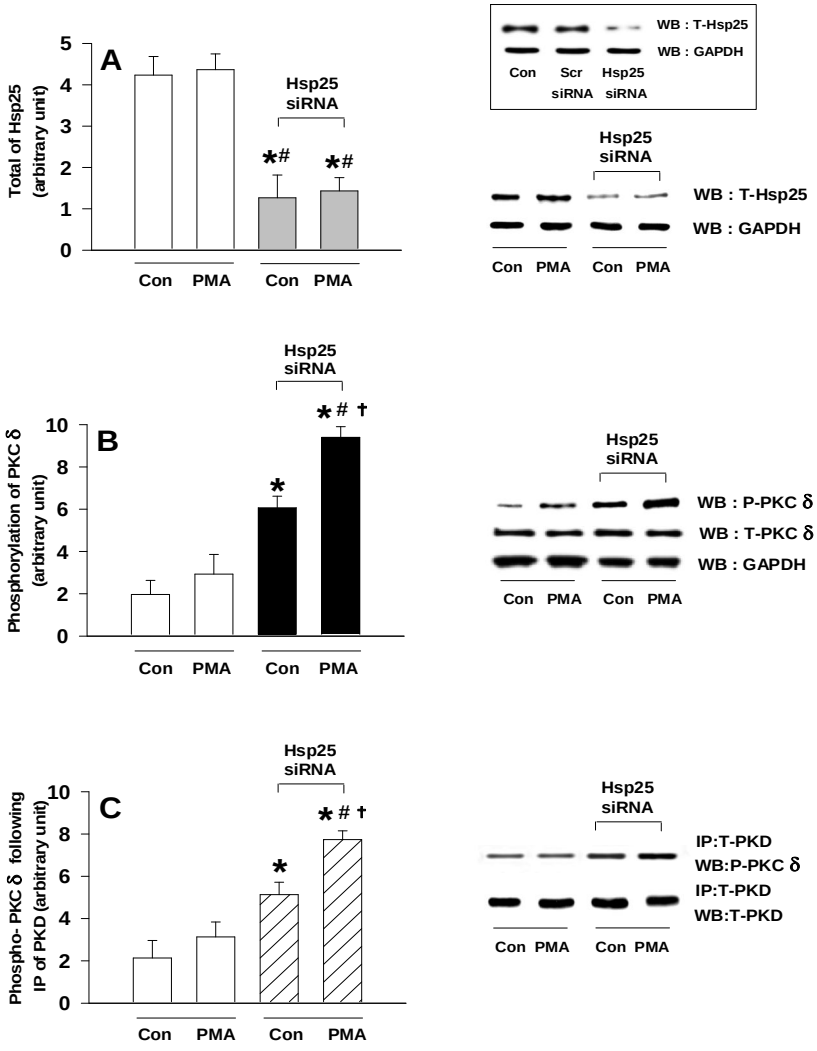

Fig. 3-6 *Cardiomyocyte PKCδ activation by PMA is only evident after silencing of Hsp25.* siRNA transfection of Hsp25 in cardiomyocytes was performed using a kit from Santa Cruz. Plated myocytes were exposed to the siRNA (or scrambled, Scr). The inset depicts transfection efficiency. After transfection, cells were treated with or without PMA (1 μM, 15 min), lysed and subjected to Western blotting for evaluating Hsp25 (A) and total or phosphorylated PKCδ (B). The association between PKCδ and PKD was determined using a PKD antibody, the immunocomplex separated into two equal portions, and each portion immunoblotted with anti-PKCδ or anti-PKD (C). Data are means ± SE. n=3 myocyte preparations from different animals. *Significantly different from unsilenced Hsp25-Con; #Significantly different from unsilenced Hsp25 + PMA, †Significantly different from silenced Hsp25-Con, $P < 0.05$. PMA, phorbol 12-myristate 13-acetate.

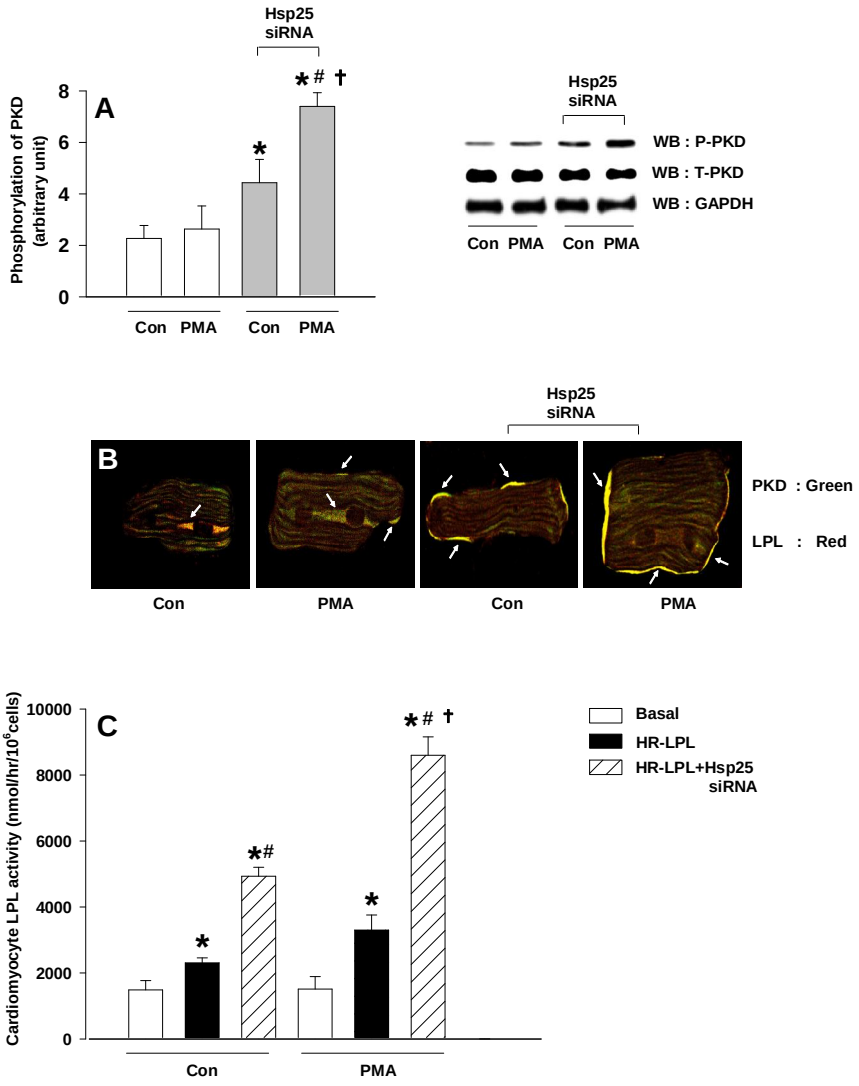

Fig. 3-7 *Augmenting PKD phosphorylation by PMA in Hsp25 silenced cardiomyocytes substantially increases LPL movement to the plasma membrane.* After transfection of Hsp25 siRNA, cells treated with or without PMA (1 μM, 15min) were used to determine total or phosphorylated PKD using Western blotting (A). In some experiments, cells were fixed, incubated with primary antibodies (rabbit polyclonal PKD and polyclonal chicken antibody against bovine LPL) followed by incubation with secondary antibodies [goat anti-rabbit IgG-FITC (green) and rabbit anti-chicken IgG with streptavidin-conjugated Cy3 fluorescent probe (red)] and visualized with a confocal microscope (B). LPL activity was determined by adding heparin (8 U/ml) to the incubation medium, and the release of surface-bound LPL activity into the medium determined (C). *Significantly different from unsilenced Hsp25-Con; #Significantly different from unsilenced Hsp25 + PMA treated, †Significantly different from silenced Hsp25-Con, $P < 0.05$.

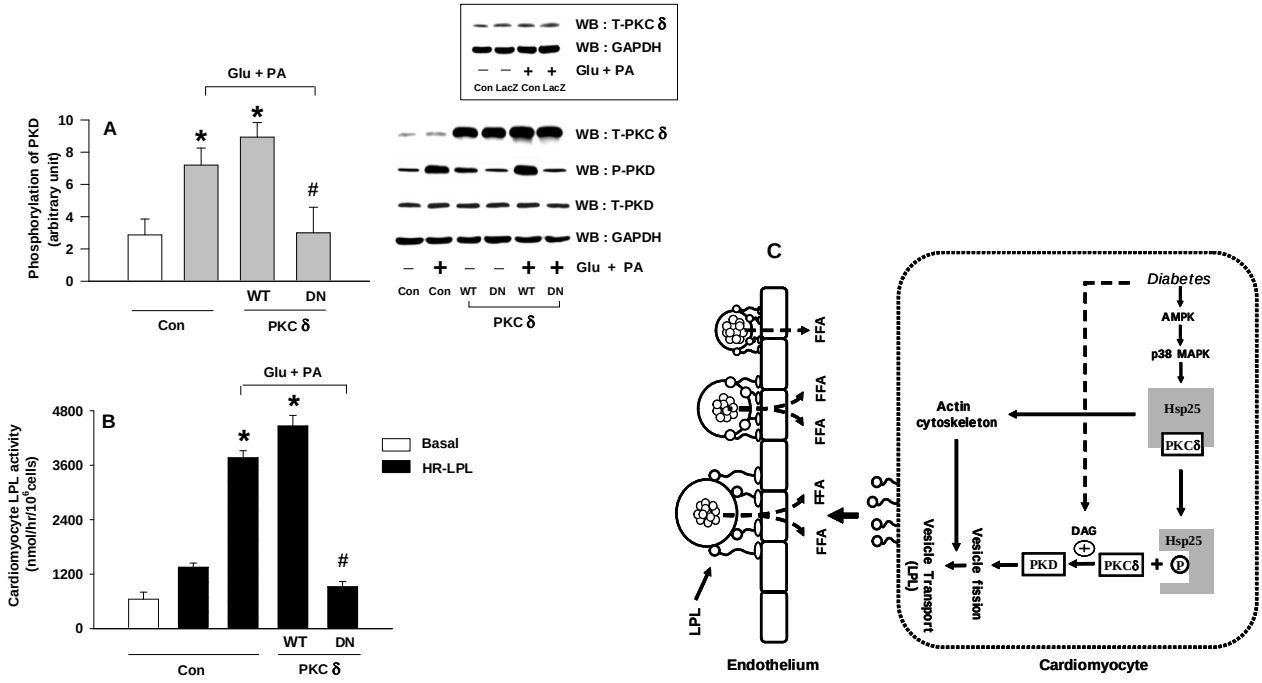

Fig. 3-8 *Protein kinase D is a key regulator of cardiomyocyte LPL secretion following diabetes and requires prior activation of PKCδ.* Cardiomyocytes were infected with recombinant adenovirus vectors carrying wild-type (WT) PKCδ and dominant-negative (DN) PKCδ. Mock infection as a control was performed using LacZ (inset). Infected cells were incubated for a further 36 hours before treatment in the absence or presence of high glucose and palmitic acid (2h). Phosphorylated PKD (A) and heparin releasable LPL activity (B) was subsequently determined. *Significantly different from untreated Con; #Significantly different from WT PKCδ, $P < 0.05$. Schematic mechanism of how diabetes regulates cardiomyocyte LPL is depicted in C. Following diabetes and development of hyperglycemia and hyperlipidemia, AMPK/p38 MAPK induced formation of actin cytoskeleton together with dissociation of PKCδ from its complex with Hsp25 allows DAG to activate PKD. PKD is responsible for vesicle formation, allowing LPL to be transported along the actin cytoskeleton network and eventually bind to HSPGs on the plasma membrane. From here, LPL is transported onto similar HSPG-binding sites on the luminal surface of the capillary endothelium. At this location, hydrolysis of circulating lipoprotein-TG occurs, providing FA to the underlying cardiomyocyte.

3.6. Bibliography

1. Avogaro A, Nosadini R, Doria A, Fioretto P, Velussi M, Vigorito C, Sacca L, Toffolo G, Cobelli C, Trevisan R, et al.: Myocardial metabolism in insulin-deficient diabetic humans without coronary artery disease. *Am J Physiol* 258:E606-618, 1990

2. Saddik M, Lopaschuk GD: Myocardial triglyceride turnover and contribution to energy substrate utilization in isolated working rat hearts. *J Biol Chem* 266:8162-8170, 1991

3. Lopaschuk GD, Belke DD, Gamble J, Itoi T, Schonekess BO: Regulation of fatty acid oxidation in the mammalian heart in health and disease. *Biochim Biophys Acta* 1213:263-276, 1994

4. Paulson DJ, Crass MF, 3rd: Endogenous triacylglycerol metabolism in diabetic heart. *Am J Physiol* 242:H1084-1094, 1982

5. Haffner SM: Lipoprotein disorders associated with type 2 diabetes mellitus and insulin resistance. *Am J Cardiol* 90:55i-61i, 2002

6. Blanchette-Mackie EJ, Masuno H, Dwyer NK, Olivecrona T, Scow RO: Lipoprotein lipase in myocytes and capillary endothelium of heart: immunocytochemical study. *Am J Physiol* 256:E818-828, 1989

7. Merkel M, Eckel RH, Goldberg IJ: Lipoprotein lipase: genetics, lipid uptake, and regulation. *J Lipid Res* 43:1997-2006, 2002

8. Augustus AS, Kako Y, Yagyu H, Goldberg IJ: Routes of FA delivery to cardiac muscle: modulation of lipoprotein lipolysis alters uptake of TG-derived FA. *Am J Physiol Endocrinol Metab* 284:E331-339, 2003

9. Camps L, Reina M, Llobera M, Vilaro S, Olivecrona T: Lipoprotein lipase: cellular origin and functional distribution. *Am J Physiol* 258:C673-681, 1990

10. Eckel RH: Lipoprotein lipase. A multifunctional enzyme relevant to common metabolic diseases. *N Engl J Med* 320:1060-1068, 1989

11. Pillarisetti S, Paka L, Sasaki A, Vanni-Reyes T, Yin B, Parthasarathy N, Wagner WD, Goldberg IJ: Endothelial cell heparanase modulation of lipoprotein lipase activity. Evidence that heparan sulfate oligosaccharide is an extracellular chaperone. *J Biol Chem* 272:15753-15759, 1997

12. Blanchette-Mackie EJ, Dwyer NK, Amende LA: Cytochemical studies of lipid metabolism: immunogold probes for lipoprotein lipase and cholesterol. *Am J Anat* 185:255-263, 1989

13. Rodrigues B, Cam MC, McNeill JH: Myocardial substrate metabolism: implications for diabetic cardiomyopathy. *J Mol Cell Cardiol* 27:169-179, 1995

14. Pulinilkunnil T, Abrahani A, Varghese J, Chan N, Tang I, Ghosh S, Kulpa J, Allard M, Brownsey R, Rodrigues B: Evidence for rapid "metabolic switching" through lipoprotein lipase occupation of endothelial-binding sites. *J Mol Cell Cardiol* 35:1093-1103, 2003

15. Sambandam N, Abrahani MA, St Pierre E, Al-Atar O, Cam MC, Rodrigues B: Localization of lipoprotein lipase in the diabetic heart: regulation by acute changes in insulin. *Arterioscler Thromb Vasc Biol* 19:1526-1534, 1999

16. Sambandam N, Abrahani MA, Craig S, Al-Atar O, Jeon E, Rodrigues B: Metabolism of VLDL is increased in streptozotocin-induced diabetic rat hearts. *Am J Physiol Heart Circ Physiol* 278:H1874-1882, 2000

17. Qi D, Kuo KH, Abrahani A, An D, Qi Y, Heung J, Kewalramani G, Pulinilkunnil T, Ghosh S, Innis SM, Rodrigues B: Acute intralipid infusion reduces cardiac luminal lipoprotein lipase but recruits additional enzyme from cardiomyocytes. *Cardiovasc Res* 72:124-133, 2006

18. Pulinilkunnil T, An D, Ghosh S, Qi D, Kewalramani G, Yuen G, Virk N, Abrahani A, Rodrigues B: Lysophosphatidic acid-mediated augmentation of cardiomyocyte lipoprotein lipase involves actin cytoskeleton reorganization. *Am J Physiol Heart Circ Physiol* 288:H2802-2810, 2005

19. Kim MS, Kewalramani G, Puthanveetil P, Lee V, Kumar U, An D, Abrahani A, Rodrigues B: Acute diabetes moderates trafficking of cardiac lipoprotein lipase through p38 mitogen-activated protein kinase-dependent actin cytoskeleton organization. *Diabetes* 57:64-76, 2008

20. Foy JM, Furman BL: Effect of single dose administration of diuretics on the blood sugar of alloxan-diabetic mice or mice made hyperglycaemic by the acute administration of diazoxide. *Br J Pharmacol* 47:124-132, 1973

21. Pulinilkunnil T, Qi D, Ghosh S, Cheung C, Yip P, Varghese J, Abrahani A, Brownsey R, Rodrigues B: Circulating triglyceride lipolysis facilitates lipoprotein lipase translocation from cardiomyocyte to myocardial endothelial lining. *Cardiovasc Res* 59:788-797, 2003

22. Schafer G, Portenhauser R, Trolp R: Inhibition of mitochondrial metabolism by the diabetogenic thiadiazine diazoxide. I. Action on succinate dehydrogenase and TCA-cycle oxidations. *Biochem Pharmacol* 20:1271-1280, 1971

23. Song J, Li J, Lulla A, Evers BM, Chung DH: Protein kinase D protects against oxidative stress-induced intestinal epithelial cell injury via Rho/ROK/PKC-delta pathway activation. *Am J Physiol Cell Physiol* 290:C1469-1476, 2006

24. Rodrigues B, Cam MC, Jian K, Lim F, Sambandam N, Shepherd G: Differential effects of streptozotocin-induced diabetes on cardiac lipoprotein lipase activity. *Diabetes* 46:1346-1353, 1997

25. Haworth RS, Roberts NA, Cuello F, Avkiran M: Regulation of protein kinase D activity in adult myocardium: novel counter-regulatory roles for protein kinase Cepsilon and protein kinase A. *J Mol Cell Cardiol* 43:686-695, 2007

26. Pulinilkunnil T, An D, Yip P, Chan N, Qi D, Ghosh S, Abrahani A, Rodrigues B: Palmitoyl lysophosphatidylcholine mediated mobilization of LPL to the coronary luminal surface requires PKC activation. *J Mol Cell Cardiol* 37:931-938, 2004

27. Wang L, Rolfe M, Proud CG: Ca(2+)-independent protein kinase C activity is required for alpha1-adrenergic-receptor-mediated regulation of ribosomal protein S6 kinases in adult cardiomyocytes. *Biochem J* 373:603-611, 2003

28. An D, Pulinilkunnil T, Qi D, Ghosh S, Abrahani A, Rodrigues B: The metabolic "switch" AMPK regulates cardiac heparin-releasable lipoprotein lipase. *Am J Physiol Endocrinol Metab* 288:E246-253, 2005

29. Innis SM, Dyer RA: Brain astrocyte synthesis of docosahexaenoic acid from n-3 fatty acids is limited at the elongation of docosapentaenoic acid. *J Lipid Res* 43:1529-1536, 2002

30. Li W, Zhang J, Bottaro DP, Pierce JH: Identification of serine 643 of protein kinase C-delta as an important autophosphorylation site for its enzymatic activity. *J Biol Chem* 272:24550-24555, 1997

31. Van Lint J, Rykx A, Maeda Y, Vantus T, Sturany S, Malhotra V, Vandenheede JR, Seufferlein T: Protein kinase D: an intracellular traffic regulator on the move. *Trends Cell Biol* 12:193-200, 2002

32. Lu G, Chen J, Espinoza LA, Garfield S, Toshiyuki S, Akiko H, Huppler A, Wang QJ: Protein kinase D 3 is localized in vesicular structures and interacts with vesicle-associated membrane protein 2. *Cell Signal* 19:867-879, 2007

33. Lee YJ, Lee DH, Cho CK, Bae S, Jhon GJ, Lee SJ, Soh JW, Lee YS: HSP25 inhibits protein kinase C delta-mediated cell death through direct interaction. *J Biol Chem* 280:18108-18119, 2005

34. An D, Rodrigues B: Role of changes in cardiac metabolism in development of diabetic cardiomyopathy. *Am J Physiol Heart Circ Physiol* 291:H1489-1506, 2006

35. Taegtmeyer H, McNulty P, Young ME: Adaptation and maladaptation of the heart in diabetes: Part I: general concepts. *Circulation* 105:1727-1733, 2002

36. Liberek K, Lewandowska A, Zietkiewicz S: Chaperones in control of protein disaggregation. *Embo J* 27:328-335, 2008

37. Wisen S, Gestwicki JE: Identification of small molecules that modify the protein folding activity of heat shock protein 70. *Anal Biochem* 374:371-377, 2008

38. Gorman AM, Szegezdi E, Quigney DJ, Samali A: Hsp27 inhibits 6-hydroxydopamine-induced cytochrome c release and apoptosis in PC12 cells. *Biochem Biophys Res Commun* 327:801-810, 2005

39. Okuyama R, Fujiwara T, Ohsumi J: High glucose potentiates palmitate-induced NO-mediated cytotoxicity through generation of superoxide in clonal beta-cell HIT-T15. *FEBS Lett* 545:219-223, 2003

40. Cheng A, Chan SL, Milhavet O, Wang S, Mattson MP: p38 MAP kinase mediates nitric oxide-induced apoptosis of neural progenitor cells. *J Biol Chem* 276:43320-43327, 2001

41. Wang QJ: PKD at the crossroads of DAG and PKC signaling. *Trends Pharmacol Sci* 27:317-323, 2006

42. Maingrette F, Renier G: Leptin increases lipoprotein lipase secretion by macrophages: involvement of oxidative stress and protein kinase C. *Diabetes* 52:2121-2128, 2003

43. Ranganathan G, Song W, Dean N, Monia B, Barger SW, Kern PA: Regulation of lipoprotein lipase by protein kinase C alpha in 3T3-F442A adipocytes. *J Biol Chem* 277:38669-38675, 2002

44. Ranganathan G, Kaakaji R, Kern PA: Role of protein kinase C in the translational regulation of lipoprotein lipase in adipocytes. *J Biol Chem* 274:9122-9127, 1999

45. Aronson D: Hyperglycemia and the pathobiology of diabetic complications. *Adv Cardiol* 45:1-16, 2008

46. Das Evcimen N, King GL: The role of protein kinase C activation and the vascular complications of diabetes. *Pharmacol Res* 55:498-510, 2007

47. Inoguchi T, Xia P, Kunisaki M, Higashi S, Feener EP, King GL: Insulin's effect on protein kinase C and diacylglycerol induced by diabetes and glucose in vascular tissues. *Am J Physiol* 267:E369-379, 1994

48. Montell E, Turini M, Marotta M, Roberts M, Noe V, Ciudad CJ, Mace K, Gomez-Foix AM: DAG accumulation from saturated fatty acids desensitizes insulin stimulation of glucose uptake in muscle cells. *Am J Physiol Endocrinol Metab* 280:E229-237, 2001

49. Bossard C, Bresson D, Polishchuk RS, Malhotra V: Dimeric PKD regulates membrane fission to form transport carriers at the TGN. *J Cell Biol* 179:1123-1131, 2007

50. Markou T, Yong CS, Sugden PH, Clerk A: Regulation of protein kinase C delta by phorbol ester, endothelin-1, and platelet-derived growth factor in cardiac myocytes. *J Biol Chem* 281:8321-8331, 2006

51. Yagyu H, Chen G, Yokoyama M, Hirata K, Augustus A, Kako Y, Seo T, Hu Y, Lutz EP, Merkel M, Bensadoun A, Homma S, Goldberg IJ: Lipoprotein lipase (LpL) on the surface of cardiomyocytes increases lipid uptake and produces a cardiomyopathy. *J Clin Invest* 111:419-426, 2003

52. Chiu HC, Kovacs A, Blanton RM, Han X, Courtois M, Weinheimer CJ, Yamada KA, Brunet S, Xu H, Nerbonne JM, Welch MJ, Fettig NM, Sharp TL, Sambandam N, Olson KM, Ory DS, Schaffer JE: Transgenic expression of fatty acid transport protein 1 in the heart causes lipotoxic cardiomyopathy. *Circ Res* 96:225-233, 2005

53. Finck BN, Lehman JJ, Leone TC, Welch MJ, Bennett MJ, Kovacs A, Han X, Gross RW, Kozak R, Lopaschuk GD, Kelly DP: The cardiac phenotype induced by PPARalpha overexpression mimics that caused by diabetes mellitus. *J Clin Invest* 109:121-130, 2002

54. Chiu HC, Kovacs A, Ford DA, Hsu FF, Garcia R, Herrero P, Saffitz JE, Schaffer JE: A novel mouse model of lipotoxic cardiomyopathy. *J Clin Invest* 107:813-822, 2001

55. King LM, Sidell RJ, Wilding JR, Radda GK, Clarke K: Free fatty acids, but not ketone bodies, protect diabetic rat hearts during low-flow ischemia. *Am J Physiol Heart Circ Physiol* 280:H1173-1181, 2001

56. Hafstad AD, Solevag GH, Severson DL, Larsen TS, Aasum E: Perfused hearts from Type 2 diabetic (db/db) mice show metabolic responsiveness to insulin. *Am J Physiol Heart Circ Physiol* 290:H1763-1769, 2006

57. Fauconnier J, Andersson DC, Zhang SJ, Lanner JT, Wibom R, Katz A, Bruton JD, Westerblad H: Effects of palmitate on Ca(2+) handling in adult control and ob/ob cardiomyocytes: impact of mitochondrial reactive oxygen species. *Diabetes* 56:1136-1142, 2007

58. Mazumder PK, O'Neill BT, Roberts MW, Buchanan J, Yun UJ, Cooksey RC, Boudina S, Abel ED: Impaired cardiac efficiency and increased fatty acid oxidation in insulin-resistant ob/ob mouse hearts. *Diabetes* 53:2366-2374, 2004

59. Chen V, Bagby GJ, Spitzer JJ: Exogenous substrate utilization by isolated myocytes from chronically diabetic rats. *Am J Physiol* 245:C46-51, 1983

60. Sato K, Takahashi T, Takahashi Y, Shiono H, Katoh N, Akiba Y: Preparation of chylomicrons and VLDL with monoacid-rich triacylglycerol and characterization of kinetic parameters in lipoprotein lipase-mediated hydrolysis in chickens. *J Nutr* 129:126-131, 1999

4. Cleavage of protein kinase D following acute hypoinsulinemia prevents excessive LPL-mediated cardiac triglyceride accumulation[3]

4.1. Introduction

Cardiac muscle has a high demand for energy and can use multiple substrates(1). Among these, glucose (~30%) and fatty acid (FA, ~70%) are the major sources from which the heart derives most of its energy(2). FA delivery and utilization by the heart involves: i) release from adipose tissue and transport to the heart after complexing with albumin(3), ii) provision through the breakdown of endogenous cardiac triglyceride (TG)(4), iii) internalization of whole lipoproteins(5), and iv) hydrolysis of circulating TG-rich lipoproteins to FA by lipoprotein lipase (LPL) positioned at the endothelial surface of the coronary lumen(6). The molar concentration of FA bound to albumin is ~10-fold less than that of FA in lipoprotein-TG(7) and LPL-mediated hydrolysis of TG-rich lipoproteins is suggested to be the principal source of FA for cardiac utilization(8). Coronary endothelial cells do not synthesize LPL(9). In the heart, this enzyme is produced in cardiomyocytes and subsequently secreted onto heparan sulphate proteoglycan (HSPG) binding sites on the myocyte cell surface(10). From here, LPL is transported onto comparable binding sites on the luminal surface of endothelial cells(11). At the lumen, LPL actively metabolizes the TG core of lipoproteins; the released FA's are then transported into the heart.

The earliest change that occurs in the Type 1 diabetic heart is altered energy metabolism

[3]A version of this chapter has been published. **Kim, M**., Wang, F., Puthanveetil, P., Kewalramani, G., Marzban, L., Steinberg, S.F., Webber, T.D., Kieffer, T.J., Abrahani, A., and Rodrigues, B. (2009) Cleavage of protein kinase D following acute hypoinsulinemia prevents excessive LPL mediated triglyceride accumulation. **Diabetes** 58: 2464-2475.

where in the presence of lower glucose utilization, the heart switches to using more FA for energy supply(12). One means by which this is possible is through an increase in LPL at the coronary lumen. Using retrograde perfusion of the heart with heparin to displace vascular LPL, we found elevated LPL following diabetes(13-15). We determined that the increased enzyme is: i) not the result of increased gene expression(13), ii) unrelated to an increase in the number of endothelial HSPG binding sites(13), iii) associated with an acute reduction in insulin (within 60 min)(16), and iv) functionally relevant and capable of hydrolyzing lipoprotein-TG(17). More recently, we have examined the contributions of the cardiomyocyte and endothelial cell in enabling this increased enzyme at the vascular lumen. Within the myocyte, LPL vesicle fission was regulated by protein kinase D (PKD)(18), whereas recruitment of LPL to the cardiomyocyte surface was controlled by stress kinases like AMPK(19) and p38 MAPK that allowed for provision of an actin network that facilitated LPL movement(20). Translocation of LPL from the cardiomyocyte surface to the apical side of endothelial cells is then dependent on the ability of the endothelium to release heparanase(21,22), which enables myocyte HSPG cleavage and transfer of LPL towards the coronary lumen.

Selective β-cell death and an ensuing diabetic state can be produced after a single i.v. dose of streptozotocin (STZ)(23). In Wistar rats, a dose-dependent increase in severity of diabetes is produced by 25-100 mg/kg STZ(24). After injection of 55 mg/kg (D-55), stable hyperglycemia develops within 24-48 h in concert with a ~50% reduction in plasma insulin(16,24). Although these animals were insulin deficient, they did not require insulin supplementation for survival, and did not develop ketoacidosis. In the absence of any changes in plasma FA and TG, these animals demonstrated an increase in coronary vascular LPL(13-15). Rats administered 100 mg/kg STZ (D-100) demonstrated intense β-cell necrosis, loss of 98% pancreatic insulin stores,

and severely reduced plasma insulin(16). Compared to D-55 diabetic rats, these D-100 animals show a remarkable elevation of plasma FA and TG. Importantly, LPL activity decreases(14,25) in D-100 hearts, suggesting a potential mechanism to restrain LPL derived FA when the supply of this substrate from other reservoirs is in surplus. The objective of the present study was to determine the mechanisms by which the hypoinsulinemic heart limits its LPL derived FA under conditions of hyperlipidemia. Our data demonstrate that caspase-3 activation, by cleaving PKD, attempts to restrict the hydrolysis of circulating TG by LPL, to limit FA provision and cardiac TG overload. Thus, although caspase-3 inhibition could be protective in reducing cell death, its augmentation of LPL may induce profound cardiac TG accumulation.

4.2. Materials and Methods

4.2.1. Experimental animals

The investigation conforms to the guide for the care and use of laboratory animals published by the US National Institutes of Health and the University of British Columbia. Adult male Wistar rats (260-300 g) were injected i.v. with streptozotocin (STZ), a selective beta cell toxin, which induces hypoinsulinemia, and causes hyperglycemia(13). Two different doses of STZ (55 and 100 mg/kg, dissolved in saline) were used to cause moderate and severe diabetes, and the animals were kept for 4 days. Control animals were injected with saline. Subsequently, hearts were removed for measurement of coronary luminal LPL activity, immunoprecipitation, immunofluorescence, and Western blot. Some D-100 animals were treated twice daily with Z-DEVD-fmk (3.2 mg/kg, i.p.) for 3 days, to inhibit caspase-3 activity. Blood samples were obtained from the tail vein and glucose was determined using a glucometer (Accu-Chek Advantage; Roche). Following centrifugation and its separation, plasma was assayed for insulin (rat ELISA kit), triglyceride (TG; Infinity) and non-esterified fatty acids (NEFA; Wako) using diagnostic kits.

4.2.2. Isolated heart perfusion

Rats were anesthetized with 65 mg/kg sodium pentobarbital i.p. and the heart carefully excised. Following cannulation of the aorta, hearts were perfused retrogradely with Krebs-Henseleit buffer. The rate of coronary flow (7-8 ml/min) was controlled by a peristaltic pump(14). To measure coronary endothelium-bound LPL, the perfusion solution was changed to buffer containing heparin (5 U/ml). The coronary effluent was collected in timed fractions (10 sec) over 5 min, and assayed for LPL activity by measuring the hydrolysis of a [^{3}H] triolein substrate emulsion(16). The standard assay conditions were 0.6 mM glycerol tri[9,10-^{3}H]oleate (1

mCi/mmol; 1 Ci = 37 GBq), 25 mM PIPES (pH 7.5), 0.05% (w/v) albumin, 50 mM $MgCl_2$, 2% (v/v) heat-inactivated chicken serum (containing the LPL activator, apolipoprotein CII), plus 100 μl of either medium or heart perfusate in a total volume of 400 μl.

4.2.3. Real time-PCR

14-3-3ζ and LPL mRNA expression were analyzed by real-time quantitative PCR using a light cycler and SYBR Green PCR Mix (Roche). Total RNA from hearts (50 mg) was extracted using Trizol (Invitrogen). After spectrophotometric quantification, reverse transcription was carried out using an oligo-(dT) primer and superscript II RT (Invitrogen). The real time PCR mixture with cDNA was amplified using 14-3-3ζ and LPL specific primers. 14-3-3ζ(26): 5'-CACAGCAAGCATACCAAGAA-3'(left) and 5'-AGAATGAGGCAGACAAAGGT-3'(right); LPL(19): 5'-ATCCAGCTGGGCCTAACTTT-3'(left) and 5'-AATGGCTTCTCCAATGTTGC-3'(right). The amplification parameters were set at 95 °C for 1 s and 60 °C for 6 s and 72 °C for 10 s (40 cycles total). The fluorescence signals were analyzed using light cycler relative quantification (Roche). Relative expression was evaluated by normalizing to 18S-ribosomal RNA.

4.2.4. Isolated cardiac myocytes and transfection

Ventricular calcium-tolerant myocytes were prepared by a previously described procedure(13,15). To examine the role of PKD on cardiomyocyte LPL, cells were plated on laminin-coated 6-well culture plates (to a density of 200,000 cells/well). Cells were maintained using Media-199, and incubated at 37 °C under an atmosphere of 95% O_2/5% CO_2. Cardiomyocytes were infected with recombinant adenovirus vectors carrying PKD-S744E/S748E (phosphomimetic active form) and PKD-kinase dead (PKD-KD), as described previously(18). Mock infection as a control was performed using EGFP. Infected cells were

incubated for a further 36 h before being used for either Western blot, immunofluorescence or measurement of basal and heparin-releasable (heparin 8 U/mL; 1 min) LPL activity. Cardiomyocytes were also transfected with PKD-wild type (Addgene 10808) or PKD-D378A (GenScript; non-cleavable by caspase-3) using lipofectamine 2000 (Invitrogen). These cells were used for Western blot and measurement of basal and heparin-releasable LPL activity.

4.2.5. Silencing of caspase-3 and 14-3-3ζ by siRNA

siRNA (Santa Cruz) transfection in cardiomyocytes was carried out using a kit (Invitrogen)(18). Briefly, in 6-well culture plates, 0.1 x 10^6 cells were plated and subsequently exposed to the siRNA (or scrambled, Scr) solution for 8 h at 37 °C in a CO_2 incubator. Following this, the media was changed to Media 199 and the cells incubated for another 18 h. After transfection of caspase-3 siRNA, cells were treated with or without PAC-1 (10 μM for 30 min), lysed, and subjected to Western blotting. Caspase-3 activity was measured using a fluorometric assay kit that detects cleavage of substrate DEVD-AMC (Biovision). In these cells, LPL activity was determined by adding heparin (8 U/ml for 1 min) to the incubation medium, and the release of surface-bound LPL activity into the medium determined. Bryostatin-1 (Bry, 1 nM for 30 min) was used to activate PKD. In cardiomyocytes transfected with the *14-3-3ζ* siRNA, cells were lysed, the obtained cytosolic fraction incubated with caspase-3 for 30 min, and immunoblotted for detection of PKD.

4.2.6. Western blotting

Western blot was done as described previously(19). Briefly, ventricular tissue (50 mg) or plated myocytes (0.4 x 10^6) were homogenized in ice-cold lysis buffer. Samples were quantified, boiled with loading dye, and 50 μg used in gel electrophoresis. After blotting, membranes were incubated with rabbit PKD, phospho-PKD (Ser 916 or Ser 744/748), cleaved caspase-3

(Asp175), caspase-3, 14-3-3ζ, LPL (5D2 generously provided by Dr. J. Brunzell, University of Washington, Seattle, WA) and VAMP antibodies, and subsequently with secondary goat anti-rabbit or mouse HRP-conjugated antibody. Bands were visualized using an ECL® detection kit, and quantified by densitometry.

4.2.7. Immunoprecipitation

Following STZ, hearts were lysed in lysis buffer (20 mM Tris-HCl, 2 mM EDTA, 5 mM EGTA, 50 mM 2-mercaptoethanol, 25 μg leupeptin, 4 μg aprotinin, pH 7.5) and immunoprecipitated using PKD antibodies overnight at 4 °C. The immunocomplex was pulled down with protein A/G-sepharose for 1 h, and then heated for 5 min at 95 °C. The immunocomplex was immunoblotted with anti-14-3-3ζ. Where indicated, GST-PKD (5 μg) or immunoprecipitated PKD (5 μg) from control heart were incubated with or without caspase-3 (5 units), and full length and cleaved PKD determined using Western blot.

4.2.8. Immunofluorescence

Heart-Hearts were perfused with 10% formalin and kept for 24 h. After formalin fixation and paraffin embedding, 3-μm sections were cut on silane-coated glass slides. Immunostaining was carried out as described before(19). Slides were incubated with chicken anti-bovine LPL antibody (1:400 dilution) for 3 h. After being washed with TBS, slides were incubated with biotinylated rabbit anti-chicken IgG-conjugated Cy3 (1:150 dilution; Chemicon) for 1 h. Slides were visualized using a fluorescent microscope.

Cardiomyocyte-Following transfection, myocytes were fixed for 10 min with 4% paraformaldehyde in PBS, permeabilized with 0.1% Triton X-100 in PBS for 3 min, treated with PBS containing 1% BSA for 20 min, and finally rinsed with PBS. Cells were incubated with rabbit polyclonal PKD, mouse monoclonal TGN38, or chicken anti-bovine LPL antibody

followed by incubation with secondary antibodies (goat anti-rabbit IgG-FITC, donkey anti-mouse IgG-TR, donkey anti-mouse IgG-FITC, streptavidin-conjugated Cy3 fluorescent probe) to localize PKD (green), TGN38 (Green and Red), and LPL (red) respectively. Slides were visualized using a Zeiss Pascal confocal microscope.

4.2.9. Separation and measurement of cardiac triglyceride

Total cardiac lipids were extracted and solubilized in chloroform: methanol: acetone: hexane (4:6:1:1 v/v/v/v). Separation and quantification of TG was achieved using HPLC (Waters 2690 Alliance HPLC, Milford, MA), as described previously(27). Heart sections were also stained with Oil-Red-O and counter stained with haematoxylin to visualize cardiac lipid accumulation.

4.2.10. Heart fractionation and determination of OXPAT

OXPAT is a lipid-storage droplet protein that is highly enriched in tissues that have high rates of fatty acid β-oxidation(28). To determine whether the cardiac lipid droplet is coated with OXPAT, we fractionated heart tissue by a previously described method(28). Briefly, cardiac tissues were homogenized and centrifuged (2000g for 5 min) with 45% sucrose and lysis buffer. The supernatants obtained were overlaid with 40% and 10% sucrose solutions and subjected to centrifugation at increasing force (2,700-172,000g). The different fractions obtained at a particular force were then subjected to Western blot for OXPAT or used for determination of TG.

4.2.11. Transmission electron microscopy

To assess accumulation of lipid droplets, morphological evaluation of hearts was carried out using transmission electron microscopy(29). Briefly, left ventricular tissue was fixed in 1.5% glutaraldehyde and paraformaldehyde, cut into small blocks (~1 x 0.5 x 0.2 mm), and fixed for 8 h at 4 °C. After washing, tissue was post fixed with 1% osmium tetroxide and further treated

with 1% uranyl acetate and dehydrated using increasing concentrations of ethanol (50–100%). Blocks were embedded in epoxy resin and sectioned at ~90 nm. Sections were stained with 1% uranyl acetate and Reynolds lead citrate. Images were obtained with a Hitachi H7600 electron microscope.

4.2.12. Plasma membrane CD36

Heart membrane fractions were isolated by a previously described method using a sucrose density gradient(30). Using Western blot, identification of CD36 protein was done using rabbit polyclonal CD36 as the primary antibody and mouse anti-rabbit horseradish peroxidase as the secondary antibody. Na^+-K^+-ATPase was used as a plasma membrane marker.

4.2.13. Palmitate oxidation in isolated cardiomyocytes

FA oxidation was performed as described previously(31). Following attachment of cardiomyocytes from the different groups to laminin-coated 60-mm center-well organ culture dishes, cells were incubated in glucose-free DMEM containing 0.4 mM palmitic acid, 3% FA-free BSA, and 0.5 μCi [1-^{14}C]palmitic acid. Incubation was carried out for 2 h at 37 °C with 95% O_2-5% CO_2 gassing. 5% KOH was then injected into the center wells, and oxidation stopped by injecting 1 M H_2SO_4 into the incubation buffer. The dishes were sealed, stored at 4 °C overnight, and KOH assessed for $^{14}CO_2$ by scintillation counting. Oxidation was calculated by subtracting $^{14}CO_2$ at zero time from trapped $^{14}CO_2$ after 2 h of incubation. Results are expressed as nmol CO_2/h/mg of protein (BCA Protein Assay Kit). It should be noted that measurement of palmitate oxidation in isolated quiescent cardiomyocytes may not truly reflect what happens in the working heart.

4.2.14. Separation of Golgi and measurement of vesicles

Golgi membranes were isolated from heart tissues using a Golgi isolation kit (Sigma). 5 g of heart tissue was minced and resuspended in 0.25 M sucrose using a Dounce homogenizer. The homogenate was centrifuged at 3,000 g for 15 min. The supernatant was adjusted to 1.25 M by adding 2.3 M sucrose and then overlaid with 1.84 M and 1.1 M sucrose. The density gradient solution was centrifuged at 120,000 g for 3 h. The Golgi enriched fraction was collected at the 1.1/0.25 M sucrose interphase and confirmed using Western blotting with TGN38 antibody (trans-Golgi specific marker). Golgi-enriched membranes were diluted with buffer containing 25 mM KCl, 2.5 mM MgSO4, 25 mM Hepes, 0.2 M sucrose, 1 mM dithiothreitol, and 30 μM GTP-γS. GST-PKD (5 μg), caspase-3 (5 units) or cytosol (0.2 mg of protein) from control and D-100 hearts was then added to the membranes, and incubation continued for 15 min at 37 °C(32). After centrifugation (12000 g, 10 min, 4 °C), pellets were re-suspended in the previous buffer plus 0.25 M KCl, and centrifuged at 250,000 g for 1 h to obtain a pellet. Pellets were re-suspended in lysis buffer, and subjected to SDS/PAGE and Western blot for VAMP and LPL.

4.2.15. Materials

[^{3}H]triolein, [1-^{14}C]palmitic acid, and the ECL® detection kit were purchased from Amersham Canada. Heparin sodium injection (Hapalean; 1000 USP U/ml) was obtained from Organon Teknika. PKD, phospho-PKD (Ser 916 or Ser 744/748), cleaved caspase-3 (Asp175), and caspase-3 antibodies were obtained from Cell Signaling (Danvers, MA). 14-3-3ζ, VAMP and β-actin antibodies were obtained from Santa Cruz biotechnology, Inc. (Delaware Avenue, CA). Caspase-3 enzyme, GST (Glutathione S transferases)-PKD protein, and Z-DEVD-fmk were purchased from Biovision. Bryostatin-1 and PAC-1 were from Calbiochem. All other chemicals were obtained from Sigma Chemical.

4.2.16. Statistical analysis

Values are means ± SE. Wherever appropriate, one-way ANOVA followed by the Bonferroni test was used to determine differences between group mean values. The level of statistical significance was set at $P<0.05$.

4.3. Results

4.3.1. Severity of diabetes determines the magnitude of LPL at the coronary lumen

By exploiting two different doses of STZ, we induced moderate (55 mg/kg) and severe (100 mg/kg) hypoinsulinemia. Although both groups were equally hyperglycemic (Figure 4-1A, inset), D-100 rats showed a more profound loss of circulating insulin (Figure 4-1A). During hypoinsulinemia, excessive lipolysis and loss of adipose tissue mass results in an increase in both plasma FA and TG(24). Indeed, both plasma FA (Figure 4-1B) and TG (Figure 4-1B, inset) levels were elevated in D-100 animals. Interestingly, measurement of these parameters in D-55 showed no significant differences when compared to control (Figure 4-1B). During hypoinsulinemia with its attendant loss of glucose utilization, LPL activity increases at the vascular lumen(13). Compared to control hearts, there was substantial increase in heparin-releasable LPL activity in D-55 animals (Figure 4-1C), with most of the enzyme located at the vascular lumen as shown using immunofluorescence (Figure 4-1E). Contrary to the results obtained with D-55 rats, heparin-releasable LPL activity (Figure 4-1C) and LPL immunofluorescence (Figure 4-1E) in severely hypoinsulinemic D-100 animals were unchanged when compared to control. Both hypoinsulinemic groups showed no significant change in cardiac LPL gene expression (Figure 4-1D).

4.3.2. Caspase-3 produces proteolysis of cardiac PKD

Recently, we have reported that phosphorylation of PKD is a key element to increase cardiac LPL after hyperglycemia (D-55) by regulating fission of vesicles from Golgi membranes(18). In the present study, measurement of PKD revealed that only D-100 hearts showed a decrease in full length PKD (Figure 4-2A, inset), with a corresponding robust increase in the cleaved form (Figure 4-2A), that increases its activity(33) but limits its Golgi binding capability(34). In U-937

leukemic monocyte lymphoma cells, caspase-3 has been suggested to control PKD by cleaving its cysteine rich domain(33), which is necessary for binding to trans-Golgi(34). Measurement of caspase-3 in D-100 rat hearts demonstrated an increase in its activity (Figure 4-2B). This increase was modest; PAC-1, a procaspase-3 activator, increased caspase-3 activity 2-fold higher than D-100. TUNEL and DAPI nuclear staining were used to assess cell apoptosis. Hearts from D-100 animals exhibited a higher number of apoptotic cells. However, the overall percentage of these cells was very low (~0.01%) (data not shown). Given the effect of caspase-3 to cleave PKD, purified GST-PKD was incubated with active caspase-3 enzyme. As predicted, GST-PKD was rapidly cleaved by caspase-3 (Figure 4-2C). Replicating this experiment using PKD isolated from control hearts also showed cleavage of PKD by caspase-3. However, caspase-3's proteolysis of GST-PKD was faster than its cleavage of isolated PKD from control hearts (Figure 4-2D). Interestingly, although D-55 hearts also showed an increase in caspase-3 activity (Figure 4-2B), this was not associated with cleaved PKD (Figure 4-2A) suggesting that in D-55 hearts, some protein is preventing PKD cleavage. 14-3-3 proteins are binding proteins known to interact with a number of enzymes protecting them against proteolytic degradation(35), and diabetes is known to decrease the gene and protein expression of 14-3-3ζ(36). Measurement of 14-3-3ζ showed a decrease in its mRNA (Figure 4-2E) and protein (Figure 4-2E, inset), only in D-100 hearts. In addition, severe hypoinsulinemia also resulted in a decreased attachment of PKD to 14-3-3ζ (Figure 4-2F). Silencing of 14-3-3ζ in cardiomyocytes had no influence on PKD expression (Figure 4-2G, inset). Nevertheless, in these cells, exposure to caspase-3 accelerated PKD cleavage (Figure 4-2G, boxed inset). Our data suggest that both activation of caspase-3 together with loss of 14-3-3ζ is required for cleavage of PKD following severe hypoinsulinemia.

4.3.3. Manipulating PKD in isolated cardiomyocytes is sufficient to regulate heparin-releasable LPL

In cardiomyocytes, phospho-mimetic (PKD-S744E/S748E) and kinase-dead (KD) mutants of PKD were over expressed by adenoviral vectors to establish the relationship between PKD and LPL. We first validated successful transduction using Western blotting (Figure 4-3A). Both PKD-S744E/S748E and KD mutants increased total PKD expression (Figure 4-3A, inset); only the phospho-mimetic mutant demonstrated higher Ser916 phosphorylation, which is related to its catalytic activity(37). The S744/S748 phosphorylation site has been shown to have a critical role in recruiting PKD to the trans-Golgi(34). Simply increasing the expression of the phospho-mimetic and KD mutants augmented their association with the trans-Golgi (Appendix Fig B-1). However, PKD-S744E/S748E also increased the co-localization of LPL to the trans-Golgi (Figure 4-3C), with a striking increase in heparin releasable LPL activity (Figure 4-3B).

Using a different strategy, cardiomyocytes were transfected with PKD-D378A, point mutated to prevent caspase-3 mediated proteolysis(33). Successful transfection of PKD-WT and PKD-D378A is demonstrated in Appendix Fig B-1B. Although PKD-WT and PKD-D378A themselves elevated PKD phosphorylation at Ser 916, phosphorylation of Ser 744/748 (Appendix Fig B-1B) and heparin-releasable LPL activity (Appendix Fig B-1C) remained unchanged compared to EGFP. Bryostatin-1 is a potent activator of PKD(38). Control cardiomyocytes treated with bryostatin-1 increased phosphorylation (both S744/S748 and Ser 916) of PKD and heparin-releasable LPL activity (Figure 4-3D, inset). In WT and D378A cardiomyocytes, bryostatin-1 was not only capable of further increasing Ser 916 phosphorylation but also Ser 744/748 phosphorylation (Appendix Fig B-1B). In these myocytes, bryostatin-1 also elicited a robust increase in heparin-releasable LPL activity (Appendix Fig B-1C). Pre-treating

EGFP and WT cells with PAC-1 followed by bryostatin-1 induced significant cleavage of PKD, an effect that was not apparent in PKD-D378A cardiomyocytes (Figure 4-3D). More importantly, caspase-3 activation in D378A did not decrease LPL activity as seen in EGFP and WT (Figure 4-3E). It should be noted that in this experiment using non-diabetic myocytes, 14-3-3 ζ was unable to protect PKD from cleavage by PAC-1, which elicited a more robust increase in caspase-3 compared to D-100. Overall, these data suggest that LPL transport to the cell surface is dependent on PKD phosphorylation at S744/S748 rather than PKD's intrinsic activity, and that cleavage of PKD by caspase-3 is sufficient to prevent PKD mediated increase in LPL activity.

4.3.4. Silencing of caspase-3 prevents PKD proteolysis and increases cardiac LPL activity

We used siRNA to silence caspase-3 in isolated cardiomyocytes. We first validated successful caspase-3 inhibition using Western blotting (Figure 4-4A, inset). In myocytes in which caspase-3 was silenced, PAC-1 was unable to increase caspase-3 activity (Figure 4-4A) or to increase PKD cleavage (Figure 4-4B). Furthermore, in myocytes in which caspase-3 was silenced, the PAC-1 induced decrease in LPL activity was prevented (Figure 4-4C).

4.3.5. Caspase-3 restricts PKD-mediated LPL vesicle formation

PKD, by associating with vesicle associated membrane protein (VAMP, one of v-SNAREs), is known to trigger vesicular movement(39). To further elucidate the interactions between caspase-3, PKD and LPL, purified Golgi were incubated in the presence or absence of GST-PKD and caspase-3, and vesicle formation determined using antibodies against VAMP. As predicted, VAMP associated vesicle formation significantly increased on incubation with GST-PKD; the GST-PKD induced vesicles contained high levels of LPL (Figure 4-5A and B). These effects of PKD on VAMP associated vesicle formation and LPL content were impeded by caspase-3 (Figure 4-5A and B). We applied a similar approach *in vivo*, using Z-DEVD to inhibit caspase-3

in D-100 hearts. Interestingly, when the cytosolic fraction from Z-DEVD treated D-100 hearts was incubated with isolated Golgi, VAMP associated vesicular formation together with LPL vesicle content increased significantly (Figure 4-5C and D).

4.3.6. Inhibiting caspase-3 in D-100 rats increases LPL at the vascular lumen

Given the strong relationship between caspase-3 and LPL, D-100 rats were treated with the caspase-3 inhibitor, Z-DEVD and LPL activity determined. Z-DEVD was very effective in preventing caspase-3 cleavage and its subsequent activation (Figure 4-6A). More importantly, this caspase-3 inhibitor prevented the cleavage of PKD that is seen in D-100 hearts (Figure 4-6B). This effect on PKD in Z-DEVD treated D-100 hearts increased the appearance of LPL at the vascular lumen (Figure 4-6D), in addition to augmenting heparin-releasable LPL activity (Figure 4-6C) to levels observed in D-55 hearts. Z-DEVD had no influence on total LPL expression, which remained approximately 20% lower than control (Figure 4-6E). In addition, Z-DEVD had no further influence in increasing vascular LPL in D-55 hearts (data not shown). In summary, activation of caspase-3 in D-100 hearts restrains the transfer of LPL to the coronary lumen by affecting proteolysis of PKD.

4.3.7. Caspase-3 inhibition in D-100 promotes excessive cardiac TG accumulation

Interestingly, the augmented amount of LPL in Z-DEVD treated D-100 rats corresponded to an increased clearance of circulating TG (Figure 4-7A), without affecting plasma FA (Figure 4-7B). In these animals, unlike the drop in plasma TG, there was a striking accumulation of cardiac TG, which was almost 2-fold higher than that in the untreated D-100 animals (Figure 4-7C and D). Sucrose fractionation and subjection of the different fractions to Western blot for OXPAT or determination of TG revealed that in D-100, the fractions (top) that had highest amount of TG were associated with OXPAT (Appendix Fig B-2); caspase inhibition in D-100 induced a further

increase of OXPAT in these fractions (Appendix Fig B-2). Hearts from D-100 animals demonstrated an approximately two-fold increase in CD36 protein (Figure 4-7E). Treatment of these animals with Z-DEVD did not initiate a further increase in plasma membrane CD36 (Figure 4-7E). Cardiac palmitate oxidation in D-100 rats treated and untreated with Z-DEVD remained high (Figure 4-7F).

4.4. Discussion

During diabetes, when cardiac glucose uptake, glycolysis and pyruvate oxidation are impaired, the heart rapidly adapts to using a greater amount of FA for ATP generation, allowing it to maintain its function(40). This change occurs not only as a consequence of increased exogenous FA (due to release of FA from adipose tissue and hydrolysis of TG-rich lipoproteins by LPL) and endogenous FA (hormone sensitive lipase hydrolysis of intracellular stored TG) supply, but also through an intrinsic adaptation/maladaptation to elevated FA that includes an augmented FA oxidation and expression of genes that control utilization of this substrate(40). To avoid over supply of this potentially lethal substrate, the heart can exquisitely regulate its LPL content at the vascular lumen. Thus following moderate acute STZ diabetes (that resembles a poorly controlled T1D patient), when circulating FA and TG have yet to increase, significantly elevated luminal LPL protein and activity is observed(14). Given that vascular endothelial LPL is acquired from the cardiomyocyte, we previously examined the mechanisms by which diabetes increases cardiomyocyte cell surface LPL, a reservoir that can rapidly augment coronary luminal LPL when the need for FA is intensified. In the myocyte, we reported that recruitment of LPL to the cell surface was controlled by protein kinase D (which regulated LPL vesicle fission)(18), whereas stress kinases like AMPK and p38 MAPK allowed for actin cytoskeleton polymerization, providing the cardiomyocyte with an infrastructure to facilitate LPL movement(20). In the present study, our data demonstrate that following severe hypoinsulinemia (with its attendant elevation of plasma FA and TG), caspase-3 activation, by cleaving PKD, restricts amplification of LPL, thereby limiting FA provision and overwhelming cardiac TG accumulation.

The cytosolic serine-threonine kinase, PKC-μ, also known as PKD, regulates vesicular fission from the trans-Golgi network, allowing cargo proteins to be delivered to the plasma membrane(34). Within PKD, a cysteine-rich domain has been shown to have critical role in recruiting and binding PKD to the trans-Golgi(34). We have recently reported that PKD is a key modulator of LPL vesicular trafficking within cardiomyocytes, and is related, not only to binding of PKD to the Golgi(18), but also to phosphorylation of Ser 744/748 in its catalytic domain. In D-55 animals, PKD phosphorylation was strongly correlated to an increase in LPL on the luminal surface of the capillary endothelium. Given the observation that in hearts from D-100 animals, LPL activity remained unchanged after 4 days, or decreases after one week(14,25), we hypothesized that a signal deficiency for LPL translocation exists within these hearts. Interestingly, measurement of PKD revealed that only D-100 hearts showed a decrease in full length PKD, with a corresponding robust increase in the cleaved form. Our data suggest that following severe hypoinsulinemia, proteolysis of PKD may be an important event to limit an increase in LPL activity at the vascular lumen.

In U-937 cells, caspase-3 has been suggested to control PKD by cleaving its cysteine rich domain(33). Given the relationship between caspase-3 and PKD, we measured caspase-3 and determined that both D-55 and D-100 hearts demonstrated an increase in its activity, likely mediated by reactive oxygen species(41). It should be noted that the observed increase of caspase-3 in these hearts did not reach the upper limit seen with PAC-1, the caspase-3 activator that induces apoptosis (programmed cell death). Thus, although caspase-3 plays a key role in apoptosis(42), in the acute hypoinsulinemic heart, caspase-3 may also have a non-apoptotic function. Other studies have also suggested that caspase-3 has a regulatory function in cell proliferation, differentiation and shaping(43). This secondary function of caspase-3 in D-100

hearts included cleavage of PKD, an observation that was absent following moderate hypoinsulinemia, even though these hearts showed an increase in caspase-3 activity. Given that a) measurement of 14-3-3ζ showed a decrease in its mRNA and protein, only in D-100 hearts, b) caspase-3's proteolysis of cardiac-PKD was slower than its cleavage of GST-PKD, and c) silencing of 14-3-3ζ in cardiomyocyte accelerated PKD cleavage on exposure of these cells to caspase-3, our data suggest that this 14-3-3ζ binding protein protects PKD against proteolytic degradation by caspase-3 in D-55. Using control myocytes, we confirmed the relationship between PKD, LPL, and caspase-3. Thus, the phospho-mimetic PKD co-localized with LPL in the trans-Golgi, facilitating LPL secretion to cardiomyocyte cell surface. In addition, PKD mutated to prevent its cleavage by caspase-3 or silencing of caspase-3 was able to increase LPL activity. Overall, our data suggest that caspase-3, by cleaving PKD, limits LPL vesicle formation and eventual increase of LPL at the vascular lumen.

Z-DEVD-fmk is a potent, irreversible and cell permeable inhibitor of caspase-3. Using this compound in D-100 animals, we effectively lowered caspase-3 activity, prevented PKD cleavage and increased LPL vesicle formation and translocation to the vascular lumen. This increase in LPL at the vascular lumen occurred even though the total LPL protein expression remained approximately 20% lower than control. It should be noted that electron microscopy using immunogold-labeling established that, in the heart, 78% of total LPL is present in cardiac myocytes, 3-6% in the interstitial space, and 18% at the coronary endothelium(6). Thus, LPL at the vascular lumen is likely more dependent on the signaling which promotes transfer of this enzyme from the cardiomyocyte to the coronary lumen rather than its absolute cardiomyocyte content.

Cardiac LPL is a major determinant of plasma TG(44). Thus, the increase in cardiac luminal LPL in Z-DEVD treated D-100 animals could explain the decline in circulating TG. Whether other tissue LPL contributes towards this observed fall in plasma TG is unknown as heparin perfusion to release vascular bound LPL is difficult to accomplish in other tissues. As no apparent change was noted in plasma FA levels in these animals, our data suggest that following LPL mediated TG hydrolysis, FA can be taken up rapidly and directly into tissues. In support of this suggestion, cardiac and skeletal muscle specific overexpression of LPL decreased plasma TG, elevated TG storage in muscle tissue but was without effect when plasma FA was measured(45). In the event of an increased availability of FA, its disposal can occur either via oxidation or its conversion into TG, which serves as the primary storage form of FA. Caspase-3 inhibition did not alter the high FA uptake and oxidation in D-100 rats. However, measurement and visualization of cardiac TG revealed a striking accumulation in Z-DEVD treated D-100 hearts, which was almost 2-fold higher than that in the untreated D-100 animals. This TG was richly associated with the lipid-storage droplet protein, OXPAT(28). Overall, these data suggest that in D-100 hearts treated with Z-DEVD, FA uptake and oxidation are likely operating at their maximum capacity. The additional TG accumulation in this group is thus most likely a consequence of an increase in LPL and vascular lipolysis, with the released fatty acids rapidly taken up and stored as TG with the assistance of OXPAT. Other studies have also reported excessive TG overload when LPL is specifically overexpressed in the heart(46). It should be recognized that PKD has also been linked to GLUT4-mediated glucose uptake in contracting myocytes(47). However, as STZ diabetes rapidly decreases the myocardial content of total membrane GLUT4 ($t_{1/2}$ of 3.5 days)(48), the impact of PKD in regulating glucose uptake is likely minimal under conditions of hypoinsulinemia and hyperglycemia.

In summary, severe hypoinsulinemia with its associated increase in circulating FA and TG, lowers 14-3-3ζ expression and activates caspase-3, which can cleave PKD, reduce LPL vesicle fission and restrict LPL translocation to the vascular lumen (Figure 4-7G). When caspase-3 is inhibited, this compensatory response is lost, leading to accumulation of TG (Figure 4-7G). It should be noted that in transgenic rabbits that have global overexpression of LPL, attenuation of hypertriglyceridemia was observed, an effect suggested to contribute toward amelioration of insulin resistance and obesity(49). Contrary to systemic overexpression, tissue-specific overexpression of LPL in skeletal muscle and heart is associated with lipid oversupply, insulin resistance and severe myopathy, characterized by both muscle fiber degeneration, extensive proliferation of mitochondria and peroxisomes, excessive dilatation and impaired left ventricular systolic function(18,45,46,50,51). Interestingly, drugs like pioglitazone that are known to decrease caspase-3(52), have been reported to reduce circulating TG(53,54) by increasing LPL in humans(55), and also to increase the myocardial content of lipids in rats fed a high fat diet(56). Whether this effect can explain the risk of heart failure when TZDs are used in patients with Type 2 diabetes has yet to be determined(57,58). Thus, although caspase inhibition has been considered to have therapeutic effects in many human diseases, including heart attack, neurodegenerative diseases and autoimmune disorders, its use in diabetes to prevent cardiac cell death could be lead to significant cardiac TG accumulation, and warrants further investigation.

Figures

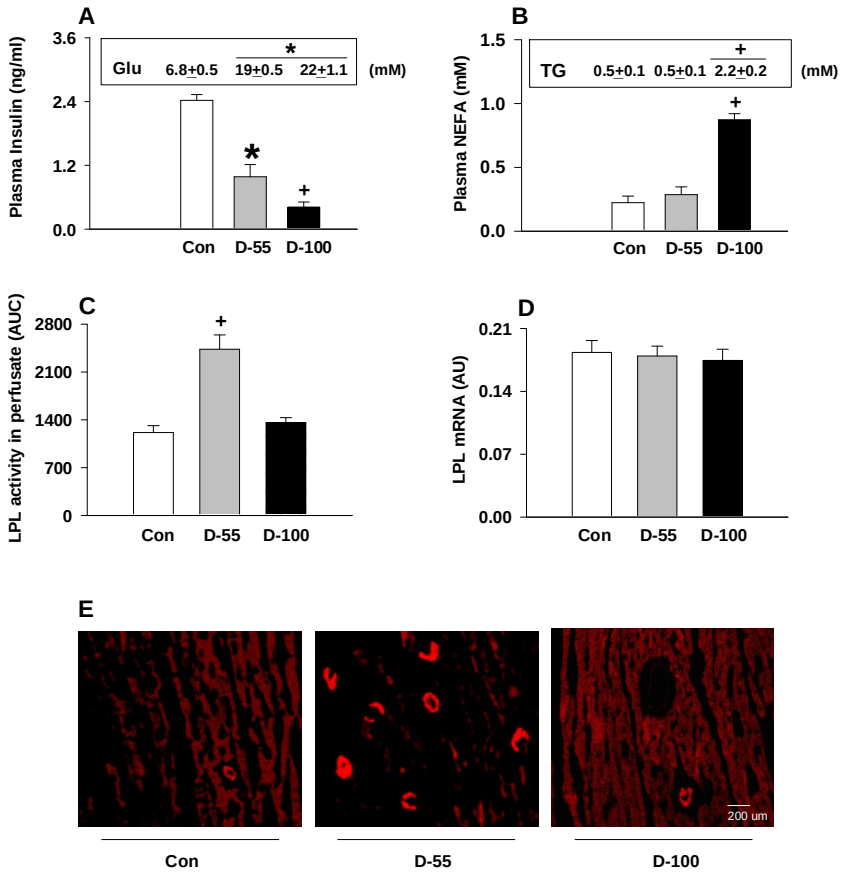

Fig. 4-1 *Moderate and severe hypoinsulinemia have dissimilar effects on cardiac LPL.* Animals were treated with two different doses of STZ [55 (D-55) and 100 (D-100) mg/kg], and kept for 4 days. Fed blood samples were obtained from the tail vein and glucose (Glu) determined using a glucometer (A, inset). Plasma was assayed for insulin (A), triglyceride (TG, B inset), and non-esterified fatty acids (NEFA, B) using diagnostic kits. Hearts were isolated and perfused in the non-recirculating retrograde mode. The coronary luminal LPL released with heparin (5 units/ml) was collected, and LPL activity was assayed using radiolabeled triolein. LPL activity was determined as nmol/h/ml. The results are expressed as area under curve (AUC) of enzyme released over 5 min (C). LPL mRNA was measured using real time PCR (D). LPL was visualized by immunofluoresence (E). Bar = 200 µm. AU = Arbitrary Units. Results are the means ± SE of 3-5 rats in each group. *Significantly different from control; $^{+}$significantly different from all other groups, $P<0.05$.

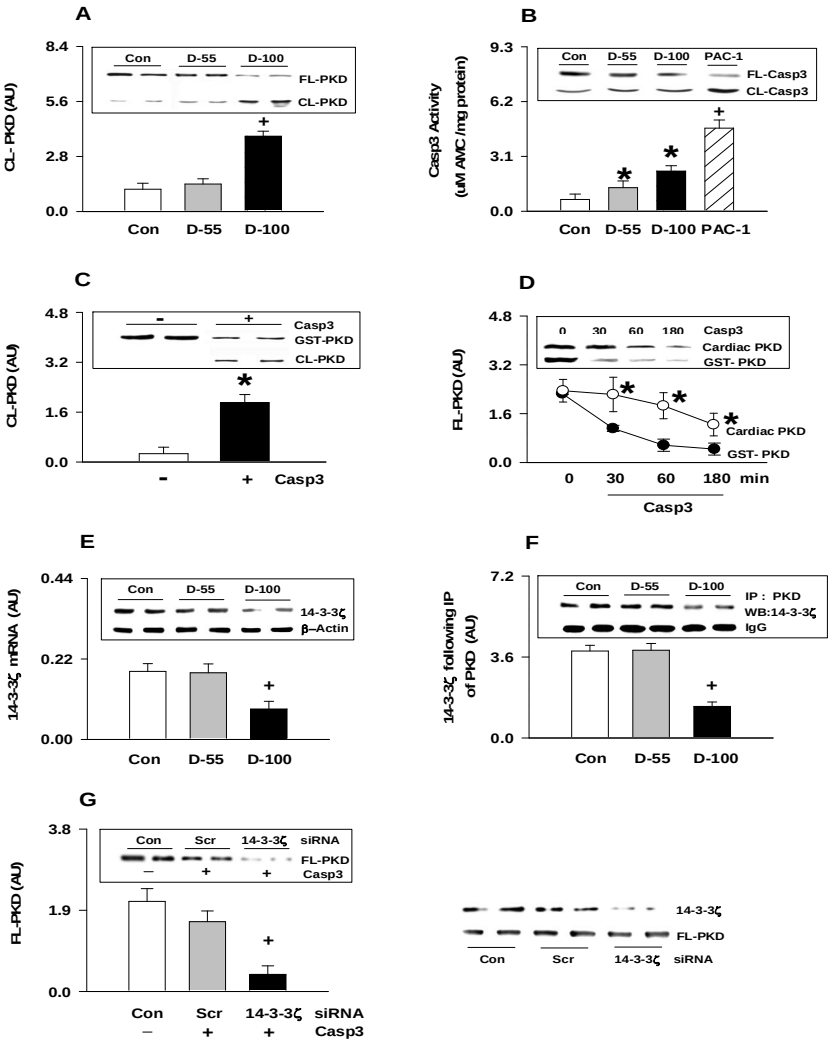

Fig. 4-2 *PKD cleavage is increased following severe hypoinsulinemia.* Full length (FL) and cleaved (CL) PKD (A) and caspase-3 (B, inset) were measured using Western blot. Caspase-3 activity was measured using a fluorometric assay kit (B). In a separate experiment, control rats injected with PAC-1 (10 mg/kg kept for 30 min) were used as a positive control (B). *In vitro*, purified GST-PKD was incubated in the absence or presence of activated caspase-3, and PKD proteolysis determined using Western blot (C). Comparison of the time dependent cleavage of GST-PKD and cardiac PKD (purified from control hearts) by capase-3 is described in D. *14-3-3ζ* protein (E, inset) and gene (E) expression were measured using Western blot and real time PCR respectively. To examine the association between PKD and *14-3-3ζ*, PKD was immunoprecipitated using a PKD antibody and immunoblotted with anti-*14-3-3ζ* (F). Plated myocytes were exposed to the 14-3-3ζ siRNA (or scrambled, Scr). The inset (G) depicts transfection efficiency. After transfection of 14-3-3ζ siRNA, cells were lysed and the cytosolic fraction incubated with or without caspase-3 (5 units for 30 min) and subjected to Western blot for evaluating FL-PKD (G and boxed inset). Results are the means ± SE of 3-5 rats in each group. *Significantly different from control/GST-PKD; +significantly different from all other groups, $P<0.05$. PAC-1, procaspase-3 activator; IP, immunoprecipitation; WB, Western blot; Casp3, Caspase-3.

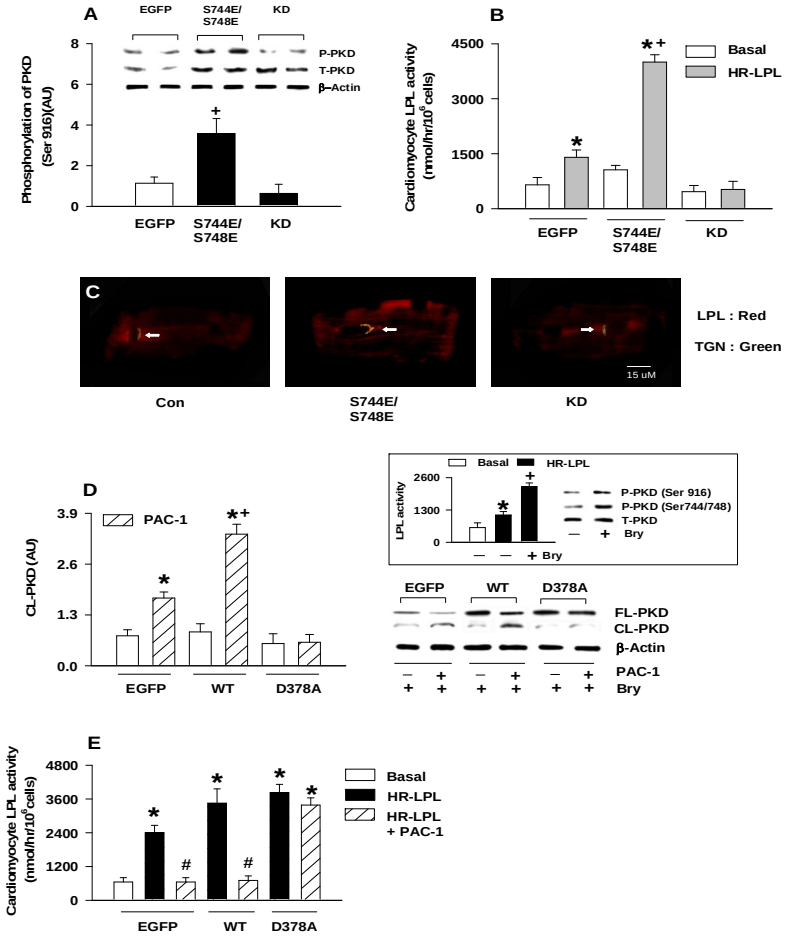

Fig. 4-3 *PKD phosphorylation at S744/S748 together with its resistance to proteolysis by caspase-3 increases cardiac LPL.* Control cardiomyocytes were infected with recombinant adenovirus vector carrying phospho-mimetic (S744E/748E) and kinase-dead (KD) mutants, or EGFP. Infected cells were incubated for a further 36 h before protein extraction for measurement of total (A, inset) and phosphorylated (Ser 916) PKD (A). In these cells, LPL activity was determined by adding heparin (8 U/ml for 1 min) to the incubation medium, and the release of surface-bound LPL activity into the medium determined (B). Representative photograph showing co-localization of LPL and trans-Golgi (TGN) is shown in C (arrow). Cardiomyocytes were fixed, incubated with primary antibodies [LPL (Red) and TGN38 (Green)] followed by incubation with secondary antibodies [Cy3 (Red) and FITC (Green)]. Bar = 15 μm. PKD phosphorylation (Ser 916, Ser 744/748) and increase in cardiomyocyte LPL activity with bryostatin-1 (Bry, 1 nM for 30 min) is indicated in D (inset). Cardiomyocytes were also transfected with PKD wild-type (WT) and PKD D378A, or EGFP. In these transfected cells exposed to bryostatin-1, cleaved PKD (D) and LPL activity (E) were determined in the absence or presence of PAC-1 (10 μM for 30 min). Results are the means ± SE of 3-5 cardiomyocyte preparations from different animals. *Significantly different from control; +significantly different from all other groups, #significantly different from heparin releasable, $P<0.05$. HR, heparin-releasable; P, phosphorylated; T, total.

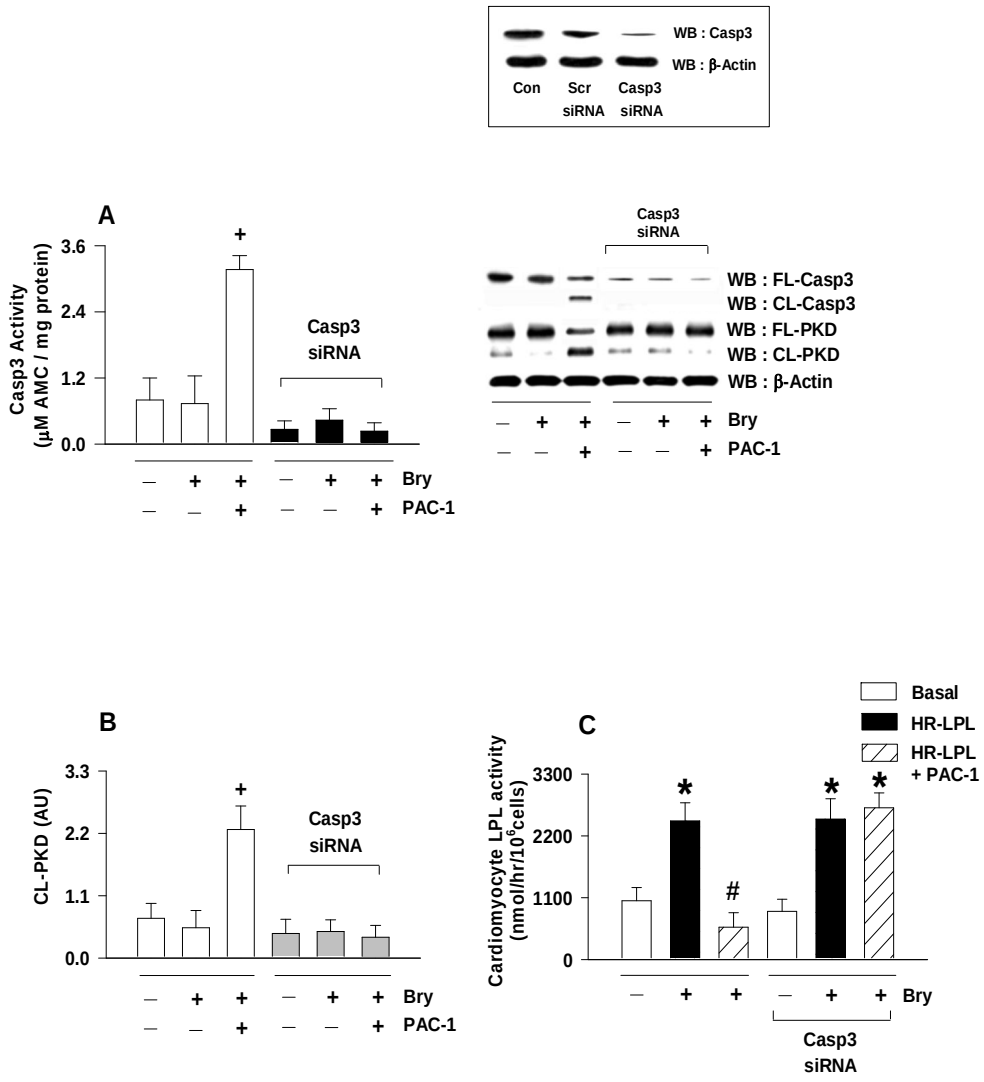

Fig. 4-4 *Impeding PKD proteolysis by silencing caspase-3 substantially increases cardiac LPL activity.* Plated myocytes were exposed to the caspase-3 siRNA (or scrambled, Scr). The inset (A) depicts transfection efficiency. After transfection of caspase-3 siRNA, cells were treated with or without PAC-1 (10 μM for 30 min), lysed, and subjected to Western blot for evaluating full length (FL) and cleaved (CL) caspase-3 and PKD (A and B). Caspase-3 activity was measured using a fluorometric assay kit (A). In these cells, LPL activity was determined by adding heparin to the incubation medium, and the release of surface-bound LPL activity into the medium determined (C). Bryostatin-1 (Bry, 1 nM for 30 min) was used to activate PKD. Results are the means ± SE of 3-5 cardiomyocyte preparations from different animals. *Significantly different from control; +significantly different from all other groups, #significantly different from heparin releasable, $P<0.05$.

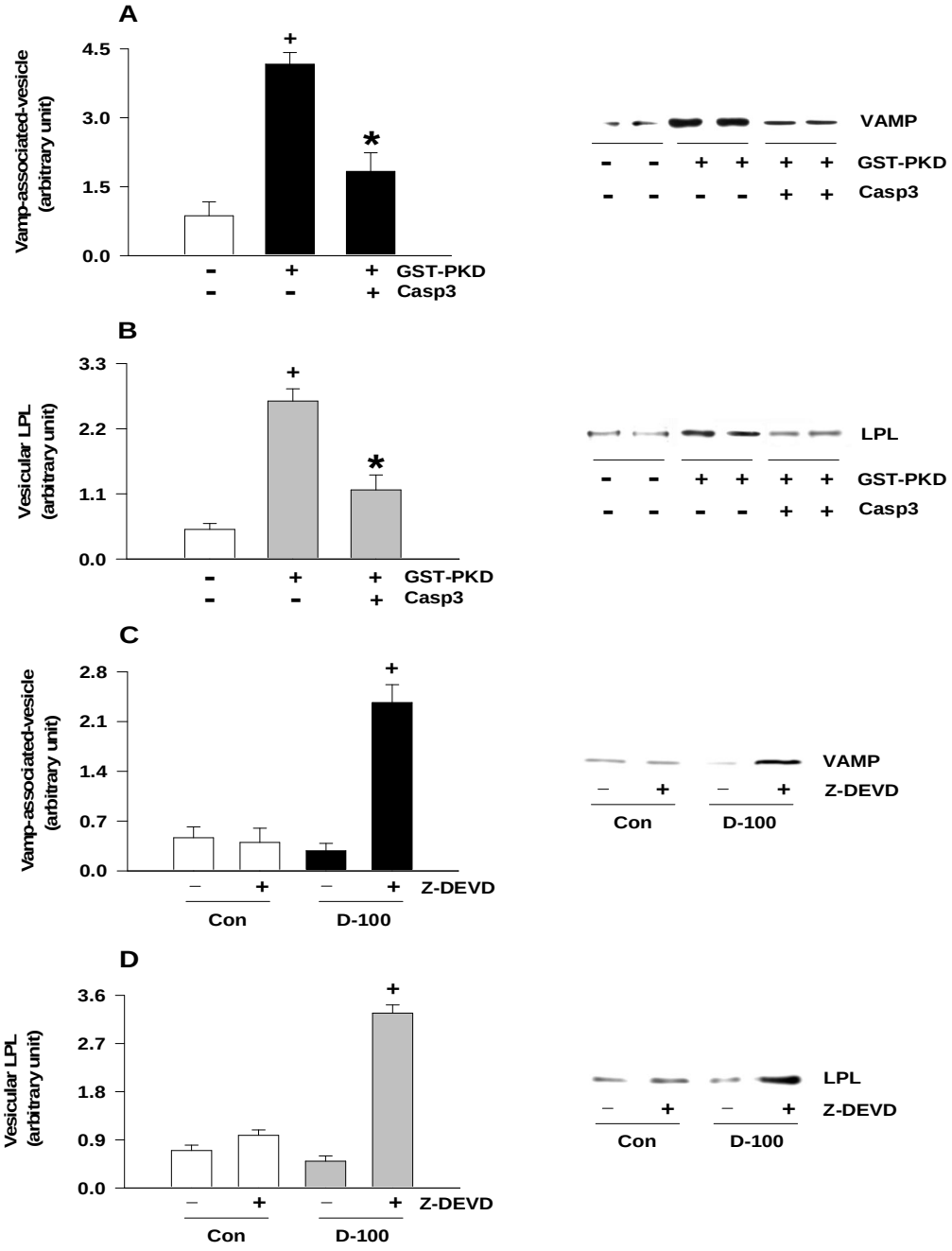

Fig. 4-5 *Full length PKD is essential for LPL vesicle formation from Golgi.* Rat heart homogenate was overlaid on sucrose solutions, and the gradients centrifuged for 2 h. A Golgi fraction was isolated from the sucrose interphase and mixed with GST-PKD (5 μg) alone or together with caspase-3 (5 units) (A and B). Isolated Golgi were also incubated with cardiac cytosol (0.2 mg) isolated from control and D-100 hearts, treated or not treated with Z-DEVD (C and D). All samples were ultra centrifuged for isolation of vesicles, which were then subjected to Western blot for evaluating VAMP and LPL. Results are the means ± SE of 3-5 experiments in each group. *Significantly different from control; +significantly different from all other groups, $P<0.05$.

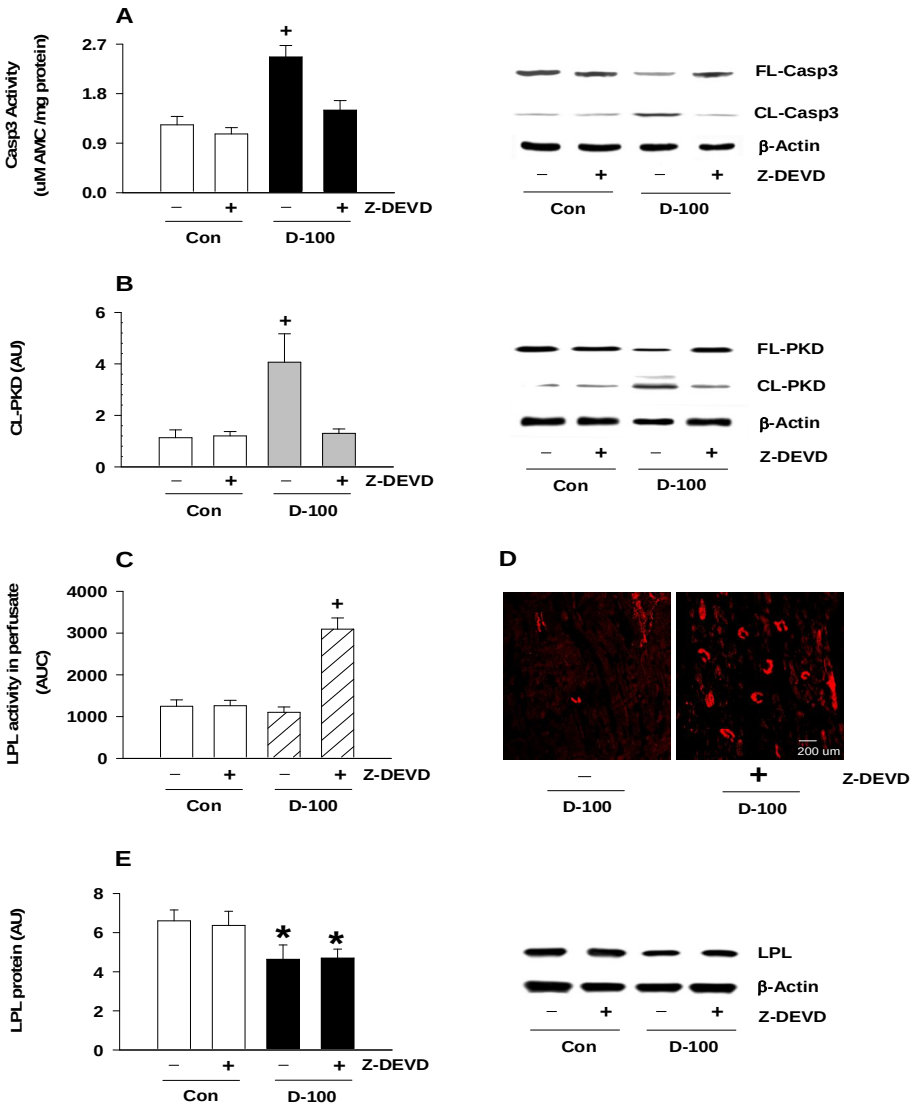

Fig. 4-6 *Activation of caspase-3 in D-100 limits vascular lumen increase in LPL.* Animals were treated with STZ (100 mg/kg, i.v.), and kept for 4 days. After 1 day of STZ, some control and D-100 rats were treated twice daily with Z-DEVD (3.2 mg/kg, i.p.) for 3 days. Cardiac caspase-3 activity was measured using a fluorometric assay kit (A). FL and CL-caspase-3 (A) and PKD (B) in the different groups were measured using Western blot. Hearts were also isolated and perfused in the non-recirculating retrograde mode. The coronary luminal LPL released with heparin (5 units/ml) was assayed using radiolabeled triolein. The results are expressed as area under curve (AUC) of enzyme released over 5 min (C). LPL was visualized by immunofluoresence (D). Bar = 200 μm. The level of LPL protein was measured using Western blot (E). Results are the means ± SE of 3-5 rats in each group. *Significantly different from control; +significantly different from all other groups, $P<0.05$.

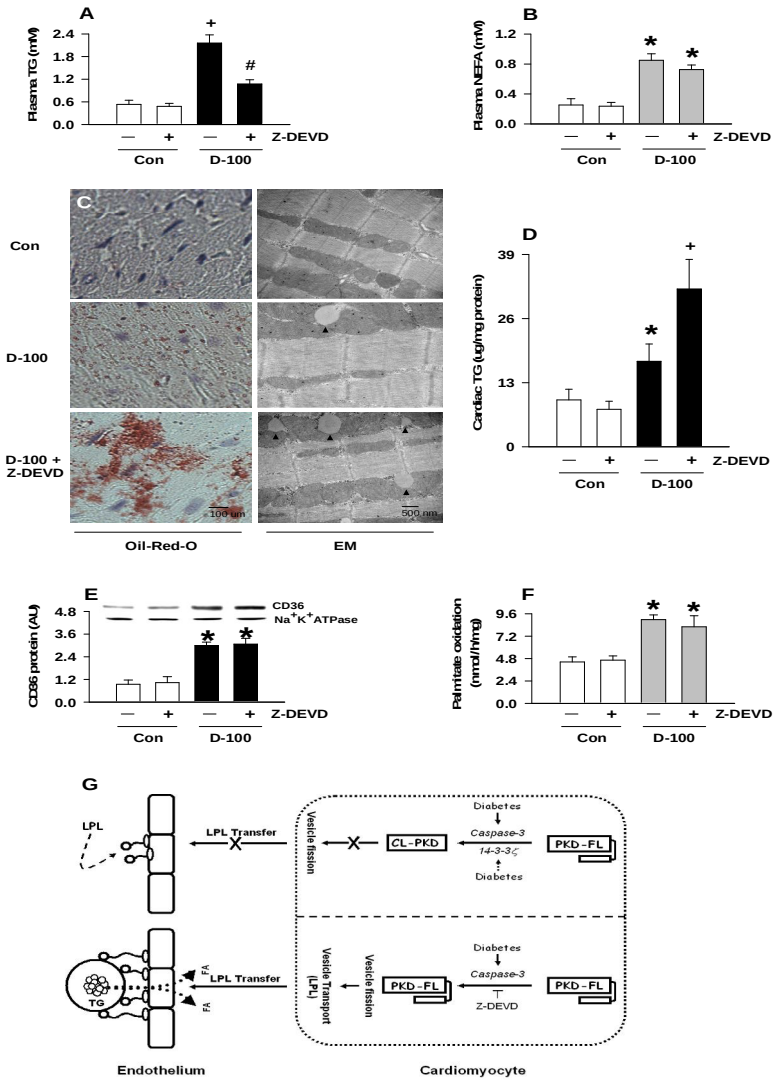

Fig. 4-7 *Inhibition of caspase-3 facilitates a striking increase in TG accumulation in D-100 hearts*. Plasma collected at termination was evaluated for TG (A) and NEFA (B) using diagnostic kits. Oil Red O staining of representative cardiac sections showing lipid accumulation is described in C (left panel). Bar = 100 μm. Representative electron micrograph of hearts from different groups is depicted in C (right panel). Bar = 500 nm. Black arrow head, lipid-like vacuoles. Cardiac TG was extracted with organic solvent, and determined using HPLC (D). Plasma membranes were isolated and used for identification of CD36 (E). Palmitate oxidation in myocytes isolated from the different groups was assessed by measuring $^{14}CO_2$ (F). Results are the means ± SE of 3-5 rats in each group. *Significantly different from control; $^{+}$significantly different from all other groups, $^{\#}$significantly different from untreated D-100, $P<0.05$. A graphic representation of caspase-3 control of cardiac metabolism is described in G. Following severe hypoinsulinemia, a decrease in full length PKD requires both activation of caspase-3 together with loss of the binding protein 14-3-3ζ. Proteolysis of PKD is unable to transfer cardiac LPL to the vascular lumen. The caspase inhibitor, Z-DEVD, effectively lowers caspase-3 activity in D-100 hearts, prevents PKD cleavage and increases LPL vesicle formation and translocation to the coronary lumen. This increase in luminal LPL is associated with a decline in circulating triglyceride (TG), but a striking cardiac TG accumulation.

4.5. Bibliography

1. Avogaro A, Nosadini R, Doria A, Fioretto P, Velussi M, Vigorito C, Sacca L, Toffolo G, Cobelli C, Trevisan R, et al.: Myocardial metabolism in insulin-deficient diabetic humans without coronary artery disease. *Am J Physiol* 258:E606-618, 1990

2. Saddik M, Lopaschuk GD: Myocardial triglyceride turnover and contribution to energy substrate utilization in isolated working rat hearts. *J Biol Chem* 266:8162-8170, 1991

3. Lopaschuk GD, Belke DD, Gamble J, Itoi T, Schonekess BO: Regulation of fatty acid oxidation in the mammalian heart in health and disease. *Biochim Biophys Acta* 1213:263-276, 1994

4. Paulson DJ, Crass MF, 3rd: Endogenous triacylglycerol metabolism in diabetic heart. *Am J Physiol* 242:H1084-1094, 1982

5. Haffner SM: Lipoprotein disorders associated with type 2 diabetes mellitus and insulin resistance. *Am J Cardiol* 90:55i-61i, 2002

6. Blanchette-Mackie EJ, Masuno H, Dwyer NK, Olivecrona T, Scow RO: Lipoprotein lipase in myocytes and capillary endothelium of heart: immunocytochemical study. *Am J Physiol* 256:E818-828, 1989

7. Merkel M, Eckel RH, Goldberg IJ: Lipoprotein lipase: genetics, lipid uptake, and regulation. *J Lipid Res* 43:1997-2006, 2002

8. Augustus AS, Kako Y, Yagyu H, Goldberg IJ: Routes of FA delivery to cardiac muscle: modulation of lipoprotein lipolysis alters uptake of TG-derived FA. *Am J Physiol Endocrinol Metab* 284:E331-339, 2003

9. Camps L, Reina M, Llobera M, Vilaro S, Olivecrona T: Lipoprotein lipase: cellular origin and functional distribution. *Am J Physiol* 258:C673-681, 1990

10. Eckel RH: Lipoprotein lipase. A multifunctional enzyme relevant to common metabolic diseases. *N Engl J Med* 320:1060-1068, 1989

11. Blanchette-Mackie EJ, Dwyer NK, Amende LA: Cytochemical studies of lipid metabolism: immunogold probes for lipoprotein lipase and cholesterol. *Am J Anat* 185:255-263, 1989

12. Rodrigues B, Cam MC, McNeill JH: Myocardial substrate metabolism: implications for diabetic cardiomyopathy. *J Mol Cell Cardiol* 27:169-179, 1995

13. Pulinilkunnil T, Abrahani A, Varghese J, Chan N, Tang I, Ghosh S, Kulpa J, Allard M, Brownsey R, Rodrigues B: Evidence for rapid "metabolic switching" through lipoprotein lipase occupation of endothelial-binding sites. *J Mol Cell Cardiol* 35:1093-1103, 2003

14. Rodrigues B, Cam MC, Jian K, Lim F, Sambandam N, Shepherd G: Differential effects of streptozotocin-induced diabetes on cardiac lipoprotein lipase activity. *Diabetes* 46:1346-1353, 1997

15. Pulinilkunnil T, Qi D, Ghosh S, Cheung C, Yip P, Varghese J, Abrahani A, Brownsey R, Rodrigues B: Circulating triglyceride lipolysis facilitates lipoprotein lipase translocation from cardiomyocyte to myocardial endothelial lining. *Cardiovasc Res* 59:788-797, 2003

16. Sambandam N, Abrahani MA, St Pierre E, Al-Atar O, Cam MC, Rodrigues B: Localization of lipoprotein lipase in the diabetic heart: regulation by acute changes in insulin. *Arterioscler Thromb Vasc Biol* 19:1526-1534, 1999

17. Sambandam N, Abrahani MA, Craig S, Al-Atar O, Jeon E, Rodrigues B: Metabolism of VLDL is increased in streptozotocin-induced diabetic rat hearts. *Am J Physiol Heart Circ Physiol* 278:H1874-1882, 2000

18. Kim MS, Wang F, Puthanveetil P, Kewalramani G, Hosseini-Beheshti E, Ng N, Wang Y, Kumar U, Innis S, Proud CG, Abrahani A, Rodrigues B: Protein kinase D is a key regulator of cardiomyocyte lipoprotein lipase secretion after diabetes. *Circ Res* 103:252-260, 2008

19. An D, Pulinilkunnil T, Qi D, Ghosh S, Abrahani A, Rodrigues B: The metabolic "switch" AMPK regulates cardiac heparin-releasable lipoprotein lipase. *Am J Physiol Endocrinol Metab* 288:E246-253, 2005

20. Kim MS, Kewalramani G, Puthanveetil P, Lee V, Kumar U, An D, Abrahani A, Rodrigues B: Acute diabetes moderates trafficking of cardiac lipoprotein lipase through p38 mitogen-activated protein kinase-dependent actin cytoskeleton organization. *Diabetes* 57:64-76, 2008

21. Pillarisetti S, Paka L, Sasaki A, Vanni-Reyes T, Yin B, Parthasarathy N, Wagner WD, Goldberg IJ: Endothelial cell heparanase modulation of lipoprotein lipase activity. Evidence that heparan sulfate oligosaccharide is an extracellular chaperone. *J Biol Chem* 272:15753-15759, 1997

22. Wang F, Kim MS, Puthanveetil P, Kewalramani G, Deppe S, Ghosh S, Abrahani A, Rodrigues B: Endothelial heparanase secretion after acute hypoinsulinemia is regulated by glucose and fatty acid. *Am J Physiol Heart Circ Physiol* 296:H1108-1116, 2009

23. Junod A, Lambert AE, Stauffacher W, Renold AE: Diabetogenic action of streptozotocin: relationship of dose to metabolic response. *J Clin Invest* 48:2129-2139, 1969

24. Kewalramani G, An D, Kim MS, Ghosh S, Qi D, Abrahani A, Pulinilkunnil T, Sharma V, Wambolt RB, Allard MF, Innis SM, Rodrigues B: AMPK control of myocardial fatty acid metabolism fluctuates with the intensity of insulin-deficient diabetes. *J Mol Cell Cardiol* 42:333-342, 2007

25. Braun JE, Severson DL: Diabetes reduces heparin- and phospholipase C-releasable lipoprotein lipase from cardiomyocytes. *Am J Physiol* 260:E477-485, 1991

26. Chen J, Lee CT, Errico SL, Becker KG, Freed WJ: Increases in expression of 14-3-3 eta and 14-3-3 zeta transcripts during neuroprotection induced by delta9-tetrahydrocannabinol in AF5 cells. *J Neurosci Res* 85:1724-1733, 2007

27. Innis SM, Dyer RA: Brain astrocyte synthesis of docosahexaenoic acid from n-3 fatty acids is limited at the elongation of docosapentaenoic acid. *J Lipid Res* 43:1529-1536, 2002

28. Wolins NE, Quaynor BK, Skinner JR, Tzekov A, Croce MA, Gropler MC, Varma V, Yao-Borengasser A, Rasouli N, Kern PA, Finck BN, Bickel PE: OXPAT/PAT-1 is a PPAR-induced lipid droplet protein that promotes fatty acid utilization. *Diabetes* 55:3418-3428, 2006

29. Qi D, Kuo KH, Abrahani A, An D, Qi Y, Heung J, Kewalramani G, Pulinilkunnil T, Ghosh S, Innis SM, Rodrigues B: Acute intralipid infusion reduces cardiac luminal lipoprotein lipase but recruits additional enzyme from cardiomyocytes. *Cardiovasc Res* 72:124-133, 2006

30. Puthanveetil P, Wang F, Kewalramani G, Kim MS, Hosseini-Beheshti E, Ng N, Lau W, Pulinilkunnil T, Allard M, Abrahani A, Rodrigues B: Cardiac glycogen accumulation after dexamethasone is regulated by AMPK. *Am J Physiol Heart Circ Physiol* 295:H1753-1762, 2008

31. Carroll R, Carley AN, Dyck JR, Severson DL: Metabolic effects of insulin on cardiomyocytes from control and diabetic db/db mouse hearts. *Am J Physiol Endocrinol Metab* 288:E900-906, 2005

32. Abousalham A, Hobman TC, Dewald J, Garbutt M, Brindley DN: Cell-permeable ceramides preferentially inhibit coated vesicle formation and exocytosis in Chinese hamster ovary compared with Madin-Darby canine kidney cells by preventing the membrane association of ADP-ribosylation factor. *Biochem J* 361:653-661, 2002

33. Endo K, Oki E, Biedermann V, Kojima H, Yoshida K, Johannes FJ, Kufe D, Datta R: Proteolytic cleavage and activation of protein kinase C [micro] by caspase-3 in the apoptotic response of cells to 1-beta -D-arabinofuranosylcytosine and other genotoxic agents. *J Biol Chem* 275:18476-18481, 2000

34. Maeda Y, Beznoussenko GV, Van Lint J, Mironov AA, Malhotra V: Recruitment of protein kinase D to the trans-Golgi network via the first cysteine-rich domain. *Embo J* 20:5982-5990, 2001

35. Tzivion G, Avruch J: 14-3-3 proteins: active cofactors in cellular regulation by serine/threonine phosphorylation. *J Biol Chem* 277:3061-3064, 2002

36. Kim YH, Kim YS, Kang SS, Noh HS, Kim HJ, Cho GJ, Choi WS: Expression of 14-3-3 zeta and interaction with protein kinase C in the rat retina in early diabetes. *Diabetologia* 48:1411-1415, 2005

37. Matthews SA, Rozengurt E, Cantrell D: Characterization of serine 916 as an in vivo autophosphorylation site for protein kinase D/Protein kinase Cmu. *J Biol Chem* 274:26543-26549, 1999

38. Matthews SA, Pettit GR, Rozengurt E: Bryostatin 1 induces biphasic activation of protein kinase D in intact cells. *J Biol Chem* 272:20245-20250, 1997

39. Lu G, Chen J, Espinoza LA, Garfield S, Toshiyuki S, Akiko H, Huppler A, Wang QJ: Protein kinase D 3 is localized in vesicular structures and interacts with vesicle-associated membrane protein 2. *Cell Signal* 19:867-879, 2007

40. An D, Rodrigues B: Role of changes in cardiac metabolism in development of diabetic cardiomyopathy. *Am J Physiol Heart Circ Physiol* 291:H1489-1506, 2006

41. Cai L, Li W, Wang G, Guo L, Jiang Y, Kang YJ: Hyperglycemia-induced apoptosis in mouse myocardium: mitochondrial cytochrome C-mediated caspase-3 activation pathway. *Diabetes* 51:1938-1948, 2002

42. Porter AG, Janicke RU: Emerging roles of caspase-3 in apoptosis. *Cell Death Differ* 6:99-104, 1999

43. Kuranaga E, Miura M: Nonapoptotic functions of caspases: caspases as regulatory molecules for immunity and cell-fate determination. *Trends Cell Biol* 17:135-144, 2007

44. Levak-Frank S, Hofmann W, Weinstock PH, Radner H, Sattler W, Breslow JL, Zechner R: Induced mutant mouse lines that express lipoprotein lipase in cardiac muscle, but not in skeletal muscle and adipose tissue, have normal plasma triglyceride and high-density lipoprotein-cholesterol levels. *Proc Natl Acad Sci U S A* 96:3165-3170, 1999

45. Levak-Frank S, Radner H, Walsh A, Stollberger R, Knipping G, Hoefler G, Sattler W, Weinstock PH, Breslow JL, Zechner R: Muscle-specific overexpression of lipoprotein lipase causes a severe myopathy characterized by proliferation of mitochondria and peroxisomes in transgenic mice. *J Clin Invest* 96:976-986, 1995

46. Yagyu H, Chen G, Yokoyama M, Hirata K, Augustus A, Kako Y, Seo T, Hu Y, Lutz EP, Merkel M, Bensadoun A, Homma S, Goldberg IJ: Lipoprotein lipase (LpL) on the surface of cardiomyocytes increases lipid uptake and produces a cardiomyopathy. *J Clin Invest* 111:419-426, 2003

47. Luiken JJ, Vertommen D, Coort SL, Habets DD, El Hasnaoui M, Pelsers MM, Viollet B, Bonen A, Hue L, Rider MH, Glatz JF: Identification of protein kinase D as a novel contraction-activated kinase linked to GLUT4-mediated glucose uptake, independent of AMPK. *Cell Signal* 20:543-556, 2008

48. Garvey WT, Hardin D, Juhaszova M, Dominguez JH: Effects of diabetes on myocardial glucose transport system in rats: implications for diabetic cardiomyopathy. *Am J Physiol* 264:H837-844, 1993

49. Kitajima S, Morimoto M, Liu E, Koike T, Higaki Y, Taura Y, Mamba K, Itamoto K, Watanabe T, Tsutsumi K, Yamada N, Fan J: Overexpression of lipoprotein lipase improves insulin resistance induced by a high-fat diet in transgenic rabbits. *Diabetologia* 47:1202-1209, 2004

50. Kim JK, Fillmore JJ, Chen Y, Yu C, Moore IK, Pypaert M, Lutz EP, Kako Y, Velez-Carrasco W, Goldberg IJ, Breslow JL, Shulman GI: Tissue-specific overexpression of lipoprotein lipase causes tissue-specific insulin resistance. *Proc Natl Acad Sci U S A* 98:7522-7527, 2001

51. Wang H, Knaub LA, Jensen DR, Young Jung D, Hong EG, Ko HJ, Coates AM, Goldberg IJ, de la Houssaye BA, Janssen RC, McCurdy CE, Rahman SM, Soo Choi C, Shulman GI, Kim JK, Friedman JE, Eckel RH: Skeletal muscle-specific deletion of lipoprotein lipase enhances insulin signaling in skeletal muscle but causes insulin resistance in liver and other tissues. *Diabetes* 58:116-124, 2009

52. Li J, Lang MJ, Mao XB, Tian L, Feng YB: Antiapoptosis and Mitochondrial Effect of Pioglitazone Preconditioning in the Ischemic/reperfused Heart of Rat. *Cardiovasc Drugs Ther* 22:283-291, 2008

53. Boyle PJ, King AB, Olansky L, Marchetti A, Lau H, Magar R, Martin J: Effects of pioglitazone and rosiglitazone on blood lipid levels and glycemic control in patients with type 2 diabetes mellitus: a retrospective review of randomly selected medical records. *Clin Ther* 24:378-396, 2002

54. Kobayashi J, Nagashima I, Hikita M, Bujo H, Takahashi K, Otabe M, Morisaki N, Saito Y: Effect of troglitazone on plasma lipid metabolism and lipoprotein lipase. *Br J Clin Pharmacol* 47:433-439, 1999

55. Nagashima K, Lopez C, Donovan D, Ngai C, Fontanez N, Bensadoun A, Fruchart-Najib J, Holleran S, Cohn JS, Ramakrishnan R, Ginsberg HN: Effects of the PPARgamma agonist pioglitazone on lipoprotein metabolism in patients with type 2 diabetes mellitus. *J Clin Invest* 115:1323-1332, 2005

56. Baranowski M, Blachnio-Zabielska A, Zabielski P, Gorski J: Pioglitazone induces lipid accumulation in the rat heart despite concomitant reduction in plasma free fatty acid availability. *Arch Biochem Biophys* 477:86-91, 2008

57. Lago RM, Singh PP, Nesto RW: Congestive heart failure and cardiovascular death in patients with prediabetes and type 2 diabetes given thiazolidinediones: a meta-analysis of randomised clinical trials. *Lancet* 370:1129-1136, 2007

58. Lipscombe LL, Gomes T, Levesque LE, Hux JE, Juurlink DN, Alter DA: Thiazolidinediones and cardiovascular outcomes in older patients with diabetes. *Jama* 298:2634-2643, 2007

59. Zhou YT, Grayburn P, Karim A, Shimabukuro M, Higa M, Baetens D, Orci L, Unger RH: Lipotoxic heart disease in obese rats: implications for human obesity. *Proc Natl Acad Sci U S A* 97:1784-1789, 2000

5. CONCLUSIONS AND FUTURE DIRECTION

5.1. Conclusions

Diabetes is a metabolic syndrome characterized by hyperglycemia caused by deficiency in insulin secretion (Type 1), insulin action (Type 2), or both. Heart disease is a leading cause of death in diabetic patients, with coronary vessel disease and atherosclerosis being primary reasons for the increased incidence of cardiovascular dysfunction(1,2). However, a predisposition to heart failure might also reflect the effects of underlying abnormalities in diastolic function that can be detected in asymptomatic patients with diabetes alone(3,4). These observations suggest a specific impairment of heart muscle (termed diabetic cardiomyopathy)(5-10).

Several etiological factors have been put forward to explain the development of diabetic cardiomyopathy including increased stiffness of the left ventricular wall associated with accumulation of connective tissue and insoluble collagen, depressed autonomic function, impaired endothelium function and sensitivity to various ligands (e.g., β-agonists), and abnormalities of various proteins that regulate ion flux, specifically intracellular calcium(11-14). More recently, the view that diabetic cardiomyopathy could also occur as a consequence of metabolic alterations has been put forward(15-17). In T1D and T2D, glucose uptake, glycolysis, and pyruvate oxidation are impaired(18,19). Under these conditions, the heart rapidly adapts to using FA exclusively for ATP generation(20). Chronically, this maladaptation is believed to play a key role in the development of cardiomyopathy(20). A number of studies have suggested that excessive FA overload induces lipotoxicity and contributes to the initiation and development of cardiomyopathy. For example, with the use of transgenic mice, studies have shown that elevation of FA uptake or utilization induces lipotoxicity in the absence of any systemic metabolic disturbance. Thus, cardiac-specific overexpression of LPL or fatty acid transport

protein 1 significantly increased FA delivery with ensuing lipid storage, lipotoxic cardiomyopathy, and contractile dysfunction(21,22). Moreover, elevating FA utilization by cardiac-specific overexpression of PPAR-α or acyl CoA synthase also causes cardiomyopathy and cardiac dysfunction, similar to that seen during diabetes(23,24). Conversely, reducing FA supply or utilization prevented the development of cardiomyopathy in obese or diabetic animals. In ZDF or transgenic mice with cardiac overexpression of LPL, a PPAR-γ agonist decreased plasma and cardiac intracellular lipids and ameliorated cardiomyopathy(25,26). Additionally, increasing lipoprotein excretion by overexpressing human apoB also reduces cardiac lipids and improves cardiomyopathy(27). Taken together, these studies provide convincing evidence that augmented FA supply during obesity or diabetes impairs cardiac lipid homeostasis and leads to lipotoxicity cardiomyopathy.

The mechanisms that mediate cardiac lipotoxicity are still not completely understood. One potential target is over production of reactive oxygen species (ROS)(24). High rate of FA oxidation increases mitochondrial action potential, leading to augmented ROS generation(24). Under normal physiological conditions, ROS is removed by cellular antioxidants. In the event of excessive generation of ROS, as observed in STZ-induced diabetic rats, ZDF rats, and *db/db* mice, it causes cardiomyocyte cell damage and augmented apoptosis(26,28,29). Another potential mechanism for lipotoxicity is accumulation of lipids, when FA uptake supercedes its oxidation. Regarding accumulation of TG, the role of this neutral lipid in inducing contractile dysfunction is still unknown, although a strong association between TG storage and lipotoxicity has been established in both animal models and human studies(26,30,31). Interestingly, a recent study suggested that TG formation actually provides protection against the deleterious effects of fatty acyl-CoA(32). Besides TG, excessive FA also leads to ceramide generation, an

intracellular messenger known to trigger apoptosis(26). Accumulation of ceramide has been found in ZDF rats (26) or in isolated cardiomyocytes incubated with high fat(33,34). Ceramide up regulates inducible nitric oxide synthase through activation of NF-κB, leading to increased generation of nitric oxide and peroxynitrite(26,35). As a highly reactive molecule, peroxynitrite causes opening of the mitochondrial permeability transition pore and release of cytochrome *c*. Additionally, ceramide directly interacts with cytochrome *c*, leading to its release from the mitochondria(36). As a consequence, caspase is activated, which initiates the apoptotic pathway in cells. High FA can also impair cardiolipin and lead to a ceramide-independent cell apoptosis(37). To avoid oversupply of potentially lethal fatty acids, my objective was to determine the mechanisms by which cardiac LPL is augmented. Previously, our lab suggested that AMPK influences LPL translocation to the cardiomyocyte cell surface, for eventual secretion to the vascular lumen. My initial study determined the molecular mechanisms by which AMPK controls LPL. Following AMPK activation, HR-LPL activity was appreciably enhanced, an effect that was reduced by preincubation with a p38 MAPK inhibitor (SB202190) or silencing of p38 MAPK using small interfering RNA (siRNA). In the absence of AMPK activation, direct stimulation of p38 MAPK was able to augment LPL activity at the cardiomyocyte cell surface, an effect that was prevented by cytochalasin D (inhibitor of actin polymerization). Following these stress kinase signals, Hsp25 is phosphorylated, releases actin monomers, and promotes actin polymerization. Overall, these data suggest that in diabetic hearts, stress kinase signals, Hsp25, and the actin cytoskeleton act in unison to promote vascular LPL increase.

In addition to stress signals, PKC has also been suggested to increase LPL activity by promoting its vesicular trafficking. Following hyperglycemia induced by diazoxide or STZ, we

demonstrate that PKCδ dissociates from Hsp25, allowing this protein kinase to phosphorylate and activate PKD, an important kinase that regulates fission of vesicles from the Golgi membrane. Rottlerin, a PKCδ inhibitor, prevented PKD phosphorylation and the subsequent increase in LPL. In myocytes in which PKD was silenced or a mutant form of PKCδ was expressed, high glucose and FA (to mimic diabetic conditions) were incapable of increasing LPL. Finally, silencing of cardiomyocyte Hsp25 elicited a significant phosphorylation of PKCδ, and activation of PKD. Overall, following diabetes, when cardiac glucose utilization is impaired, the PKCδ-PKD pathway embraces LPL vesicle formation and its secretion to cell surface. From here, LPL is transported onto similar HSPG-binding sites on the luminal surface of the capillary endothelium. At this location, hydrolysis of circulating lipoprotein-TG occurs, providing FA to the underlying cardiomyocyte.

During severe diabetes (D-100), there is an excess provision of circulating plasma FA from adipose tissue and increased hepatic VLDL-TG secretion. In this specific situation, coronary HR-LPL activity was lower compared to control hearts. It is suggested that LPL activity was reduced to limit overload of this potentially lethal substrate following severe diabetes. D-100 hearts showed cleavage of PKD, reducing its ability to interact with Golgi, and prevented LPL vesicle formation. This PKD proteolysis required activation of caspase-3 together with loss of 14-3-3ζ, a binding protein that protects enzymes against degradation. More importantly, during severe diabetes, inhibition of caspase-3 prevented PKD cleavage, augmented coronary LPL activity, and increased clearance of circulating TG. The net result of caspase-3 inhibition in D-100 rats was an increase in FA uptake into cardiac tissue, FA overload and striking accumulation in myocardial TG. As excess myocardial TG can lead to cardiac dysfunction, our data suggest

that caspase-3 inhibition can be either beneficial or harmful, depends on the prevalent physiological or pathological conditions, and requires further investigation.

5.2. Future direction

Future studies could focus on the following issues:

1. Insulin sensitizers (PPAR-γ activators) such as rosiglitazone and pioglitazone are used in the treatment of Type 2 diabetes. However, recent reports have suggested that these insulin sensitizers are associated with a statistically significant increase in the risk for heart disease. Interestingly, these drugs are known to prevent caspase-3 activation. Given that activation of caspase-3 can restrict LPL translocation to the vascular lumen, future studies should focus on identifying whether these drugs promote coronary LPL accumulation.

2. My studies indicate that following diabetes, cardiac LPL activity is increased without any change in LPL gene expression. Post translational transfer of LPL from the cardiomyocyte to the coronary lumen is a likely candidate for explaining this effect. As LPL dimerization is required for this movement, future studies should focus on identifying mechanisms that promote LPL dimerization. Interestingly, Angptl-4 in adipose tissue is known to convert LPL from a catalytically active dimer to the inactive monomer. Although cardiac Angptl-4 mRNA expression level is low in the heart compared to adipose tissue, whether its cardiac levels increase following hyperglycemia needs further investigation.

3. Since effective blood glucose control is always difficult in diabetic patients, it is possible that over time, these patients are predisposed to brief periods of hypoinsulinemia, increased luminal LPL, and abnormal FA supply and utilization by the heart leading to excessive FA and TG accumulation. Whether this excess LPL-derived FA during diabetes could contribute to heart failure remains unclear, and needs to be determined.

5.3. Bibliography

1. Burchfiel CM, Reed DM, Marcus EB, Strong JP, Hayashi T: Association of diabetes mellitus with coronary atherosclerosis and myocardial lesions. An autopsy study from the Honolulu Heart Program. *Am J Epidemiol* 137:1328-1340, 1993

2. Griffin E, Re A, Hamel N, Fu C, Bush H, McCaffrey T, Asch AS: A link between diabetes and atherosclerosis: Glucose regulates expression of CD36 at the level of translation. *Nat Med* 7:840-846, 2001

3. Boyer JK, Thanigaraj S, Schechtman KB, Perez JE: Prevalence of ventricular diastolic dysfunction in asymptomatic, normotensive patients with diabetes mellitus. *Am J Cardiol* 93:870-875, 2004

4. Annonu AK, Fattah AA, Mokhtar MS, Ghareeb S, Elhendy A: Left ventricular systolic and diastolic functional abnormalities in asymptomatic patients with non-insulin-dependent diabetes mellitus. *J Am Soc Echocardiogr* 14:885-891, 2001

5. Schannwell CM, Schneppenheim M, Perings S, Plehn G, Strauer BE: Left ventricular diastolic dysfunction as an early manifestation of diabetic cardiomyopathy. *Cardiology* 98:33-39, 2002

6. Bell DS: Diabetic cardiomyopathy. *Diabetes Care* 26:2949-2951, 2003

7. Beljic T, Miric M: Improved metabolic control does not reverse left ventricular filling abnormalities in newly diagnosed non-insulin-dependent diabetes patients. *Acta Diabetol* 31:147-150, 1994

8. Nicolino A, Longobardi G, Furgi G, Rossi M, Zoccolillo N, Ferrara N, Rengo F: Left ventricular diastolic filling in diabetes mellitus with and without hypertension. *Am J Hypertens* 8:382-389, 1995

9. Poirier P, Bogaty P, Garneau C, Marois L, Dumesnil JG: Diastolic dysfunction in normotensive men with well-controlled type 2 diabetes: importance of maneuvers in echocardiographic screening for preclinical diabetic cardiomyopathy. *Diabetes Care* 24:5-10, 2001

10. Bertoni AG, Tsai A, Kasper EK, Brancati FL: Diabetes and idiopathic cardiomyopathy: a nationwide case-control study. *Diabetes Care* 26:2791-2795, 2003

11. Farhangkhoee H, Khan ZA, Kaur H, Xin X, Chen S, Chakrabarti S: Vascular endothelial dysfunction in diabetic cardiomyopathy: pathogenesis and potential treatment targets. *Pharmacol Ther* 111:384-399, 2006

12. Cesario DA, Brar R, Shivkumar K: Alterations in ion channel physiology in diabetic cardiomyopathy. *Endocrinol Metab Clin North Am* 35:601-610, ix-x, 2006

13. Heyliger CE, Pierce GN, Singal PK, Beamish RE, Dhalla NS: Cardiac alpha- and beta-adrenergic receptor alterations in diabetic cardiomyopathy. *Basic Res Cardiol* 77:610-618, 1982

14. Candido R, Forbes JM, Thomas MC, Thallas V, Dean RG, Burns WC, Tikellis C, Ritchie RH, Twigg SM, Cooper ME, Burrell LM: A breaker of advanced glycation end products attenuates diabetes-induced myocardial structural changes. *Circ Res* 92:785-792, 2003

15. Lopaschuk GD, Rebeyka IM, Allard MF: Metabolic modulation: a means to mend a broken heart. *Circulation* 105:140-142, 2002

16. Rodrigues B, McNeill JH: The diabetic heart: metabolic causes for the development of a cardiomyopathy. *Cardiovasc Res* 26:913-922, 1992

17. Abel ED: Myocardial insulin resistance and cardiac complications of diabetes. *Curr Drug Targets Immune Endocr Metabol Disord* 5:219-226, 2005

18. Kelley DE, Mandarino LJ: Hyperglycemia normalizes insulin-stimulated skeletal muscle glucose oxidation and storage in noninsulin-dependent diabetes mellitus. *J Clin Invest* 86:1999-2007, 1990

19. Iozzo P, Hallsten K, Oikonen V, Virtanen KA, Kemppainen J, Solin O, Ferrannini E, Knuuti J, Nuutila P: Insulin-mediated hepatic glucose uptake is impaired in type 2 diabetes: evidence for a relationship with glycemic control. *J Clin Endocrinol Metab* 88:2055-2060, 2003

20. An D, Rodrigues B: Role of changes in cardiac metabolism in development of diabetic cardiomyopathy. *Am J Physiol Heart Circ Physiol* 291:H1489-1506, 2006

21. Yagyu H, Chen G, Yokoyama M, Hirata K, Augustus A, Kako Y, Seo T, Hu Y, Lutz EP, Merkel M, Bensadoun A, Homma S, Goldberg IJ: Lipoprotein lipase (LpL) on the surface of cardiomyocytes increases lipid uptake and produces a cardiomyopathy. *J Clin Invest* 111:419-426, 2003

22. Chiu HC, Kovacs A, Blanton RM, Han X, Courtois M, Weinheimer CJ, Yamada KA, Brunet S, Xu H, Nerbonne JM, Welch MJ, Fettig NM, Sharp TL, Sambandam N, Olson KM, Ory DS, Schaffer JE: Transgenic expression of fatty acid transport protein 1 in the heart causes lipotoxic cardiomyopathy. *Circ Res* 96:225-233, 2005

23. Chiu HC, Kovacs A, Ford DA, Hsu FF, Garcia R, Herrero P, Saffitz JE, Schaffer JE: A novel mouse model of lipotoxic cardiomyopathy. *J Clin Invest* 107:813-822, 2001

24. Finck BN, Lehman JJ, Leone TC, Welch MJ, Bennett MJ, Kovacs A, Han X, Gross RW, Kozak R, Lopaschuk GD, Kelly DP: The cardiac phenotype induced by PPARalpha overexpression mimics that caused by diabetes mellitus. *J Clin Invest* 109:121-130, 2002

25. Vikramadithyan RK, Hirata K, Yagyu H, Hu Y, Augustus A, Homma S, Goldberg IJ: Peroxisome proliferator-activated receptor agonists modulate heart function in transgenic mice with lipotoxic cardiomyopathy. *J Pharmacol Exp Ther* 313:586-593, 2005

26. Zhou YT, Grayburn P, Karim A, Shimabukuro M, Higa M, Baetens D, Orci L, Unger RH: Lipotoxic heart disease in obese rats: implications for human obesity. *Proc Natl Acad Sci U S A* 97:1784-1789, 2000

27. Yokoyama M, Yagyu H, Hu Y, Seo T, Hirata K, Homma S, Goldberg IJ: Apolipoprotein B production reduces lipotoxic cardiomyopathy: studies in heart-specific lipoprotein lipase transgenic mouse. *J Biol Chem* 279:4204-4211, 2004

28. Barouch LA, Gao D, Chen L, Miller KL, Xu W, Phan AC, Kittleson MM, Minhas KM, Berkowitz DE, Wei C, Hare JM: Cardiac myocyte apoptosis is associated with increased DNA damage and decreased survival in murine models of obesity. *Circ Res* 98:119-124, 2006

29. Cai L, Li W, Wang G, Guo L, Jiang Y, Kang YJ: Hyperglycemia-induced apoptosis in mouse myocardium: mitochondrial cytochrome C-mediated caspase-3 activation pathway. *Diabetes* 51:1938-1948, 2002

30. Sharma S, Adrogue JV, Golfman L, Uray I, Lemm J, Youker K, Noon GP, Frazier OH, Taegtmeyer H: Intramyocardial lipid accumulation in the failing human heart resembles the lipotoxic rat heart. *Faseb J* 18:1692-1700, 2004

31. Christoffersen C, Bollano E, Lindegaard ML, Bartels ED, Goetze JP, Andersen CB, Nielsen LB: Cardiac lipid accumulation associated with diastolic dysfunction in obese mice. *Endocrinology* 144:3483-3490, 2003

32. Listenberger LL, Han X, Lewis SE, Cases S, Farese RV, Jr., Ory DS, Schaffer JE: Triglyceride accumulation protects against fatty acid-induced lipotoxicity. *Proc Natl Acad Sci U S A* 100:3077-3082, 2003

33. Dyntar D, Eppenberger-Eberhardt M, Maedler K, Pruschy M, Eppenberger HM, Spinas GA, Donath MY: Glucose and palmitic acid induce degeneration of myofibrils and modulate apoptosis in rat adult cardiomyocytes. *Diabetes* 50:2105-2113, 2001

34. Hickson-Bick DL, Buja LM, McMillin JB: Palmitate-mediated alterations in the fatty acid metabolism of rat neonatal cardiac myocytes. *J Mol Cell Cardiol* 32:511-519, 2000

35. Unger RH, Orci L: Lipoapoptosis: its mechanism and its diseases. *Biochim Biophys Acta* 1585:202-212, 2002

36. Ghafourifar P, Klein SD, Schucht O, Schenk U, Pruschy M, Rocha S, Richter C: Ceramide induces cytochrome c release from isolated mitochondria. Importance of mitochondrial redox state. *J Biol Chem* 274:6080-6084, 1999

37. Ostrander DB, Sparagna GC, Amoscato AA, McMillin JB, Dowhan W: Decreased cardiolipin synthesis corresponds with cytochrome c release in palmitate-induced cardiomyocyte apoptosis. *J Biol Chem* 276:38061-38067, 2001

APPENDICES

Appendix A

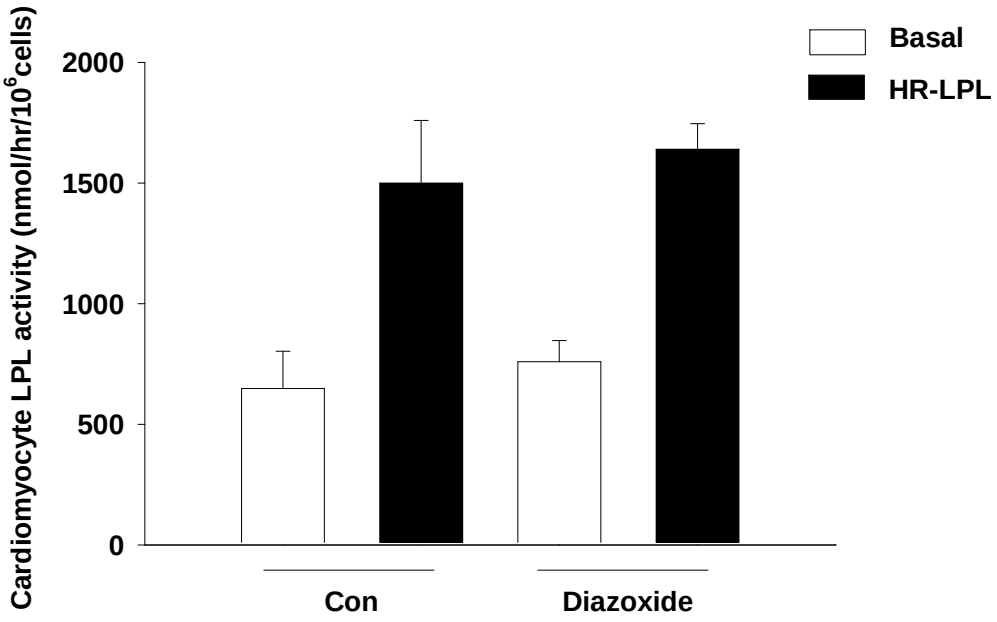

Appendix Fig. A-1 *Diazoxide has no direct effect on isolated cardiomyocyte LPL.* Cardiomyocytes were plated on laminin-coated culture plates. Cells were maintained using Media-199, and incubated at 37°C under an atmosphere of 95% O_2/5% CO_2 for 16 hours. Subsequently, DZ (1 mg/ml; calculated concentration *in vivo*) was added to the culture medium for 4 h and myocyte basal LPL activity released into the medium was measured. To release surface-bound LPL activity, heparin (8 U/mL; 1 min) was added to the culture plates, aliquots of cell medium removed, separated by centrifugation, and assayed for LPL activity. Data are means ± SE; n=3 myocyte preparations from different animals.

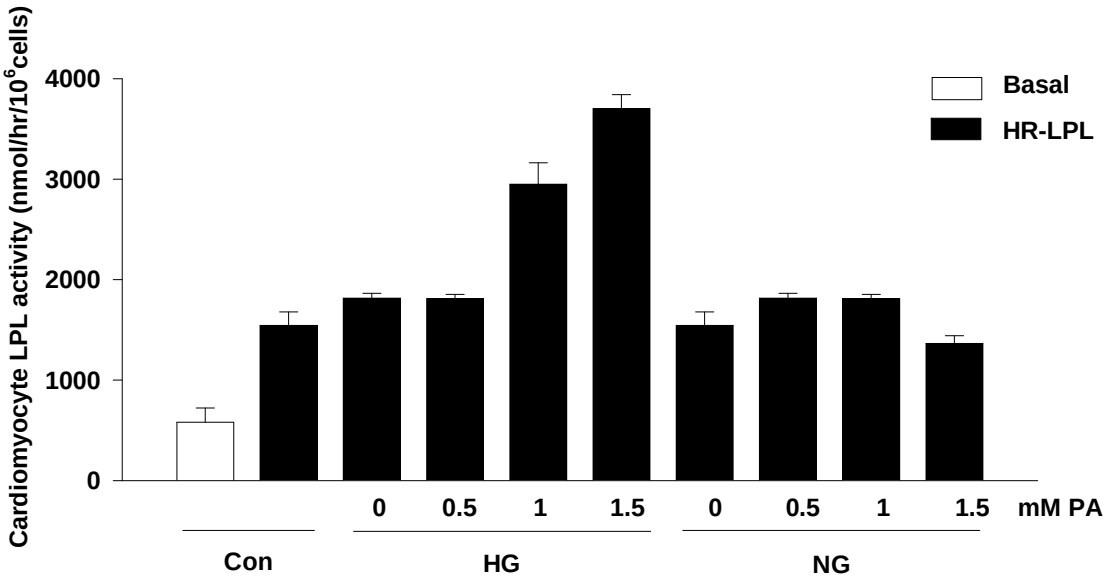

Appendix Fig. A-2 *Cardiomyocyte heparin releasable LPL activity only increases in the presence of high glucose and palmitic acid.* Laminin coated cardiomyocytes were treated with normal (NG, 5 mM) or high (HG, 20 mM) glucose and increasing concentrations of albumin bound palmitic acid (PA, 0-1.5 mM). After 2h, basal and heparin releasable LPL in the medium was determined using radio labeled triolein. Data are means ± SE; n=3 myocyte preparations from different animals.

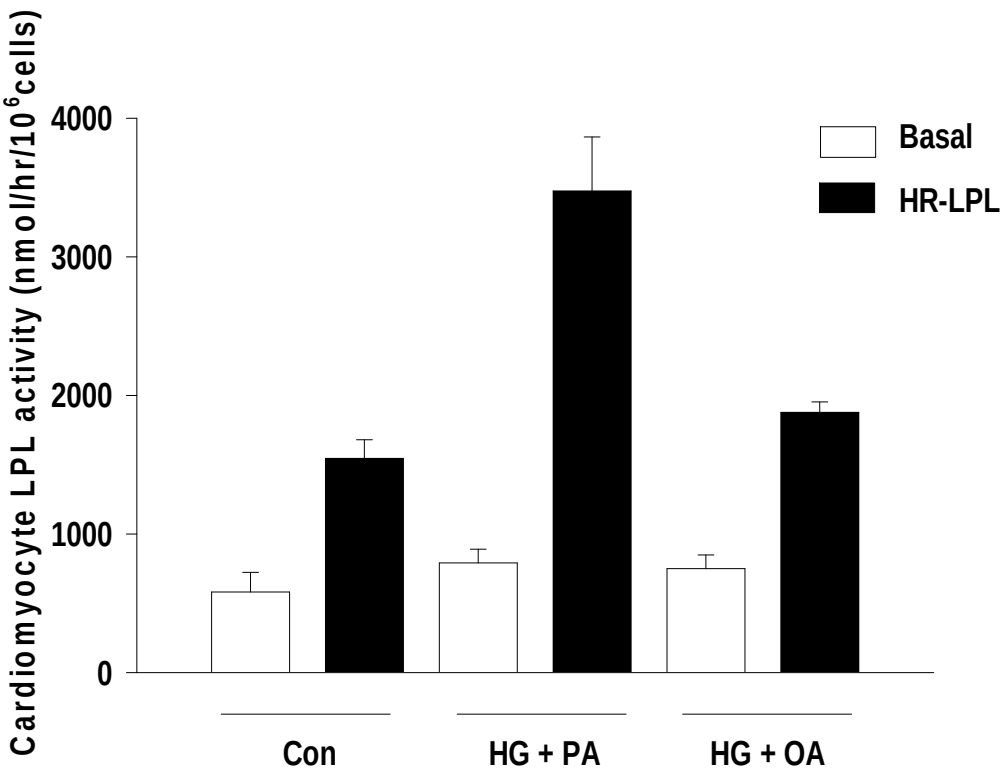

Appendix Fig. A-3 *Unlike palmitic acid, high glucose and oleic acid does not increase cardiomyocyte heparin releasable LPL.* Cardiomyocytes were treated with high glucose (20 mM) and either palmitic (1.5 mM) or oleic (1.5 mM) acid. After 2 h, basal and heparin releasable LPL in the medium was measured. Data are means ± SE; n=3 myocyte preparations from different animals. PA, palmitic acid; OA, oleic acid.

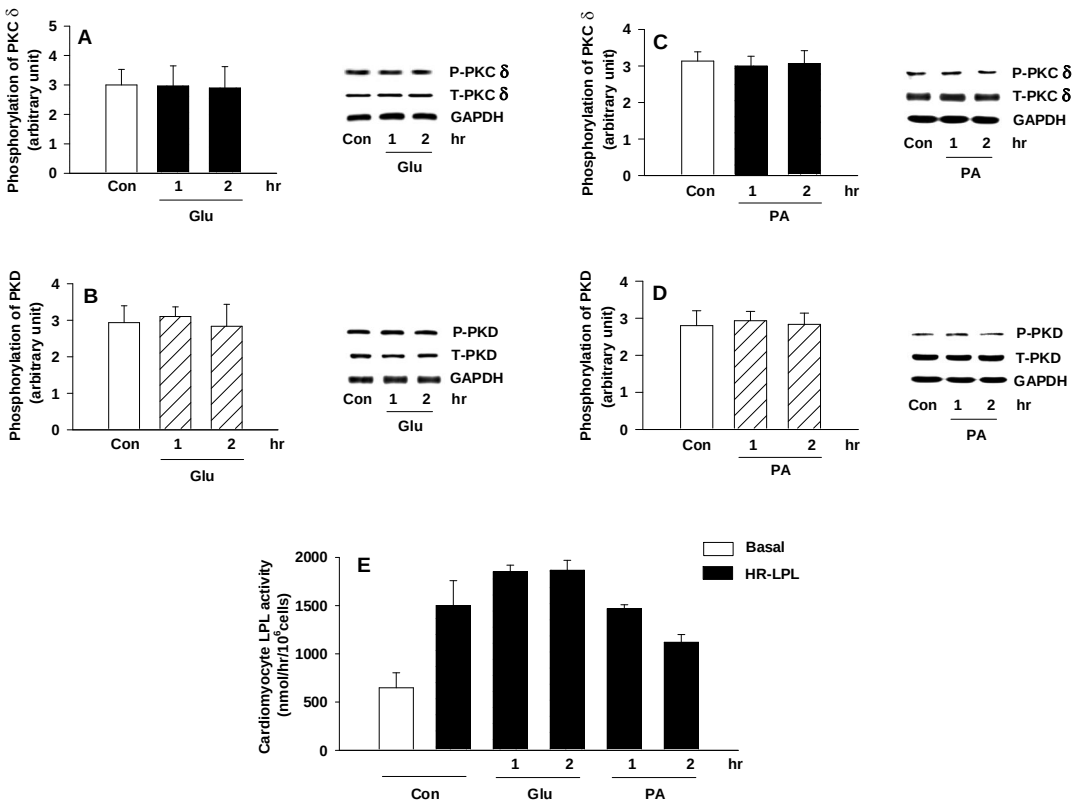

Appendix Fig. A-4 *High glucose and palmitic acid alone have no effect on cardiomyocyte LPL trafficking.* Cardiomyocytes were treated with high glucose (20 mM) or palmitic acid (1.5 mM) alone. At the indicated times, protein was extracted to determine both total and phosphorylated PKCδ (A, C) and PKD (B, D) using Western Blotting. To release surface-bound LPL activity, heparin was added to the culture plates, aliquots of cell medium removed, separated by centrifugation, and assayed for LPL activity (E). Data are means ± SE; n=3 myocyte preparations from different animals. PA, palmitic acid.

Appendix B

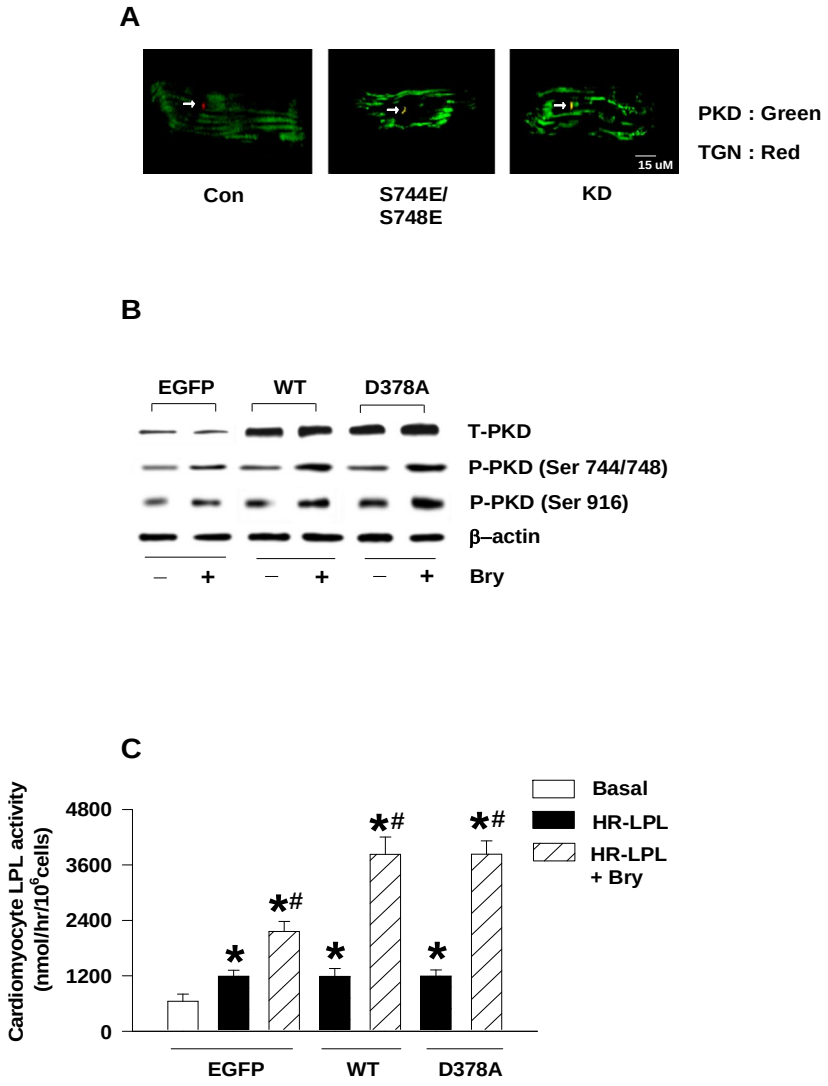

Appendix Fig B-1 *Phosphorylation at Ser 744/748 of PKD is key to increasing cardiomyocyte LPL* Control cardiomyocytes were infected with recombinant adenovirus vector carrying phospho-mimetic (S744E/748E) or kinase-dead (KD) mutants. Infected cells were incubated for a further 36 h before co-localization of PKD and trans-Golgi (TGN) was determined using immunofluoresence (arrow). Cardiomyocytes were fixed, incubated with primary antibodies [PKD (Green) and TGN38 (Red)] followed by incubation with secondary antibodies [FITC (Green) and TR (Red)] (A). Cardiomyocytes were also transfected with PKD wild-type (WT) and PKD D378A, and EGFP. Infected cells were incubated for a further 36 h before protein extraction for measurement of total and phosphorylated Ser 744/748 and Ser 916 PKD, in the absence or presence of Bryostatin-1 (B). In these cells, LPL activity was determined by adding heparin (8 U/ml for 1 minute) to the incubation medium, and the release of surface-bound LPL activity into the medium determined (C). Results are the means ± SE of 3-5 cardiomyocyte preparations from different animals. *Significantly different from control; #significantly different from heparin releasable, $P<0.05$.

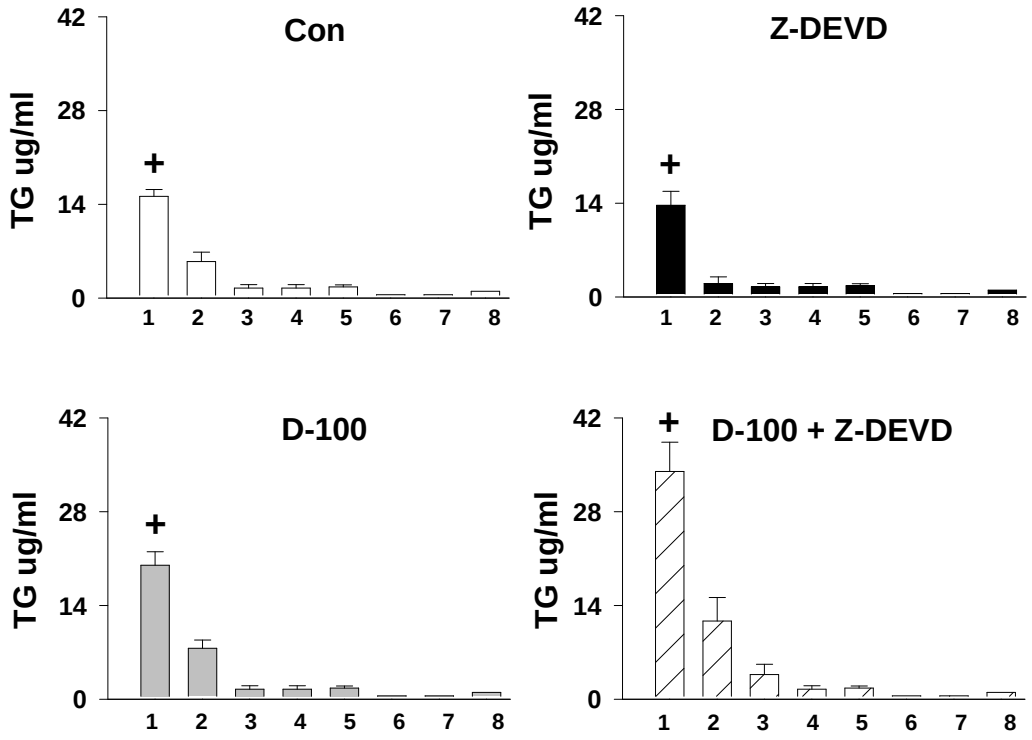

Appendix Fig B-2 *Cell fractionation and analysis of TG* Rat heart homogenates from control and D-100 hearts treated or untreated with Z-DEVD were overlaid on sucrose solutions, and the gradients centrifuged (2,700-172,000g). Following fractionation of heart tissue using sucrose density gradients, the different fractions obtained at a particular force were subjected to Western blot for OXPAT (top panel). The different fractions obtained at a particular force were then used for determination of TG (lower panel). Results are the means ± SE of 3-5 rats in each group. $^{+}$Significantly different from all other groups, $P<0.05$.

THE UNIVERSITY OF BRITISH COLUMBIA

ANIMAL CARE CERTIFICATE

Application Number: A08-0627

Investigator or Course Director: Brian B. Rodrigues

Department: Pharmaceutical Sciences

Animals:

Rats Wistar 420

Start Date: **July 1, 2008** **Approval Date:** **October 22, 2008**

Funding Sources:

Funding Agency: Canadian Diabetes Association
Funding Title: Metabolic basis for diabetic heart disease: role of cardiac lipoprotein lipase

Unfunded title: N/A

The Animal Care Committee has examined and approved the use of animals for the above experimental project.

This certificate is valid for one year from the above start or approval date (whichever is later) provided there is no change in the experimental procedures. Annual review is required by the CCAC and some granting agencies.

A copy of this certificate must be displayed in your animal facility.

Office of Research Services and Administration
102, 6190 Agronomy Road, Vancouver, BC V6T 1Z3
Phone: 604-827-5111 Fax: 604-822-5093